Cooperative Research Centre for Coastal Zone, Estuary & Waterway Management

Technical Report 38

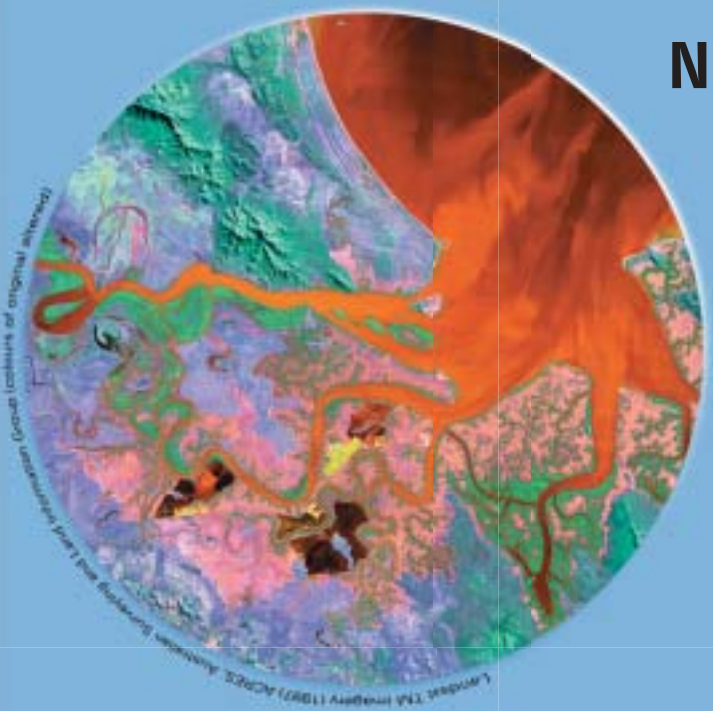

# Numerical hydrodynamic modelling of the Fitzroy Estuary

M. Herzfeld
J. R. Andrewartha
P. Sakov
I. Webster

March 2006

CSIRO
Central Queensland University
Where Students Come First.
Queensland Government
Natural Resources, Mines and Water
Australian Government
Geoscience Australia
Griffith University
CRC for Coastal Zone
Estuary & Waterway Management

# Numerical hydrodynamic modelling of the Fitzroy Estuary

M. Herzfeld, J. R. Andrewartha, P. Sakov and I. Webster

**March 2006**

CRC for Coastal Zone
Estuary & Waterway Management

Numerical hydrodynamic modelling of the Fitzroy Estuary



Written by:

Michael Herzfeld
John Andrewartha
Pavel Sakov
Ian Webster

Published by the Cooperative Research Centre for Coastal Zone, Estuary and Waterway Management (Coastal CRC)

Indooroopilly Sciences Centre
80 Meiers Road
Indooroopilly Qld 4068
Australia

www.coastal.crc.org.au



National Library of Australia Cataloguing-in-Publication data

Numerical hydrodynamic modelling of the Fitzroy Estuary

QNRM06318

ISBN 1 921017 58 9 (print and online)

# Table of contents

# Executive summary

A numerical hydrodynamic model was developed for the Fitzroy Estuary/Keppel Bay region in order to investigate the circulation, flushing and connectivity of the region. The model also served as the driver for biogeochemical and sediment transport models which were coupled to the hydrodynamic model. The model was forced with measured meteorological fields at the sea surface (wind, pressure and temperature), river discharge at the barrage and sea surface elevation, temperature and salinity at the offshore boundary. The offshore boundary forcing was obtained using a nesting strategy involving a larger-scale regional model.

The model output was compared to measured temperature and salinity data which was collected during two field exercises in the wet (February 2005) and dry (August 2004) seasons. Sea-level comparisons were also made with data measured at Port Alma. Various model parameters and processes were optimised to achieve the best comparison between measured and modelled data. This optimisation process provided insight into which parameters and processes the model was sensitive to. Simulations using the model were performed for the period March 2004 to March 2005, providing output of currents, sea level and temperature and salinity distributions.

The results from the model confirmed that the Fitzroy Estuary/Keppel Bay region is tidally dominated. Two tides occur each day and the tidal range approaches 5 m at times. This produces large currents, particularly in the vicinity of the Fitzroy mouth where current speeds may approach 2 $ms^{-1}$. Currents are directed up the estuary and tidal creeks on the flood tide, and down the estuary on the ebb tide. The tidal range undergoes a cycle of approximately 14 days, with maximum ranges of ~5 m (spring tide) and minimum of ~1 m (neap tides) during this cycle.

The large currents mix the water from the surface to the bottom, resulting in negligible gradients of temperature or salinity, except when the Fitzroy is in flood when a freshwater layer at the sea surface is present. These wet season floods effectively flush the estuary and lower salinity in Keppel Bay. After the floods the salinity in the estuary slowly increases back to marine levels over a time scale of 6–8 months.

The average, or long-term, currents in the estuary and Keppel Bay are small despite the large tidal currents. The long-term flow is a complex balance between sources of momentum at the surface (wind), sinks at the sea bed

(bottom drag) and redistribution via momentum advection. Average flow is generally directed down-estuary, becoming stronger in the wet season due to the influence of the flood water, and out of Keppel Bay along the western side of Curtis Island. There appears to be little seasonal variation in the average circulation.

Flushing times for various areas of the estuary and Keppel Bay vary according to location and time of the year. The Fitzroy Estuary is basically poorly flushed during the dry season, with flushing times generally of several months. The impact of flood waters during the wet is to flush the system very effectively in a matter of days, and these floods are predominantly responsible for annually renewing water in the estuary.

The model was able to predict concentrations of a hypothetical tracer continuously released into the estuary or Keppel Bay at specific sites. Particle tracking was also performed using these release sites. These activities revealed that the Fitzroy Estuary/Keppel Bay system is relatively poorly connected as a whole. The upper estuary and tidal creeks exchange little water with Keppel Bay on an annual basis. The upper reaches of Casuarina Creek exhibit the most limited exchange with Keppel Bay. Trajectories of particles indicated that tidal excursions are up to 15 km in Keppel Bay during spring tides, and ~10 km during neap tides.

A simple conceptual overview of the system is one where there are basically three independent systems in existence in the region. Firstly, Keppel Bay appears well connected to regions further offshore, which exchange water readily with the bay. The bay does not readily exchange water with the estuary or tidal creeks, with water transport only influencing the lower reaches of these systems. Secondly, the Fitzroy Estuary is almost de-coupled from Keppel Bay during the dry season, with limited exchange occurring due to the slow propagation of the salty water up-estuary. During the wet season the floods effectively flush the estuary, emptying water into Keppel Bay where subsequent exchanges with offshore water eventually renew the water in the system. Thirdly, the tidal creeks are also poorly coupled to Keppel Bay during the dry (exchange being restricted to the lower reaches of the creeks), and have only limited benefit from large freshwater flows during the wet to assist in flushing. The further east from the Fitzroy these creeks reside, the less impact the wet season floods appear to have.

# 1 Background

The Fitzroy Estuary and Keppel Bay region (Figure 1.1) is situated at the transition between the tropics and subtropics in Central Queensland on the eastern coast of Australia. The Fitzroy basin is a large agricultural and coal mining catchment with an extensive wetland delta and estuarine area that is a major fisheries habitat for central Queensland. Significant loads of sediment, nutrients and unknown amounts of pesticides move through the Fitzroy Estuary and offshore during summer flow events.

The Fitzroy catchment has interconnected estuarine zones with potential impacts on National Estate–listed wetlands, significant habitats for wading birds, dugong, dolphin and marine turtles and the southern lagoon of the Great Barrier Reef. Elevated sediment delivery, nutrient levels, and concentrations of the pesticide diuron originating from the Fitzroy have been identified as possible major issues for the Great Barrier Reef. With major water infrastructure development planned for the Fitzroy, there is an urgent need to relate flows and loads resulting from water and land uses in the catchments to potential impacts on the estuarine system and contiguous coastal zones including the Great Barrier Reef.

The Fitzroy Estuary/Keppel Bay is a macrotidal estuary with large barotropic tides having ranges up to 5 m. Tides undergo a neap–spring cycle over a period of approximately 14 days, with ranges at the spring of ~5 m and about 1 m during the neap. Maximum currents during the spring phase may be as large as 2 $ms^{-1}$ in the mouth of the estuary. The large tides ensure that the water column is vertically well mixed most of the time, and are also responsible for significant resuspension of fine sediment. Combined with very large deposits of silt from the hinterland in times of flood, the estuary maintains a highly turbid character. The region is characterised by extensive areas of tidal flats that become exposed at low tide and large areas of mangroves fringing the estuary which behave as a storage buffer for water at high tide. These mangroves and tidal flats have ecological significance, being home to numerous aquatic fauna and flora.

The combination of anthropogenic pressure, the presence of natural habitats and the community desire to appreciate the natural and recreational benefits of the region while sustaining agricultural demands in the catchment, make the management of the Fitzroy Estuary a challenge. The Fitzroy Contaminants project aims to provide support for the assessment of the impacts of various developments and management approaches.

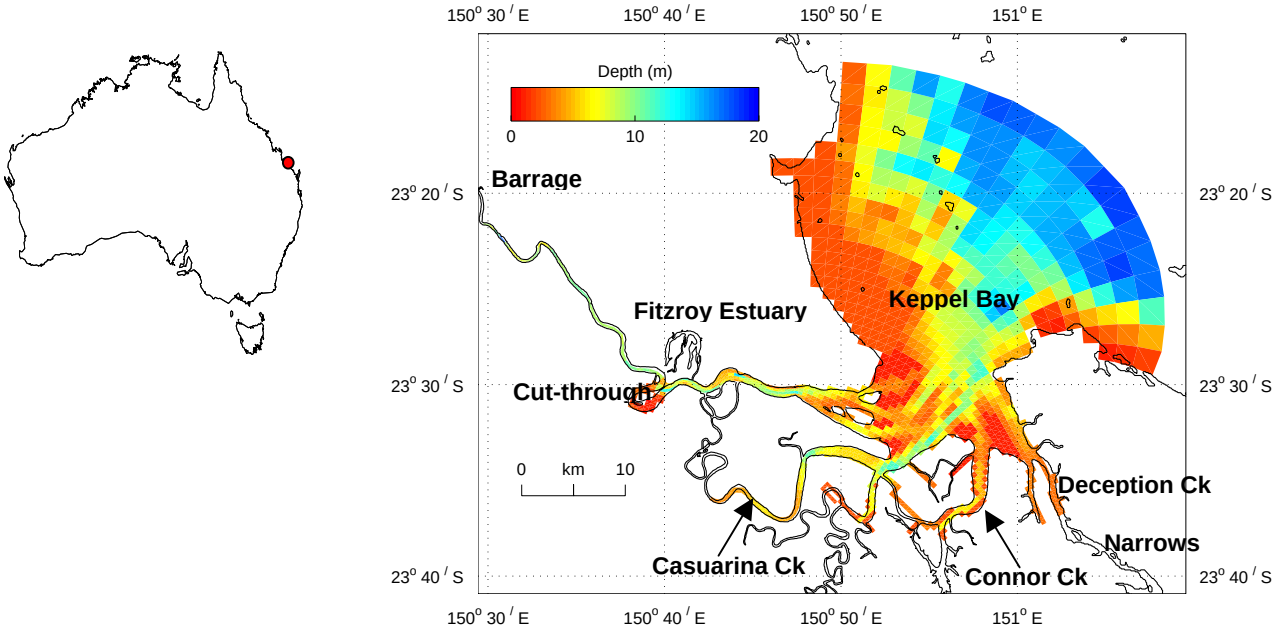


**Figure 1.1: Fitzroy Estuary/Keppel Bay Region**

# 2 Objectives

In order to assess the physical characteristics of the Fitzroy Estuary this study aims to implement a numerical hydrodynamic model that will provide predictive capacity for currents and mixing within the Fitzroy Estuary/Keppel Bay region. The model is calibrated against data collected during field excursions representative of wet and dry season conditions in the region. Insight into exchange mechanisms of the estuary with Keppel Bay, flushing times, tracer dispersal distributions and residual flows can be gained from application of the model. The model is designed to ultimately aid management decisions relating to contaminant management, and forms the basis for sediment transport and biogeochemical numerical investigations.

The model was forced with river flow, wind stress and surface elevation, temperature and salinity on the offshore limits of the domain. A regional scale hydrodynamic model which extends into the Great Barrier Reef lagoon and several hundred kilometres north and south is developed as part of this activity and used to establish boundary conditions for the coastal model. This model is represented with much larger resolution (~2 km throughout) and covers a larger area, having the sole purpose of providing boundary conditions for the coastal model.

The hydrodynamic model, its inputs, and model output are discussed in more detail below. Analyses are presented addressing the flushing characteristics of the Fitzroy Estuary, passive tracer distributions in response to the circulation, residual flow dynamics and connectivity. Limitations of the model, suggested further efforts required to improve confidence in model solutions, and data requirements to facilitate these improvements are also discussed.

# 3 The hydrodynamic model

The hydrodynamic model used to simulate the flow and mixing of Keppel Bay region is SHOC (Sparse Hydrodynamic Ocean Code; Herzfeld, 2005). This model has been developed by the Environmental Modelling group at CSIRO (Commonwealth Scientific and Industrial Research Organisation) Division of Marine Research over the last decade. SHOC is intended to be a general-purpose model applicable to scales ranging from estuaries to regional ocean domains, and has been successfully applied to a variety of applications encompassing these scales to date. SHOC is a three-dimensional finite difference hydrodynamic model based on the primitive equations. Outputs from the model include three-dimensional distributions of velocity, temperature, salinity, density, passive tracers, mixing coefficients and sea level. The equations forming the basis of the model are similar to those described by Blumberg and Herring (1987).

SHOC is based on the MECO model (Model for Estuaries and Coastal Oceans; Walker & Waring, 1998) with added functionality to allow distributed processing over multiple computing processors. SHOC also employs a sparse coordinate system internally that allows the representation of unused land in the model to be excluded. Inputs required by the model include forcing due to wind, atmospheric pressure gradients, surface heat and water fluxes and open boundary conditions (e.g. tides). A schematic of the major forcing mechanisms captured by SHOC is included as Figure 3.1. SHOC is based on the three-dimensional equations of momentum, continuity and conservation of heat and salt, employing the hydrostatic and Boussinesq assumptions. The equations of motion are discretised on a finite-difference stencil corresponding to the Arakawa C grid.

The model uses a curvilinear orthogonal grid in the horizontal and a choice of fixed ‘z’ coordinates or terrain following $\sigma$ coordinates in the vertical. The curvilinear horizontal grid was particularly useful in this application since it enabled high resolution to be specified in areas of the study region where small scale motions were present, and larger resolution where they were not. The ‘z’ vertical system allows for wetting and drying of surface cells, useful for modelling regions such as tidal flats where large areas are periodically dry. This is likely to be important in the Fitzroy Estuary which has a large tidal range and extensive drying areas. SHOC has a free surface and uses mode splitting to separate the two-dimensional (2D) mode from the three-dimensional (3D) mode. This allows fast moving gravity waves to be solved independently from the slower moving internal waves allowing the 2D and 3D modes to operate on different time steps,

resulting in a considerable improvement in computational efficiency. The model uses explicit time-stepping throughout except for the vertical diffusion scheme which is implicit. The implicit scheme guarantees unconditional stability in regions of high vertical resolution. A Laplacian diffusion scheme is employed in the horizontal on geopotential surfaces. Smagorinsky mixing coefficients may be utilised in the horizontal.

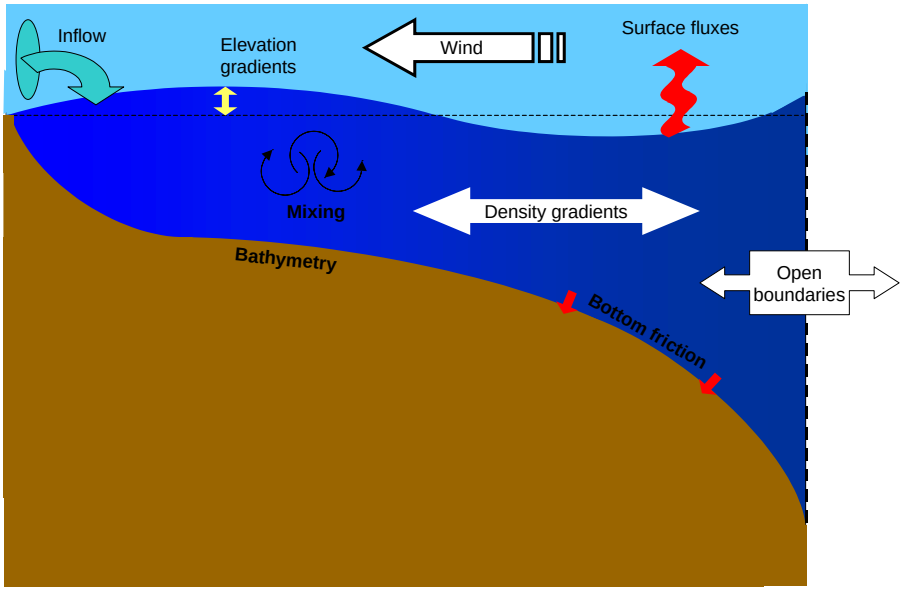


**Figure 3.1: Schematic of forcing mechanisms in SHOC**

SHOC can invoke several turbulence closure schemes, including k-ε, Mellor-Yamada 2.0 and Csanady type parameterisations. A variety of advection schemes may be used on tracers and first or second order can be used for momentum. This study used the QUICKEST advection scheme for tracers (Leonard, 1979) in conjunction with the ULTIMATE limiter (Leonard, 1991). This scheme is characterised by very low numerical diffusion and dispersion, and yielded excellent performance when resolving frontal features, which often occurred during tracer analyses.

SHOC also contains a suite of radiation, extrapolation, sponge and direct data forcing open boundary conditions. Input and output is handled through netCDF data formatted files, with the option of submitting ascii text files for simple time-series forcing. The netCDF format allows input of spatially and temporally varying forcing and initialisation data in a grid and time-step independent manner. SHOC is capable of performing particle tracking and may be directly coupled to ecological and sediment transport models.

# 4 Model domain

The simulation of the physics of the Fitzroy Estuary/Keppel Bay region required the construction of three model grids. A large scale ‘super’ grid was developed to generate tidal harmonics suitable for forcing a regional-scale grid. The regional grid supplied the initial and open boundary conditions for a smaller grid of the local study region, nested within the regional grid. In the absence of field-derived temperature, salinity and surface elevation measurements to apply to the open boundaries, this strategy is the only way of adequately driving the model through the open boundaries. The domain nesting is illustrated in Figure 4.1, the regional domain in Figure 4.2 and Fitzroy Estuary/Keppel Bay (local) domain in Figure 4.3.

The super grid was required to be executed in two-dimensional depth-averaged mode only, as the goal was to reproduce the sea level on the boundary of the regional grid. The super grid was used with a rectilinear grid of resolution 4.4 km. The regional rectilinear grid has a resolution of 2.2 km and 22 layers in the vertical with 3 m resolution at the surface and 80 m resolution near the maximum depth of 600 m. River flows representing the Fitzroy and Calliope Rivers are included, and south Keppel Bay is connected to Port Curtis estuary via The Narrows, which has approximately the same cross-sectional area as the real geography but is wider and shallower in the model owing to the discretisation used.

A curvilinear grid was used to model the Fitzroy region where high resolution is achieved in the estuary and tidal creeks, with coarser resolution near the offshore boundary. The lower estuary is resolved in three dimensions, while above the cut-through the river is resolved in two dimensions (laterally averaged). This is desirable so that very fine cross-river resolution does not adversely compromise the time step used, hence delivering unacceptable run time ratios. The grid spacing varied from ~200 m cross-river in the lower estuary and tidal creeks to ~2 km at the seaward boundary. The along-river resolution above the cut through varies from ~1 km to 250 m. There are 16 layers in the vertical with 0.5 m resolution at the surface and 2 m resolution near the maximum depth of 18 m. This domain consists of mostly land cells, with 17% of the surface layer comprising wet cells and 9% of the 3D domain being wet.

The run-time ratio of the model is approximately 180:1 (i.e. the model simulates 180 days of results in one day of real time). This is determined by the stability constraints on the model which limit the maximum time step to be used for 2D and 3D modes. These constraints are in turn dependent on the grid resolution, the water depth, stratification and the size of the grid. Considerable effort was

invested into optimising these time steps so as to achieve the largest run-time ratio possible. The model speed is quite fast, allowing a year-long simulation to be completed in around two days of real time.

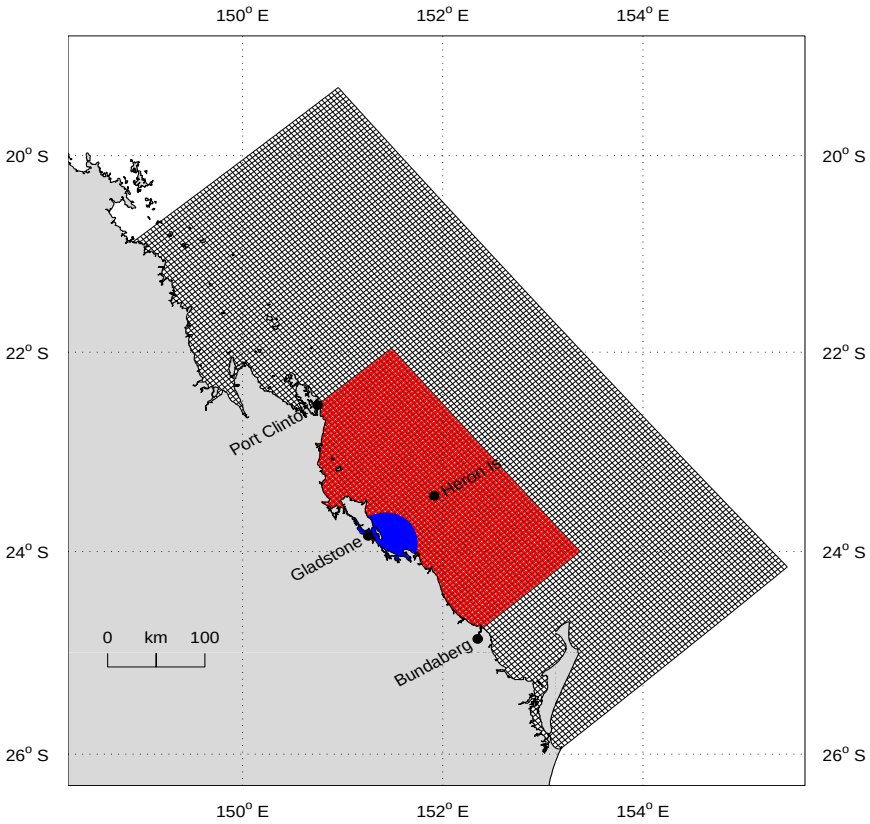


**Figure 4.1: Nested domain consisting of super grid (black), regional grid (red) and local grid (blue)**

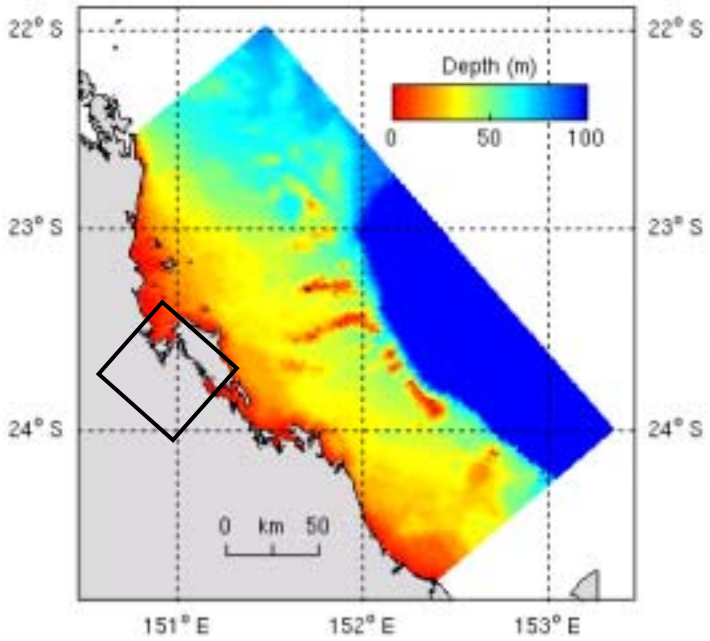


**Figure 4.2: Regional domain**

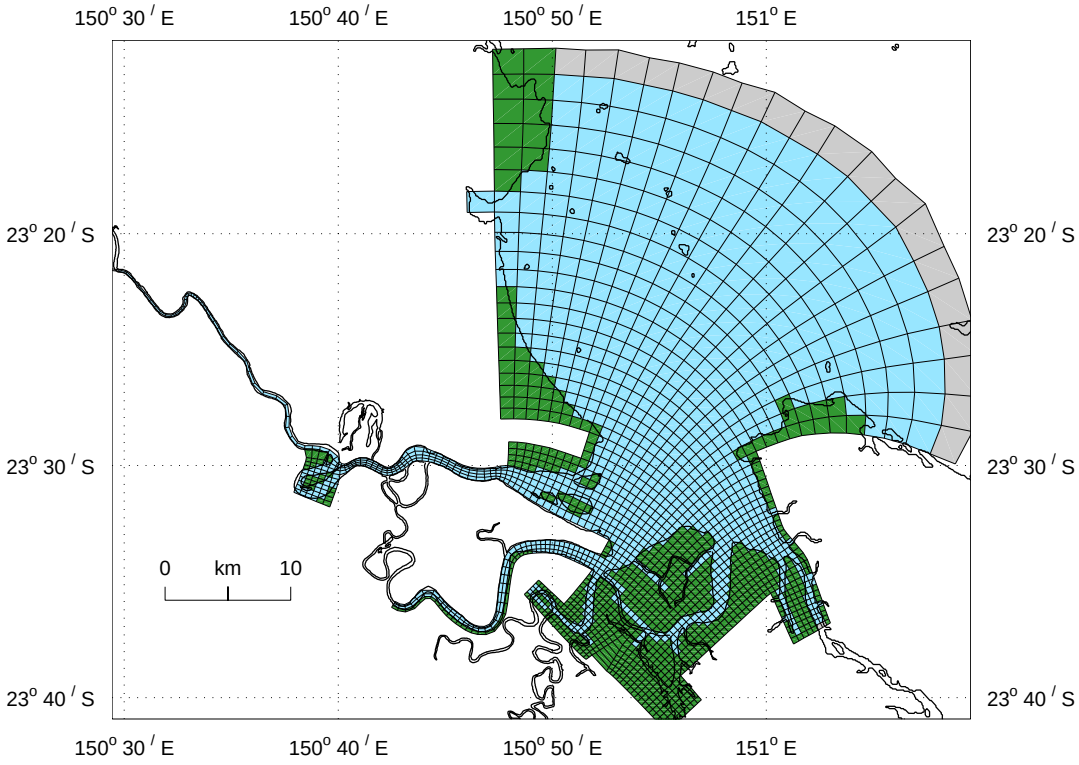


**Figure 4.3: Fitzroy/Keppel Bay domain with the discretised grid superimposed**

# 5 Input data

The model was forced with wind, river flow from the Fitzroy River and elevation, temperature and salinity on the oceanic open boundary. The regional grid was also forced with river flow from the Calliope River which was connected to the local domain via The Narrows. The model simulation period was chosen as 1 March 2004 to 28 February 2005 inclusive, providing 12 months of simulation. All data are collected to span this period. The sources of the forcing data are detailed below.

## 5.1 Wind forcing

Wind speed and direction data were obtained from the Bureau of Meteorology at the locations depicted in Figure 5.1.1 and interpolated onto the regional and Fitzroy domains to provide a temporally and spatially varying wind-field.

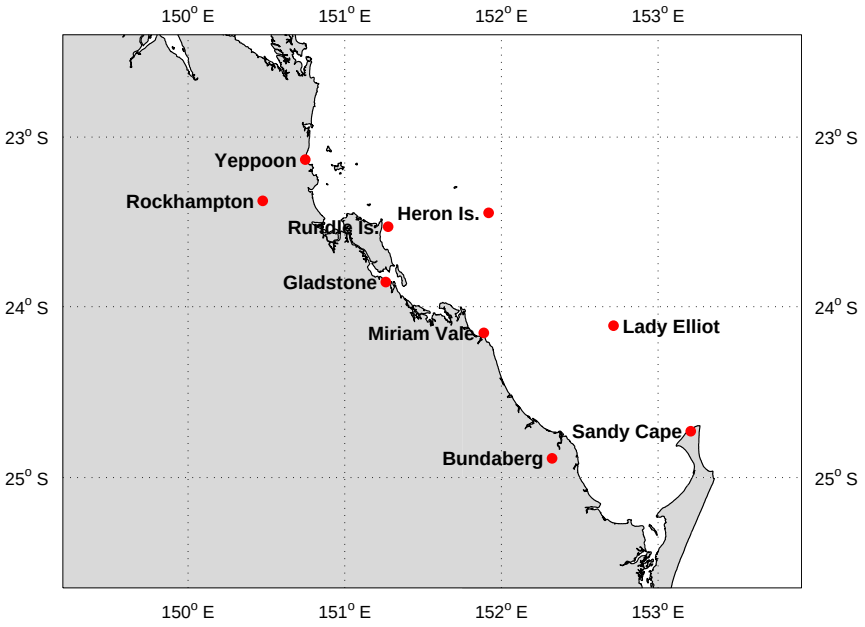


**Figure 5.1.1: Wind measurement sites**

A sample of the wind-field at selected sites is shown in Figure 5.1.2 (a) and (b) for a subsample of the simulation period. The mean wind speed and direction during the whole period is shown in Table 5.1.1.

**Table 5.1.1: Mean wind speed and direction for wind measurement sites**

| Site | Annual mean wind speed ($ms^{-1}$) | Annual mean wind direction ($^oT$) |
|---|---|---|
| Gladstone | 5.2 | 122 |
| Miriam Vale | 5.2 | 142 |
| Heron Island | 6.8 | 106 |
| Lady Elliot Island | 5.9 | 144 |
| Sandy Cape | 6.3 | 182 |
| Yeppoon | 5.1 | 124 |
| Rockhampton | 3.8 | 112 |
| Bundaberg | 4.9 | 128 |
| Rundle Island | 8.3 | 133 |
| Mean | 5.7 | 132 |

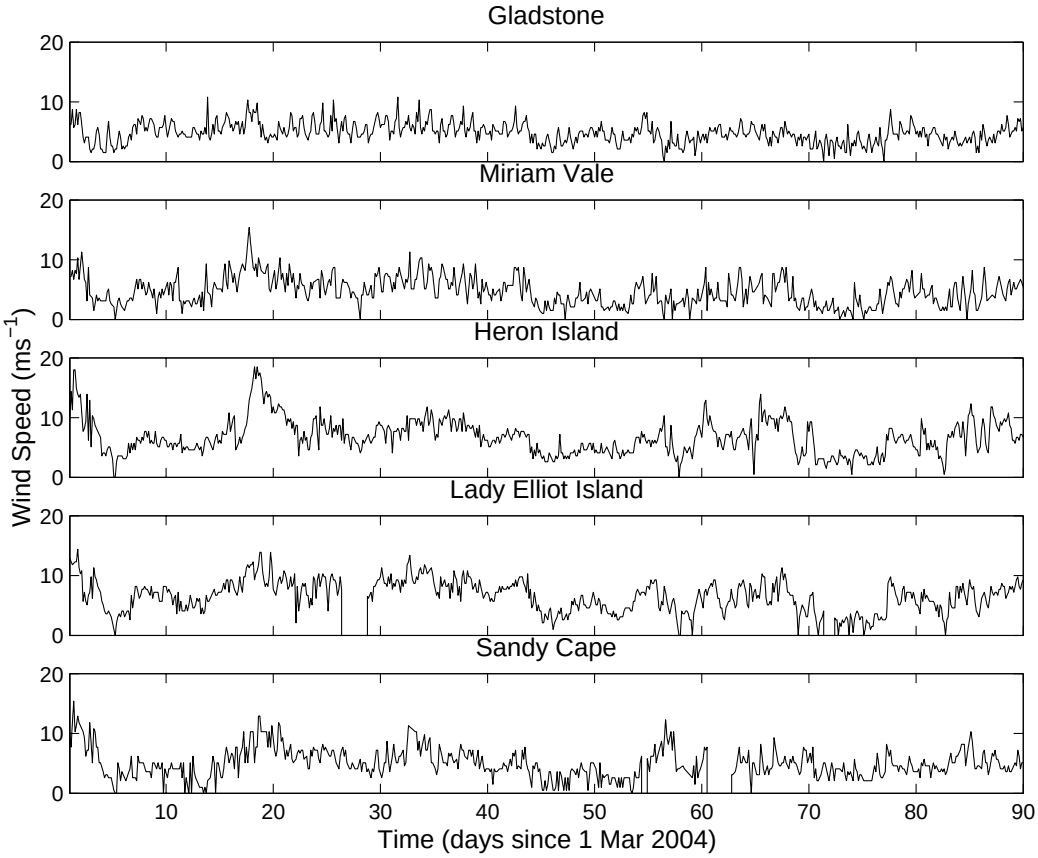


**Figure 5.1.2 (a): Wind speed at measurement sites**

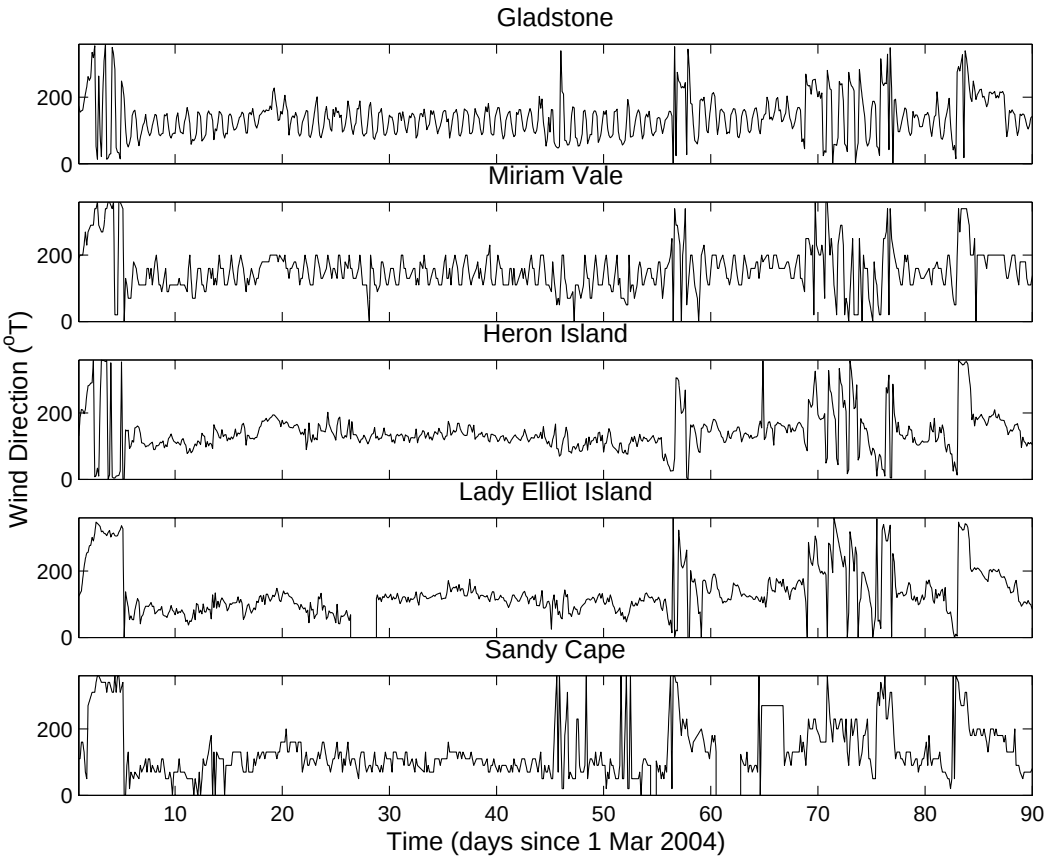


**Figure 5.1.2 (b): Wind direction at measurement sites**

Figure 5.1.2(a,b) and Table 5.1.1 indicate that for the simulation period the mean wind in the Fitzroy region was a relatively light (~6 $ms^{-1}$) south-easterly. Wind speed is generally below 10 $ms^{-1}$, with the offshore island sites experiencing higher wind-speed. A diurnal oscillation, particularly for the Gladstone and Miriam Vale sites, is evident, suggesting sea-breeze activity may be present in this region.

## 5.2 Surface elevation

The time series of surface elevation prescribed on the open boundaries of the Fitzroy domain were supplied from output of the regional model. The elevations used in the regional model consist of a high frequency component (tidal component with periods <1 day) and a low frequency component with periods of days to weeks. The tidal component applicable to the regional domain was derived from output of the super grid, which in turn was forced only on the open boundaries with tides constructed from a global tidal model (Eanes & Bettadpur, 1995).

Tidal records were obtained at hourly intervals over a variety of locations (courtesy of National Tidal Facility and Queensland Department of Transport) shown in Figure 5.2.1. Since the phase and amplitude of the tide are variable over the study region, these data do not possess adequate spatial resolution to construct an accurate tidal forcing of the regional open boundaries; hence the use of the global tide model which is capable of supplying tidal data at arbitrary resolution. However, the measured data are useful for calibrating the tide, and the Burnett Heads data were used for extracting the low frequency variations (e.g. coastally trapped waves and storm surges) with which the southern boundary of the regional model was forced.

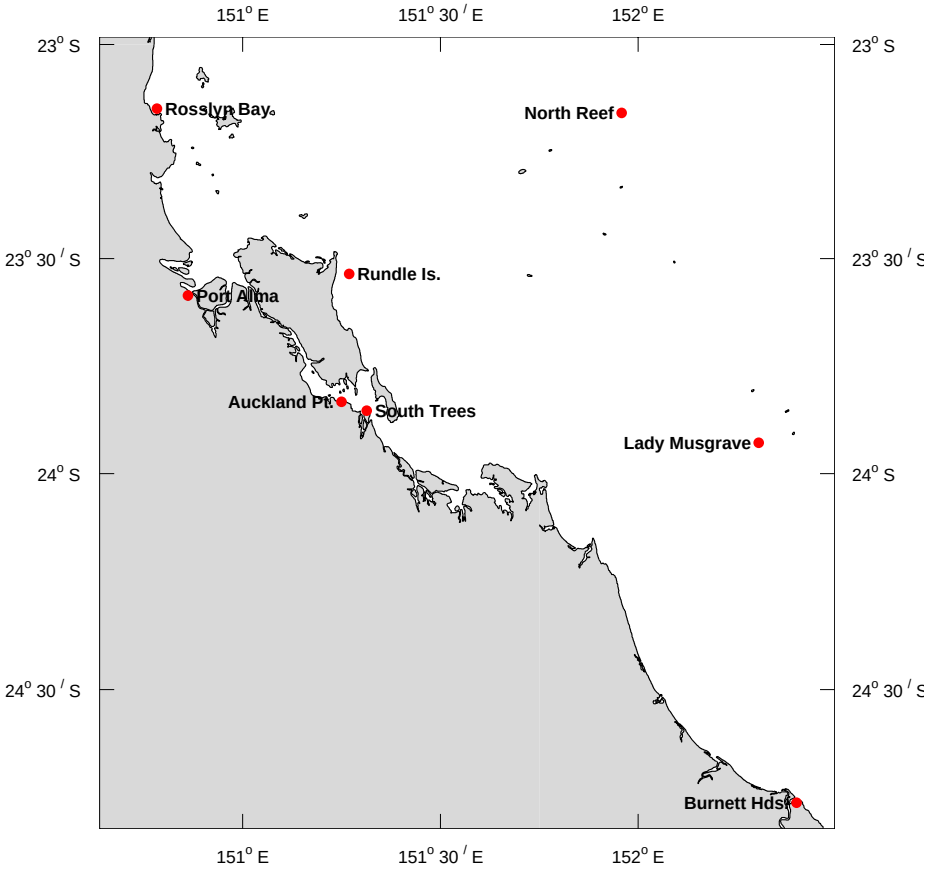


**Figure 5.2.1: Tidal observation locations**

Using the global tide model directly to force the open boundaries of the regional model resulted in poor performance in the vicinity of the northern and southern cross-shelf boundaries. This is due to the global tide model's tendency to supply inaccurate constituents near the coast, and reflection and overspecification problems with the cross-shelf open boundary conditions themselves. Further away from the cross-shelf boundaries, the model performed adequately,

suggesting that it is the offshore open boundary that is predominantly responsible for driving the tide in the domain interior.

This scenario prompted the use of the super grid, whose cross-shelf open boundaries were distant enough from the zones encompassing the regional model's open boundaries to provide accurate elevations in these areas. The super grid was run in 2-dimensional mode only for the year 1999 to provide time series of surface elevation on the regional grid's open boundaries. These time series were then decomposed into the tidal constituents, which were subsequently used to force the tidal component in the regional model over any given time period. Note that the role of the super grid is to obtain accurate sea level from tidal forcing only, and low frequency sea level changes were not included in this model.

This nesting approach provided better results than directly imposing the global tidal model tidal constituents on the regional model's boundaries. Comparison of sea level output at Burnett Heads from the super grid model and global tide model with observation (with low frequency component removed) is presented in Figure 5.2.2. The nesting procedure resulted in minimal reflection and smooth velocity distributions (i.e. lacking in eddies, recirculation and excessive speed or shear) across the boundary.

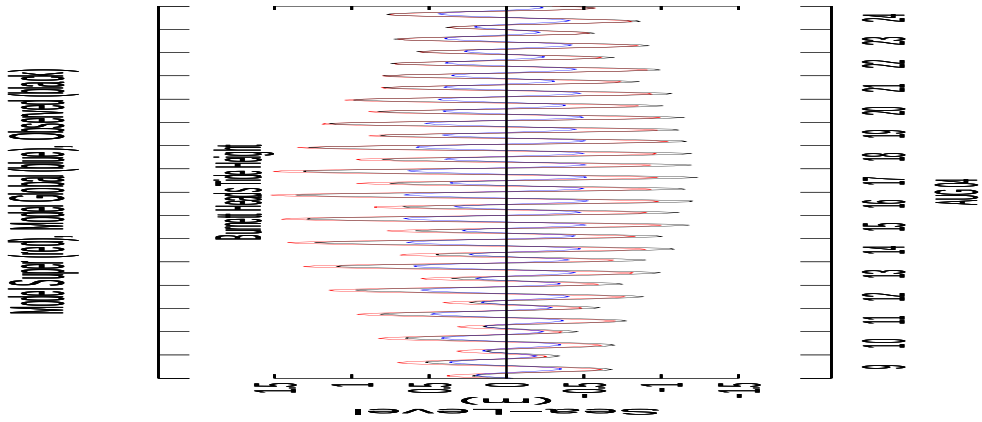


**Figure 5.2.2: Elevation from 'super' grid and global tide model: comparison to observation**

The major tidal constituents and their amplitudes derived from the super grid, at the boundary locations illustrated in Figure 5.2.3, are presented in Table 5.2.1. Note that these constituents' amplitude and phase vary spatially around the open boundary perimeter.

**Table 5.2.1: Tidal harmonics for the regional model**

| Tidal constituent name | Northern boundary amplitude (m) | Offshore boundary amplitude (m) | Southern boundary amplitude (m) |
|---|---|---|---|
| M2 | 1.230 | 0.684 | 0.891 |
| S2 | 0.449 | 0.241 | 0.306 |
| K1 | 0.322 | 0.242 | 0.233 |
| O1 | 0.153 | 0.119 | 0.110 |
| S1 | 0.002 | 0.002 | 0.002 |
| Q1 | 0.034 | 0.026 | 0.023 |
| P1 | 0.103 | 0.078 | 0.076 |
| N2 | 0.258 | 0.151 | 0.188 |
| NU2 | 0.055 | 0.029 | 0.037 |
| K2 | 0.126 | 0.065 | 0.081 |
| L2 | 0.044 | 0.019 | 0.023 |
| 2N2 | 0.046 | 0.024 | 0.027 |
| MU2 | 0.013 | 0.023 | 0.027 |
| T2 | 0.026 | 0.014 | 0.018 |

Table 5.2.1 shows that the dominant constituents in the region are those due to M2 and S2, hence the tide possesses a semi-diurnal character. It is also noted that the amplitude of these constituents is quite large. The semi-diurnal constituent N2 is also quite large. Of the diurnal constituents K1 and O1 dominate.

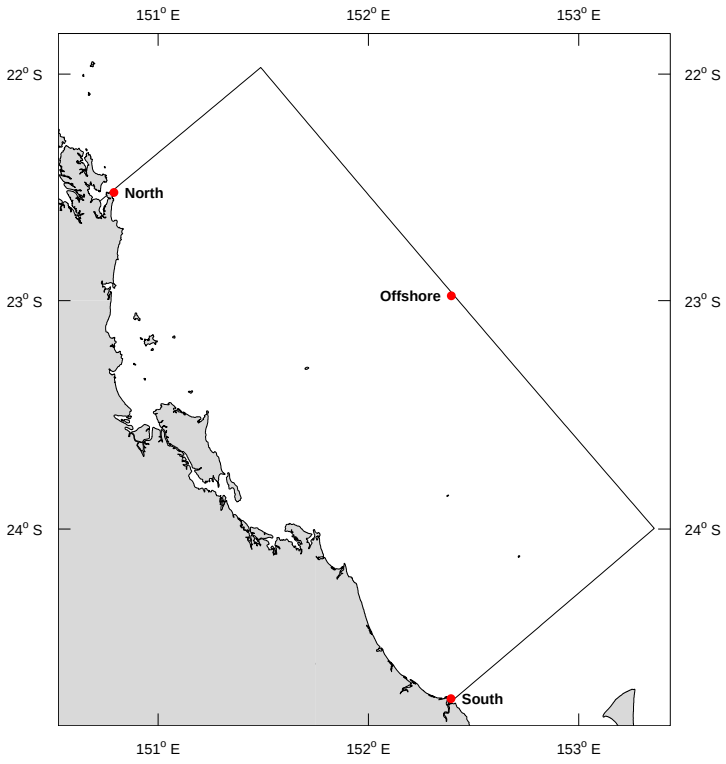


**Figure 5.2.3: Locations of tidal constituents shown in Table 5.2.2**

The long-period component was extracted from the low-passed Burnett Heads record observations (Figure 5.2.4), which is located on the southern boundary of the regional domain. The tidal component outlined above was then superimposed and the resulting sea level was applied on the southern boundary of the regional domain.

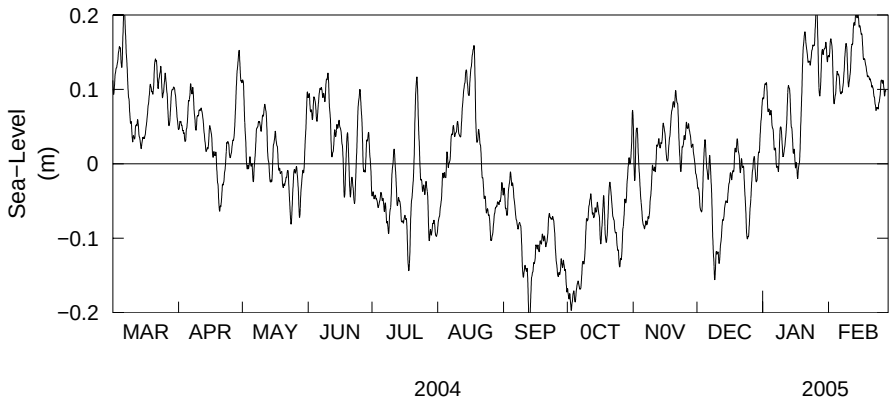


**Figure 5.2.4: Low frequency sea level at Burnett Heads**

The long-period component at Burnett Heads is applicable to the coast only, and an offshore profile was imposed on the amplitude to correctly specify the long-period wave over the shelf. The offshore extent of this wave was treated as a calibratable parameter which was tuned to provide the best match of modelled sea level to observation at Rosslyn Bay (the nearest location to the Fitzroy model offshore open boundary possessing a tide gauge). Modelled surface elevations from the regional model are compared to those measured at Rosslyn Bay in Figure 5.2.5, from which it is observed that agreement is good, that is, the model reproduces sea level well in the Fitzroy region.

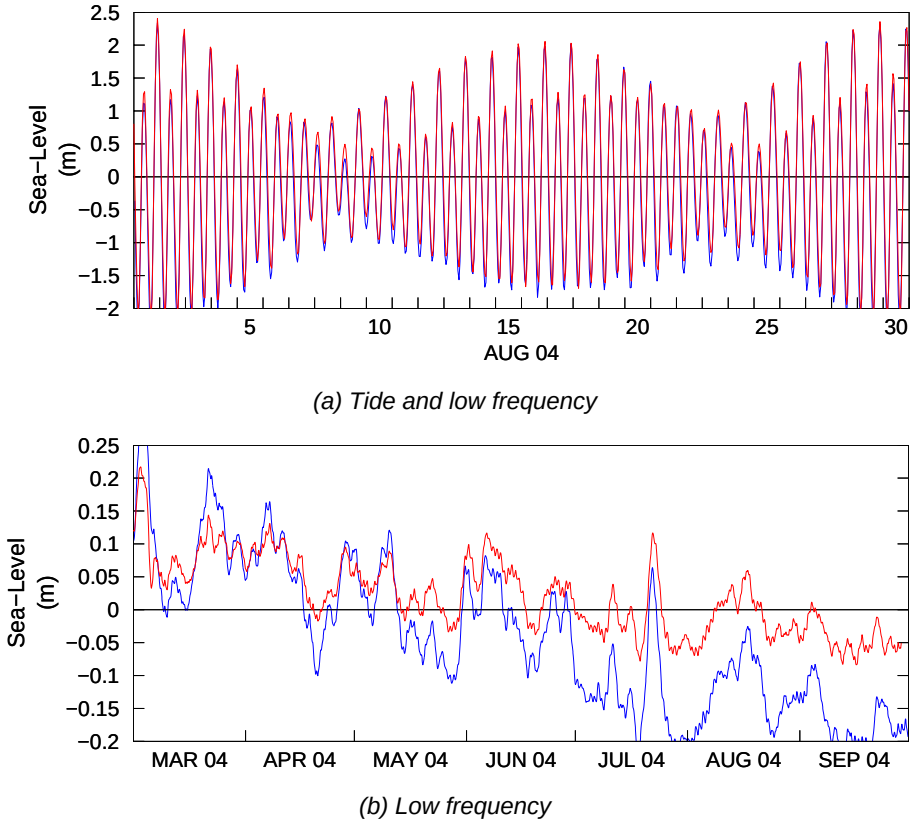


*(a) Tide and low frequency*

*(b) Low frequency*

**Figure 5.2.5: Segment of surface elevation at Rosslyn Bay from the regional model: measured (blue) and modelled (regional model, red)**

Elevations on the offshore open boundary of the Fitzroy domain were subsequently forced with output of the regional domain. Obviously these elevation signals contained both the diurnal and long-period fluctuations.

## 5.3 Temperature and salinity

The temperature and salinity (T/S) distributions used as initial conditions in the Fitzroy model were initialised to 20$^{o}$C and 36 psu respectively. The temperature solution in the local model was found to be dominated by local atmospheric exchanges (Section 6.3), and attained equilibrium with the atmospheric fluxes relatively quickly (~2 weeks), hence the choice of initial condition was not critical. Similarly, the open boundary conditions used proved relatively non-critical due to the atmospheric dominance. The salinity solution was similarly quite insensitive to the initial condition, also having a rapid spin up time. This is due in part to the simulation start time capturing the tail end of the wet season where a small flood (~50m$^3$s$^{-1}$) freshened much of the estuary, rapidly wiping out the initial condition in this part of the domain. The 36 psu prescribed for the remainder of Keppel Bay is typical of wet season salinities in this region (e.g. Figure 6.2.14), therefore any

large equilibrating salinity changes were not necessary. The salinity solution did prove to be sensitive to the open boundary condition, but there were unfortunately no suitable data to force the offshore boundary.

The CARS atlas (Climatological Atlas of Regional Seas, Ridgway *et al.*, 2002) proved to be too fresh in the Keppel Bay region, having a maximum salinity of only ~35.3 psu in September, well below the ~36 psu observed in the Bay. It was envisioned that reasonably high resolution (~10 km) global circulation model output (MOM4; Modular Ocean Model, version 4) would be available to force the boundaries, but this did not eventuate. At the time of the model construction global model output was only available up to mid 2002. Therefore, although far from optimum, the regional model was forced on the open boundaries (two cross-shelf and one offshore) with CARS and the Fitzroy model was in turn forced on the offshore open boundary with output from the regional model. As expected, the salinity solutions in the Fitzroy model resulting from this boundary forcing compared poorly with observation. This problem was ultimately addressed by inversely scaling the local model open boundary salinity values (see Section 6.2).

## 5.4 River flow

River flow records were obtained for the Fitzroy River at The Gap and the Calliope River at Castlehope. The former flow was input into the regional and Fitzroy models and the latter input at Gladstone in the regional model only. The Fitzroy flow had a base flow of 0.5 $m^3s^{-1}$ added which accounted for freshwater flow entering between The Gap and the barrage. The Boyne River was omitted in the regional model due to the presence of the Awoonga Dam reducing flows to negligible levels. Daily flows are displayed for the simulation period in Figure 5.4.1 for the Fitzroy River. The temperature of the Fitzroy and Calliope Rivers was assumed to be equal to the low pass filtered air temperature at Gladstone (Figure 5.4.2) and the input flow was assumed to be fresh (0 psu). Flow for the Calliope is displayed in Figure 5.4.3.

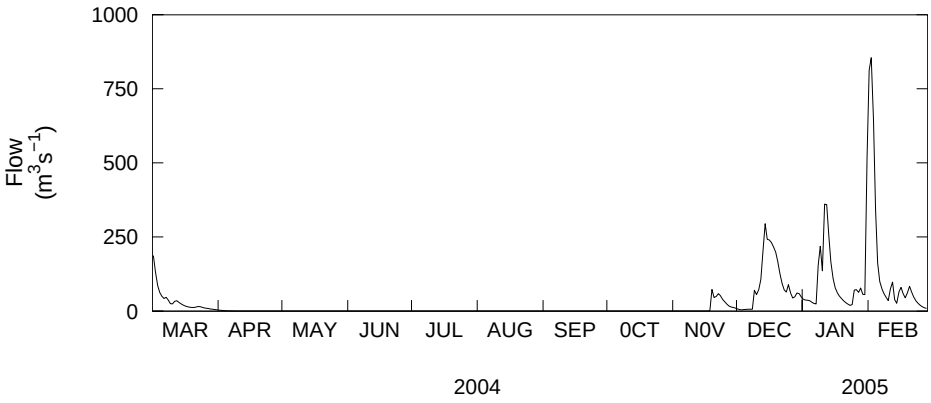


**Figure 5.4.1: Fitzroy River flow**

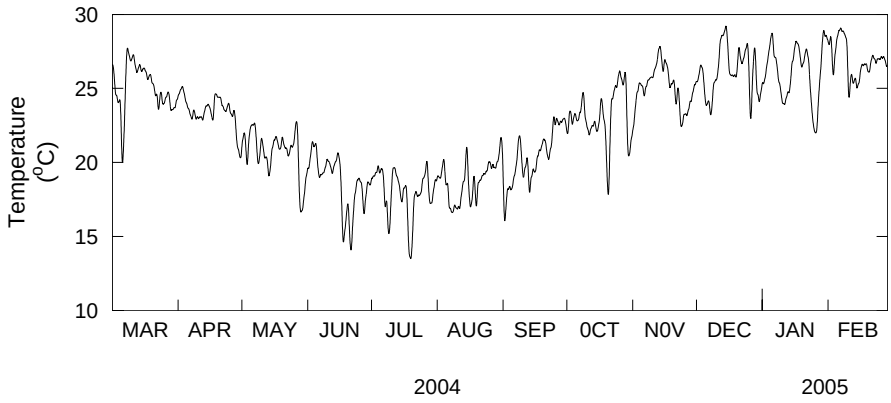


**Figure 5.4.2: Air temperature at Gladstone**

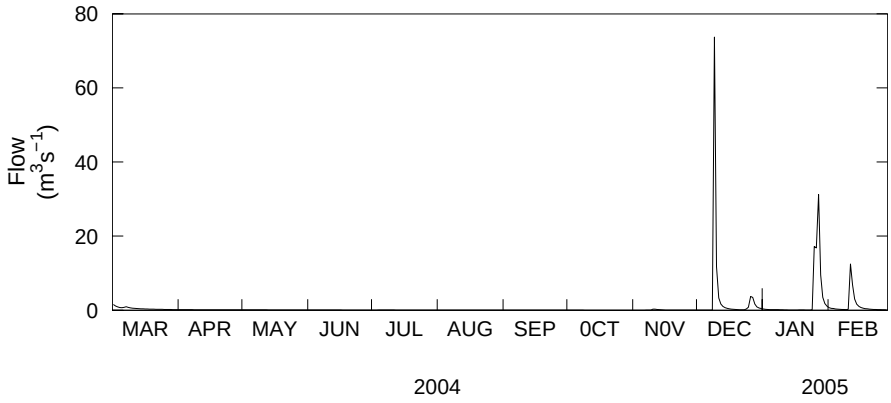


**Figure 5.4.3: Calliope River flow**

## 5.5 Heat and salt fluxes

Heat fluxes were computed from standard meteorological measurements by the methods outlined in Herzfeld (2005, Chapter 9). Short-wave radiation was estimated from the sun's hour angle at the latitude corresponding to the Fitzroy Estuary, and corrected for cloud cover. Long-wave radiation was calculated using the model sea surface temperature and measured air temperature, also correcting for cloud. Sensible and latent heat fluxes were calculated using the bulk method, requiring wet and dry bulb air temperature, pressure and wind-speed measurements as input. The heat flux components and net heat flux for the simulation period is illustrated in Figure 5.2.1. Heat fluxes are further discussed in Section 6.2.

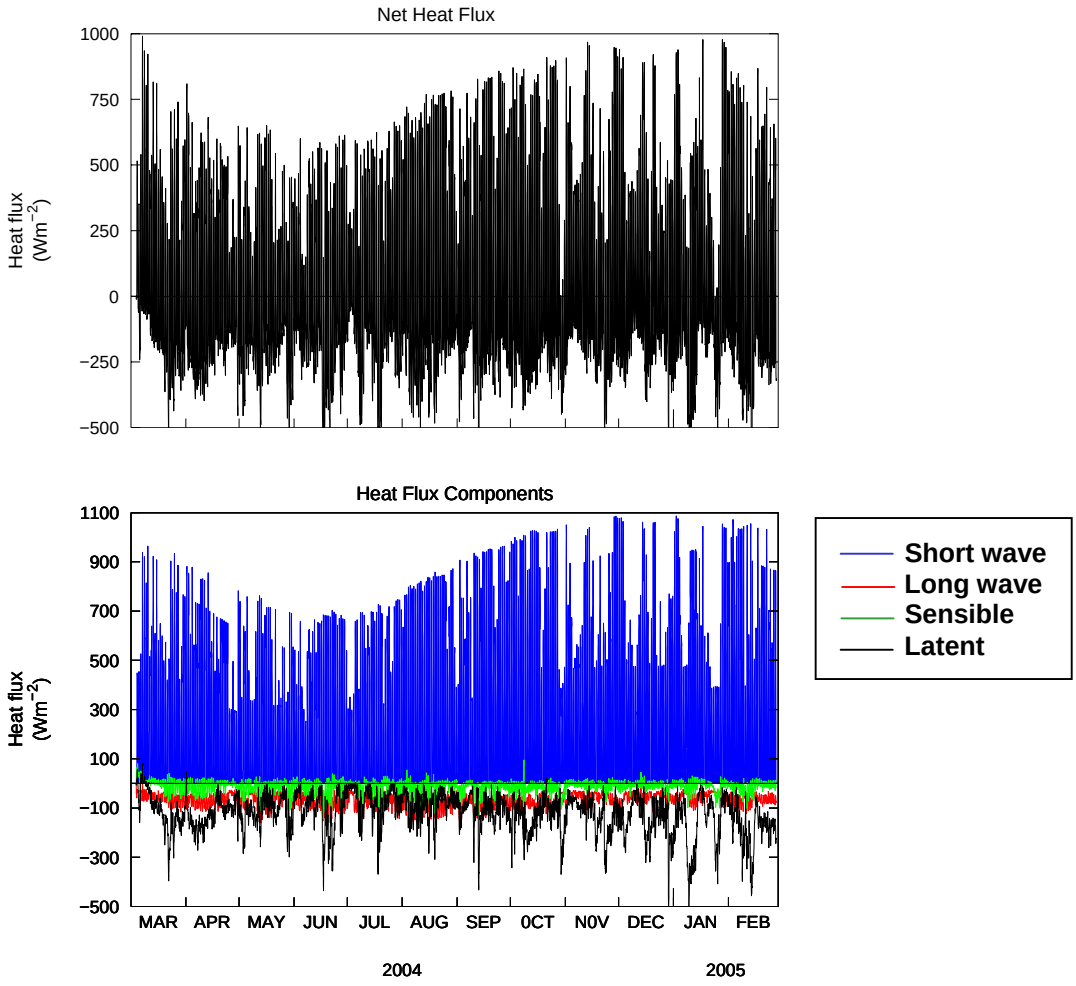


**Figure 5.5.1: Heat fluxes**

The salt flux is defined as the difference between evaporation minus precipitation. Evaporation over water is difficult to measure, and this quantity was obtained from the latent heat flux computed by the bulk method divided by the latent heat of evaporation. The precipitation used was that measured at Yeppoon, illustrated in Figure 5.5.2.

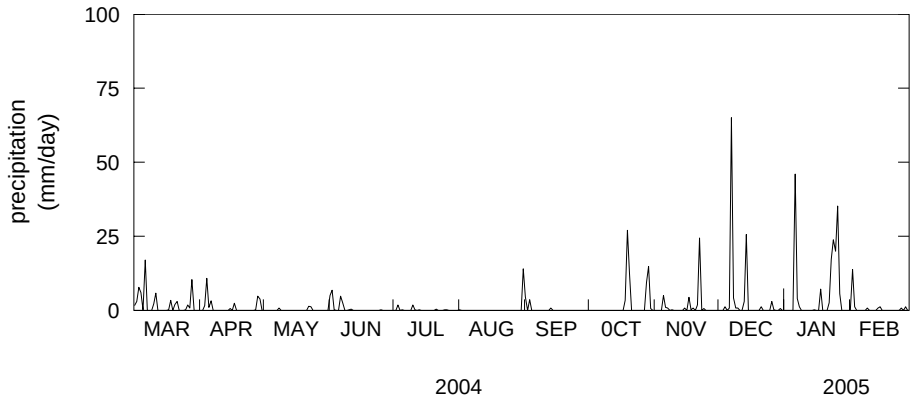


**Figure 5.5.2: Precipitation at Yeppoon**

# 6 Model output

## 6.1 Background

The Fitzroy Estuary is classified as a macrotidal, well mixed estuary. The climatic pattern at this latitude is such that there are essentially two seasons: the wet lasting from January to April and the dry from May to October. During the wet there may be vast volumes of water flowing down the Fitzroy, up to tens of thousands of cubic metres per second. These flows push marine water out of the estuary, also significantly lowering salinity in Keppel Bay and the adjoining tidal creeks. The salt wedge then slowly intrudes back into the estuary during the dry season, taking 6–8 months before again reaching the barrage and rendering the whole estuary marine. On shorter timescales a large semi-diurnal tide undergoes a neap–spring oscillation of ~14 days, with maximum ranges of ~5 m during the spring phase and ~1 m during the neap. During the spring phase the tide will wet and dry large areas of tidal flat and intertidal zones along the river. The spring tides are also responsible for the generation of large currents, which may reach ~2 $ms^{-1}$ at the Fitzroy mouth. The frictional effect of the tides on the sea bed results in a well mixed water column exhibiting little stratification.

## 6.2 Model calibration

The model was primarily calibrated against sea level, temperature and salinity. The latter two variables reflect the larger-scale circulation which is of interest in this study. Elevation calibration provides confidence that tidally driven flow is accurate, which dominates the circulation in the region. Comparisons were also made to velocity measurements obtained from ADCP, but since these measurements often reflect localised small-scale processes which may not be captured by the model, rigorous calibration to these variables was not attempted. Comparison of model output to ADCP data is presented in the sediment transport modelling study (Margvelashvili *et al*., 2006).

The modelled and measured sea level at Port Alma and Casuarina Creek is displayed in Figure 6.2.1. The low pass filtered (long-period) sea level for these two sites is displayed in Figure 6.2.2. These figures show that the model performs well in terms of sea level, capturing the semi-diurnal tidal character and neap–spring cycles.

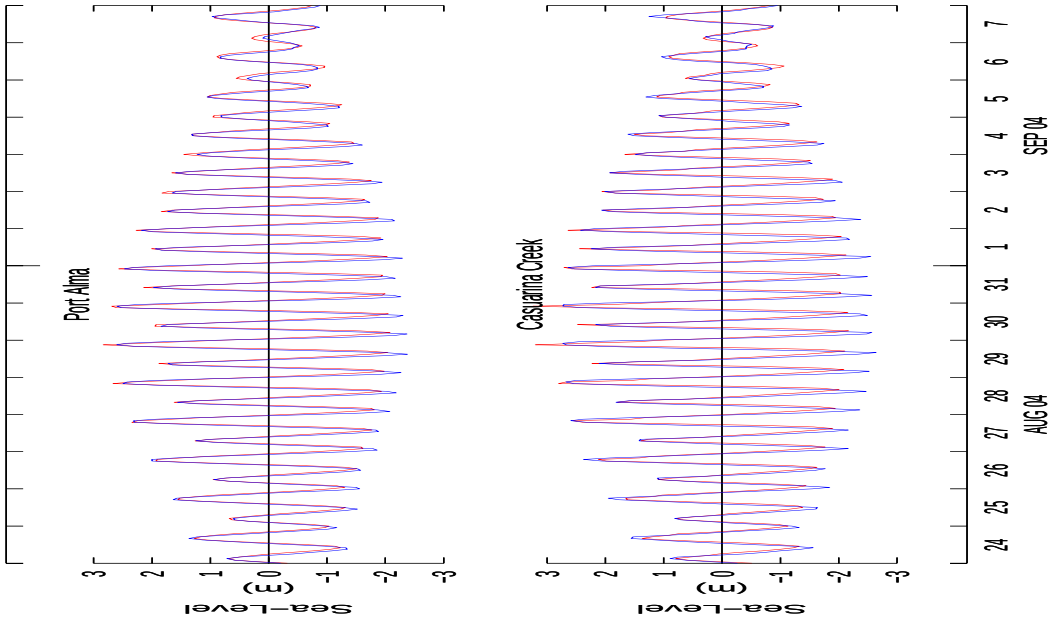


**Figure 6.2.1: Modelled and measured sea level at Port Alma and Casuarina Creek (observation = blue, model = red)**

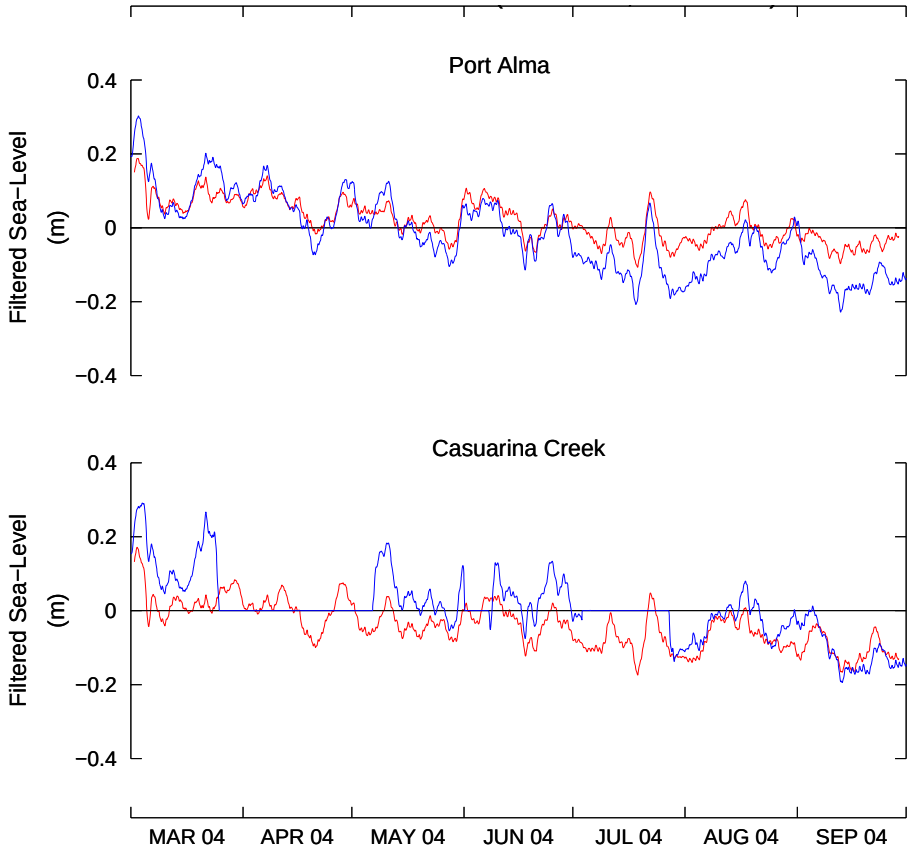


**Figure 6.2.2 : Modelled and measured sea level (observation = blue, model = red)**

The tidal signal propagating up the estuary undergoes amplification, where the amplitude near the barrage is greater than that at the mouth. This was observed in Phase 1 (Webster *et al*., 2004) and consequently the depth and width of the upper Fitzroy above the cut-through were adjusted so that the cross-sectional area matched identically to that used in the Phase 1 modelling. The tidal amplification effect in the model could not be directly verified against data since a tidal record at Lakes Creek, near the barrage, was unavailable for the simulation period. Also, the available Lakes Creek record was truncated at low tide (due to sea level receding beneath the tide gauge position), hence constituting an incomplete record from which tidal decomposition into constituents was not possible. Only a qualitative comparison is possible between measured data (July 2001) and modelled (October 2004) in order to gauge the tidal amplification effect (Figure 6.2.3).

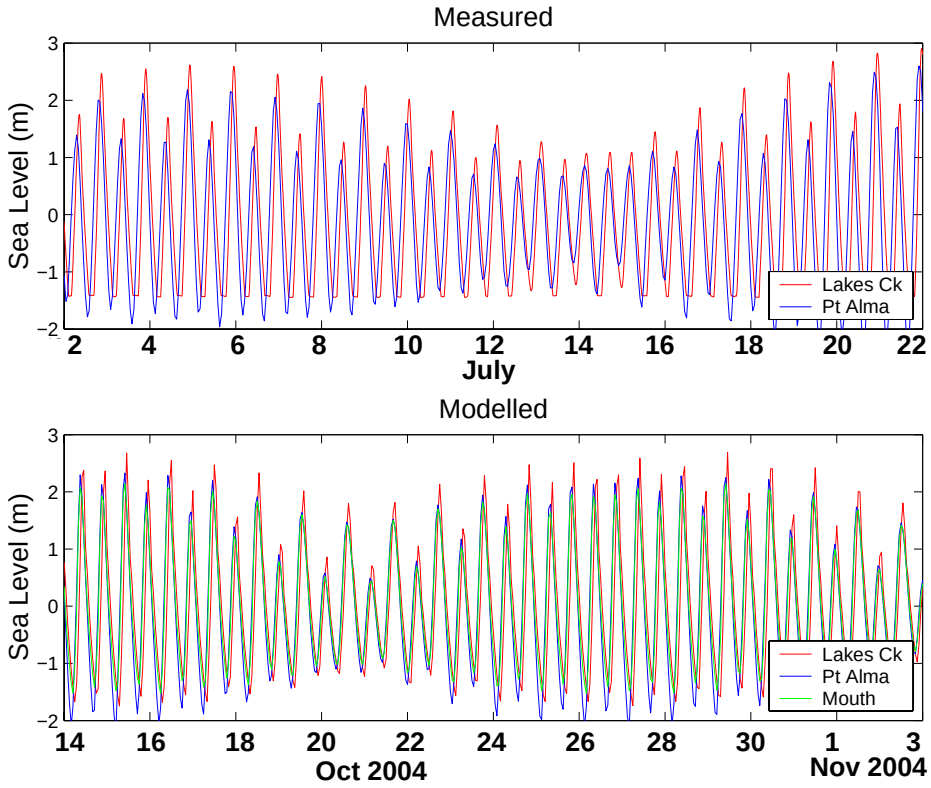


**Figure 6.2.3: Qualitative comparison of tidal amplification**

The measured data shows that the Lakes Creek tidal amplitude may be ~0.5 m greater than that at the mouth on the high tide. Amplification may only be observed at low water on the neap tide when the signal has not been truncated. The modelled results exhibit a similar trend, with amplifications at high water of the order of those measured. The low water amplification is more evident at the mouth of the Fitzroy than at Port Alma, especially during spring tides when no amplification is observed during low water at Port Alma. They exhibit a lag in the

Lakes Creek sea level relative to the Port Alma signal, which is also observed in the modelled data. Absolute maximum sea levels are also comparable between the modelled and measured data.

Comprehensive field surveys were undertaken in Keppel Bay during the dry season (15 August to 1 September, 2004, Atkinson *et al.*, 2004) and the wet season (6–9 February, 2005). These data consisted of moored CTDs at Timandra Buoy and Buoy 1, providing continuous records of temperature and salinity sampled at 5-minute frequency, and CTD profiles at numerous locations in Keppel Bay, Casuarina Creek and the Fitzroy Mouth. The moored instruments formed the basis of calibration (dry season) and verification (wet season), and were supplemented with the profiled measurements. Several profiles were obtained repetitively (half-hour intervals) at the same location, which were useful in comparing model behaviour resolved over the tidal cycle and water column.

Due to the large tidal excursion in Keppel Bay, aliasing was a problem when comparing surface distributions of temperature and salinity measured over many tidal cycles with modelled output. However, model output was interpolated to the same stations at the same times as the measurements to enable a direct comparison. The resulting surface plots cannot be considered a true snapshot of the ocean state, and are only useful for model/measurement comparison purposes.

The sites where CTD profiles were taken for the wet season are displayed in Figure 6.2.4. The model parameters were tuned so that modelled solutions optimally compared to August 2004 measurements (calibration procedure), then using this parameter, configuration in the model solutions were further compared to the February 2005 measurements (verification procedure). Model–data comparisons are outlined below.

Comparisons between time series of modelled temperature and salinity with measurements during August 2004 at Buoy 1 and Timandra Buoy (green dots in Figure 6.2.4) are displayed in Figures 6.2.5 and 6.2.6 respectively. Model data comparisons are good in both cases, except for salinity at Buoy 1 where the model appears to overestimate salinity. Upon comparison with profiled CTD measurements at this location (Figures 6.2.7 and 6.2.8), it is observed that the modelled and profile data are in agreement whereas the moored salinity at Buoy 1 is again lower, suggesting a problem with the measured salinity on the moored Buoy 1 instrument. When this instrument was retrieved it was observed to have been severely fouled, which may have compromised the salinity measurement. The magnitude of salinity oscillation at Timandra Buoy is also

larger than observation, suggesting a larger model salinity gradient in the vicinity of Timandra Buoy due to the open boundary salinity prescription.

Comparisons of the interpolated surface temperature and salinity distributions are displayed in Figure 6.2.9. The distributions were created from the measured data by simply spatially interpolating over the surface profile measurements. The modelled distributions were created by extracting the temperature or salinity values from the model output at the exact time and location of the corresponding measured value, and spatially interpolating these. As mentioned above, due to the large tidal excursion and related aliasing associated with sampling over many tidal cycles, the resulting distribution is not an accurate representation of the actual temperature or salinity distribution in Keppel Bay and is only useful for comparison purposes. Both modelled and measured salinity exhibit increased salinity of ~37 psu in the mouth of the Fitzroy Estuary, and extending up the western coast of Keppel Bay. Further offshore salinity decreases to ~36 psu. The temperature distributions both show a body of cool water towards the west side of Keppel Bay (~19$^{o}$C) with warmer water further offshore towards the north. The modelled temperature shows warmer water in the mouth of Keppel Bay which is absent in the measured data.

The continuously profiled measurements are compared to model solutions in Figures 6.2.10 (a–c) for Stations 26, 28 and 29 respectively (blue dots in Figure 6.2.4). Note that the X-axis is associated with time in these plots so that the change in vertical structure over time is represented. At station 26, the water column is seen to become warmer with time in both modelled and measured data. The modelled data is slightly warmer (~0.2$^{o}$C) than the measured data. The modelled salinity freshens towards the end of the profiling and this effect is not as evident in the measured data. Differences between model and measurement are small (<0.1 psu). At station 28, a warming and freshening is observed in both modelled and measured data, although modelled salinity is not quite as salty as the measured data at the start of the profiling. Temperature differences are again within about 0.2$^{o}$C. The measured data also appears slightly more stratified than the modelled at the end of the profiling. Moving into Casuarina Creek at Station 29, the water column is well mixed throughout and is seen to become fresher and warmer over the tidal cycle in both modelled and measured data. Differences in magnitudes are again acceptable.

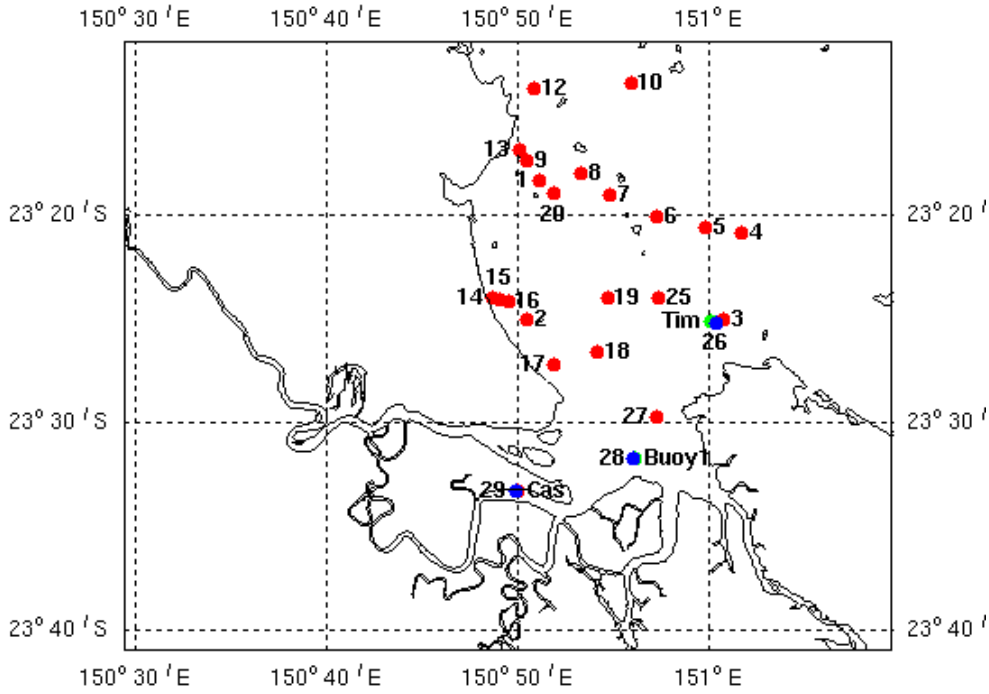


**Figure 6.2.4: Location of dry season CTD profiles**

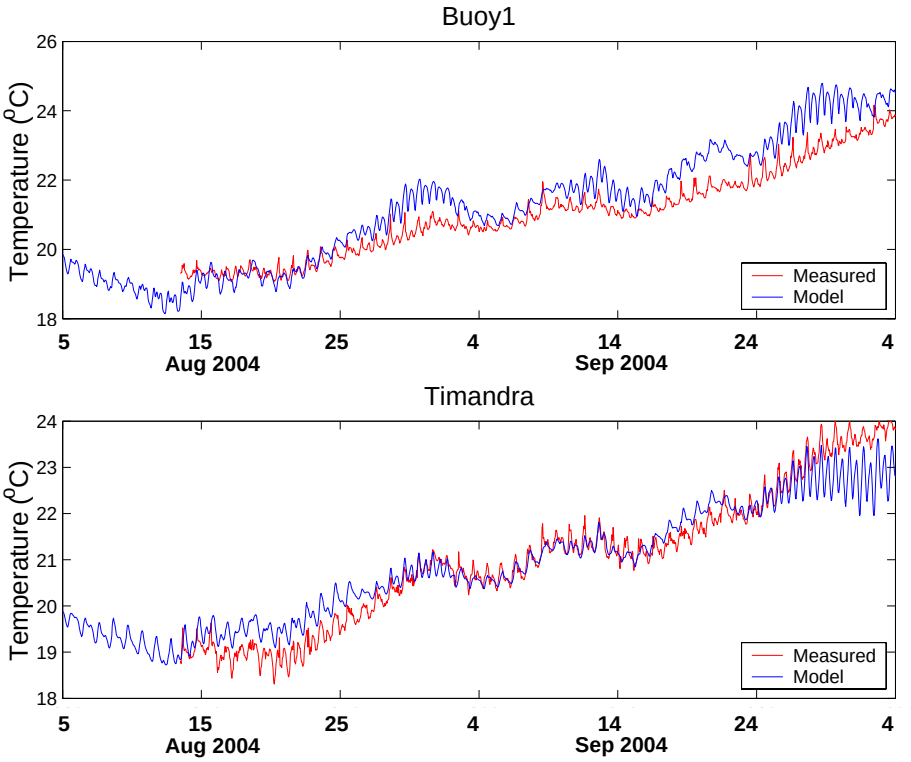


**Figure 6.2.5: Comparison of modelled and measured temperature at Buoy 1 and Timandra Buoy for the dry season (13 August 2004 to 15 October 2004)**

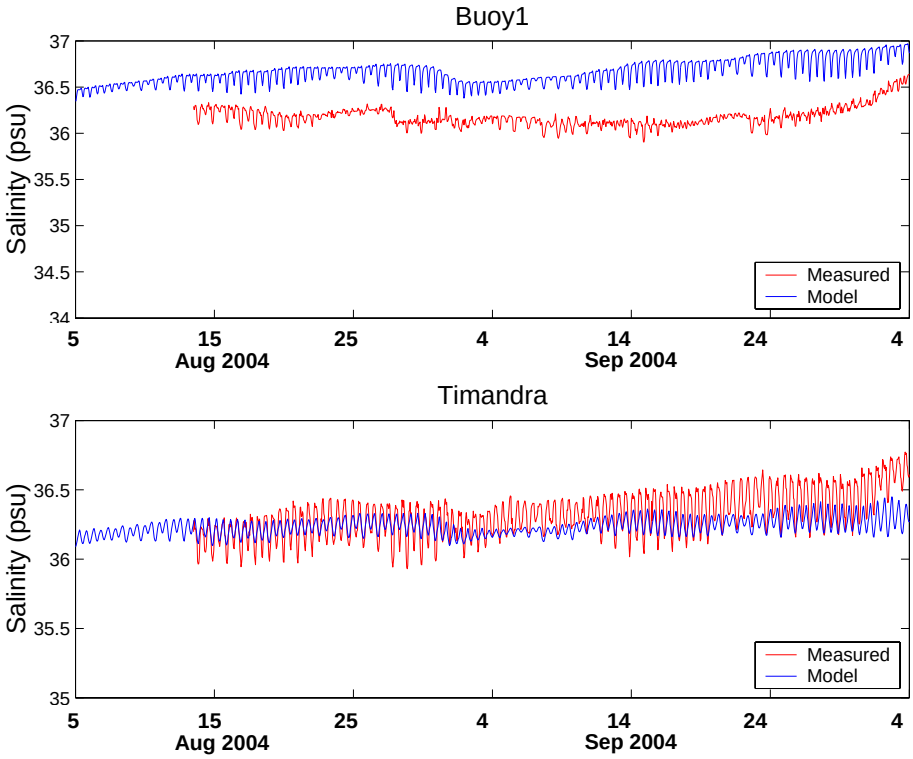

**Figure 6.2.6: Comparison of modelled and measured salinity at Buoy 1 and Timandra Buoy for the dry season (13 August 2004 to 15 October 2004)**

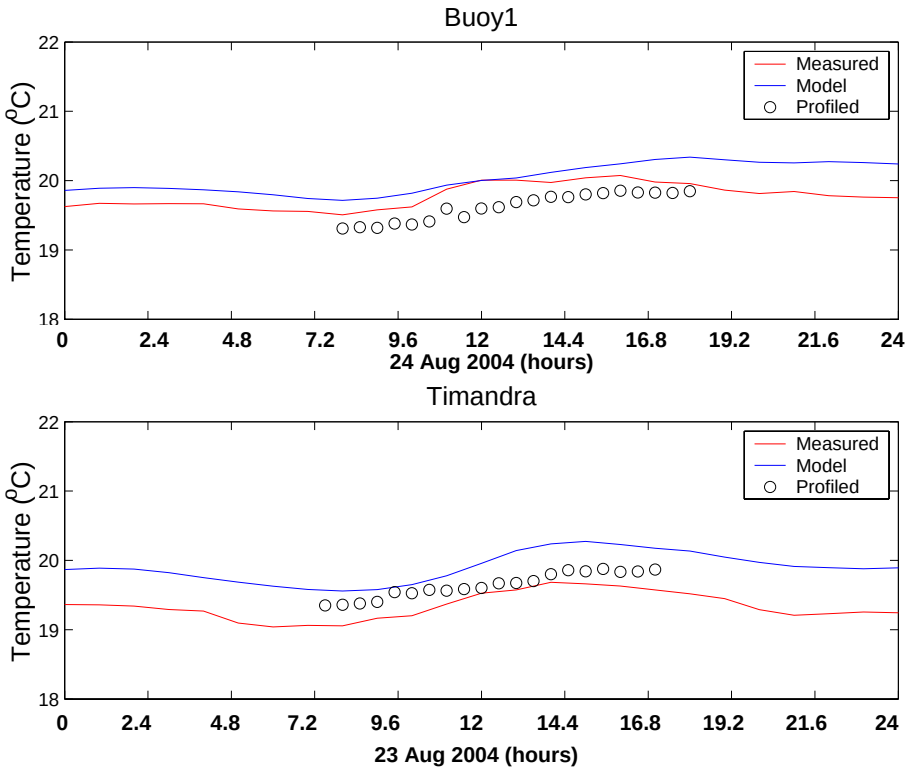


**Figure 6.2.7: Comparison of modelled and measured (profiled and moored) temperature at Buoy 1 and Timandra Buoy for the dry season**

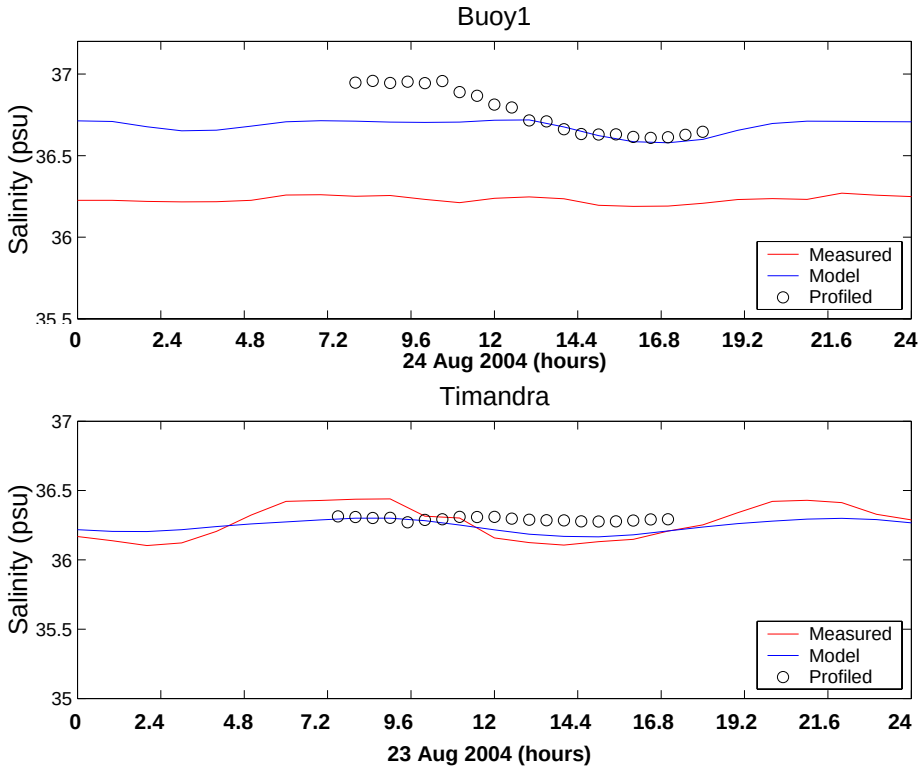


**Figure 6.2.8: Comparison of modelled and measured (profiled and moored) salinity at Buoy 1 and Timandra Buoy for the dry season**

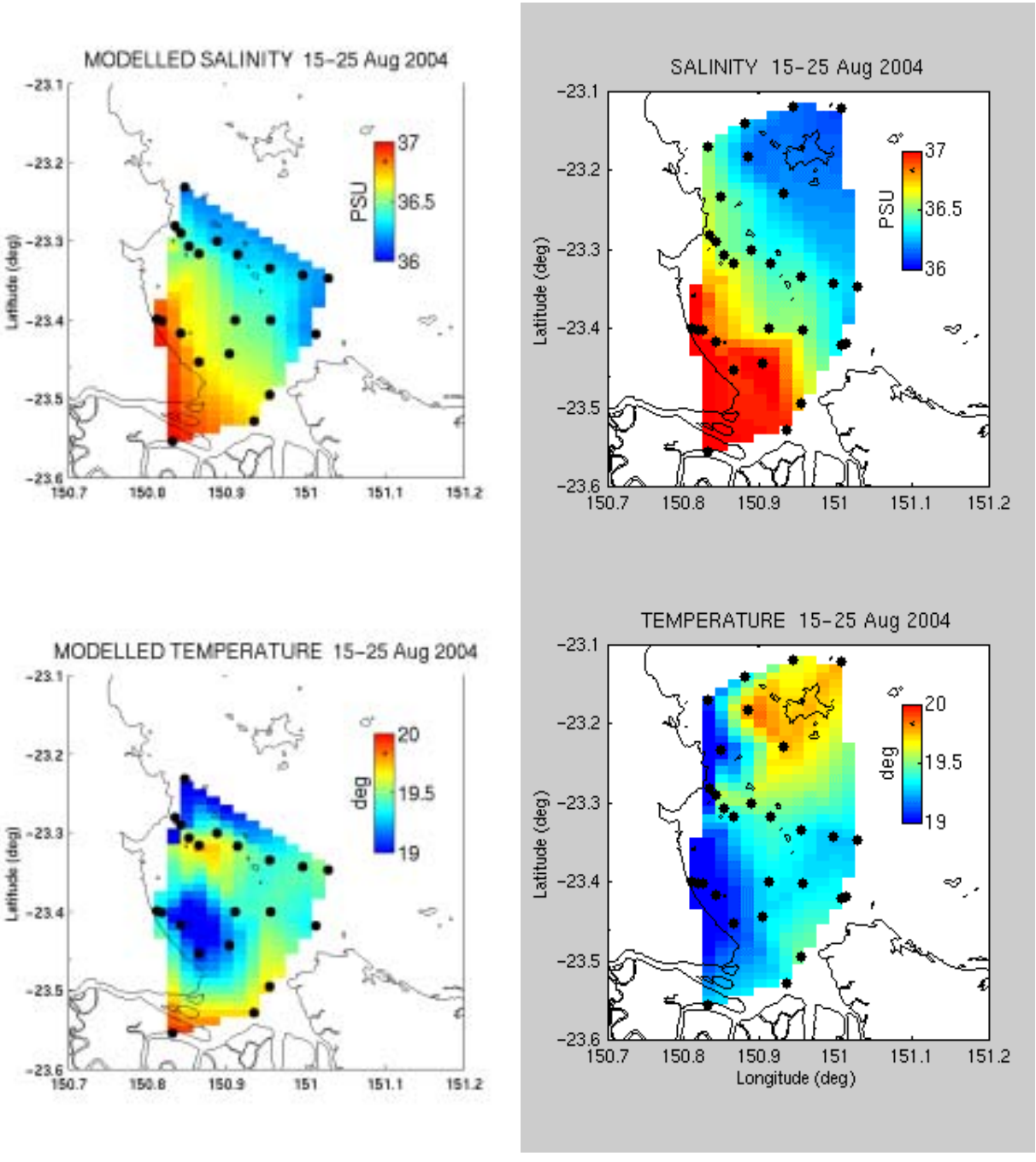


*Modelled* *Measured*

**Figure 6.2.9: Comparison of modelled and measured surface temperature and salinity for the dry season**

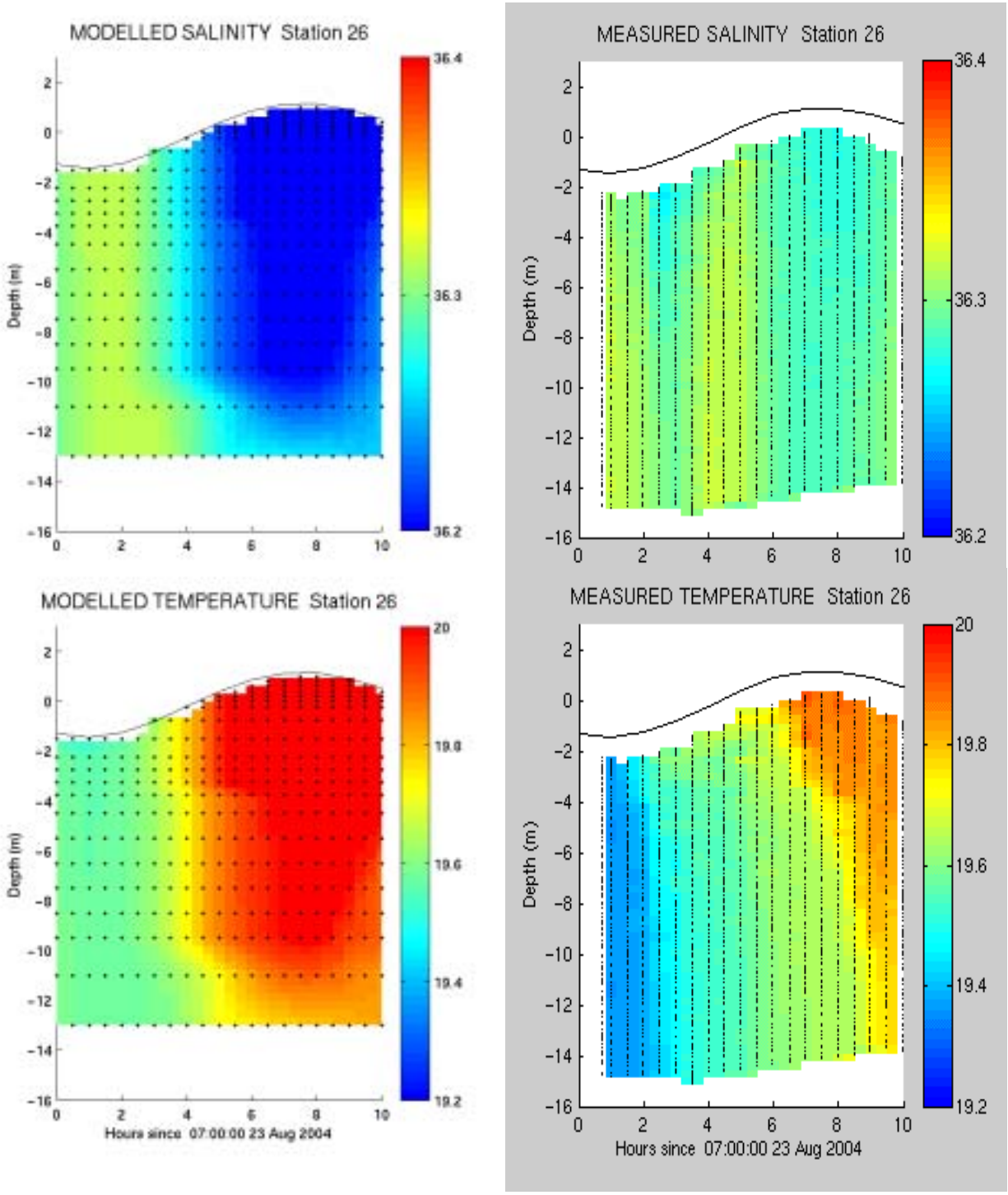


*Modelled* *Measured*

**Figure 6.2.10(a): Station 26 comparison of modelled and measured vertically profiled temperature and salinity for the dry season (25 August 2004)**

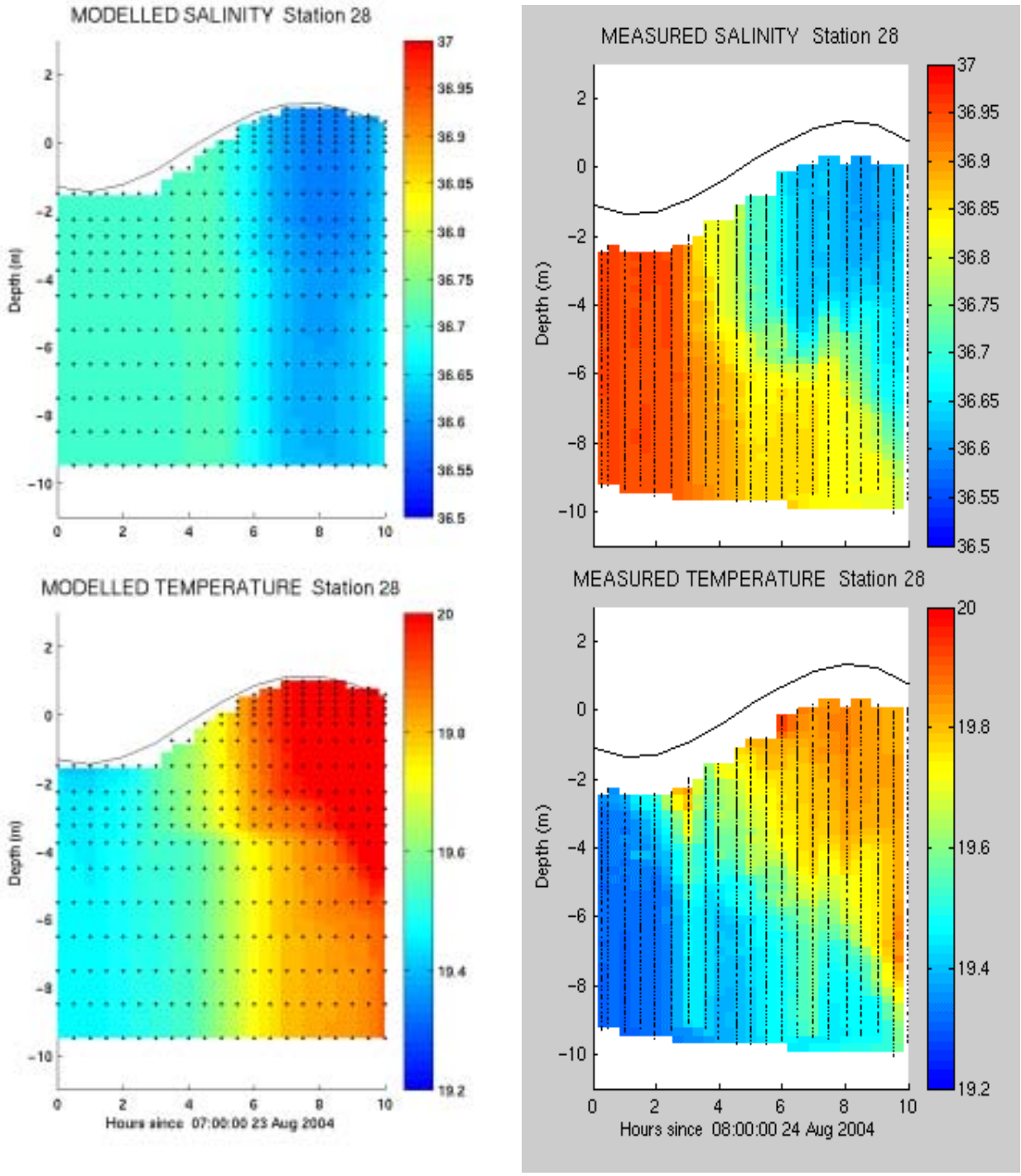


*Modelled* *Measured*

**Figure 6.2.10(b): Station 28 comparison of modelled and measured vertically profiled temperature and salinity for the dry season (23 August 2004)**

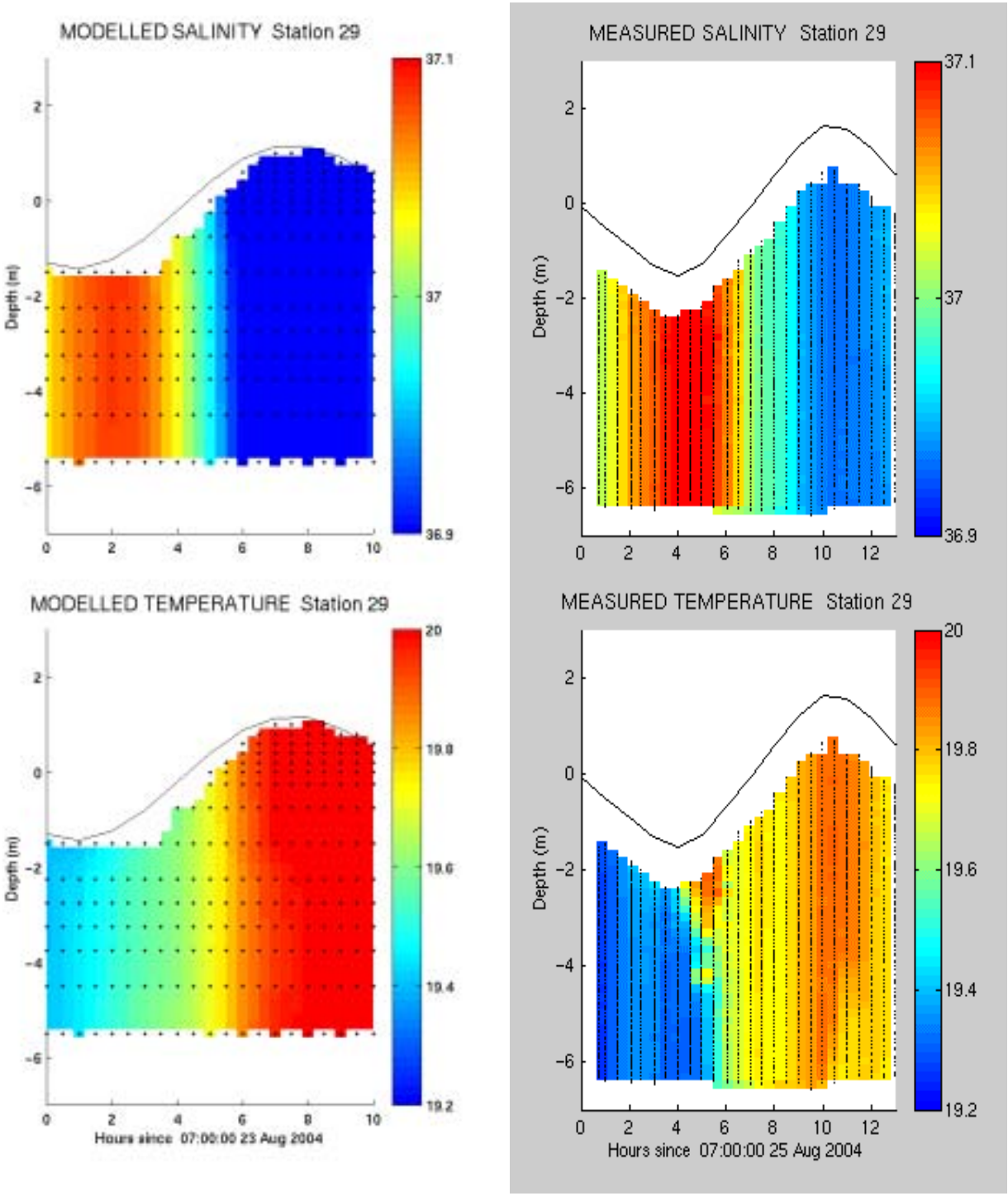


*Modelled* *Measured*

**Figure 6.2.10(c): Station 29 comparison of modelled and measured vertically profiled temperature and salinity for the dry season (25 August 2004)**

Overall the model behaves well, with the spatial distribution, magnitude and timing of events consistent with those observed in the measured data. The model solutions were compared to data collected during the wet season, February 2005, to verify the calibration. Locations of the profiling sites for this field excursion are displayed in Figure 6.2.11. Time series at Buoy 1 and Timandra Buoy derived from moored instruments are displayed in Figures 6.2.12 and 6.2.13.

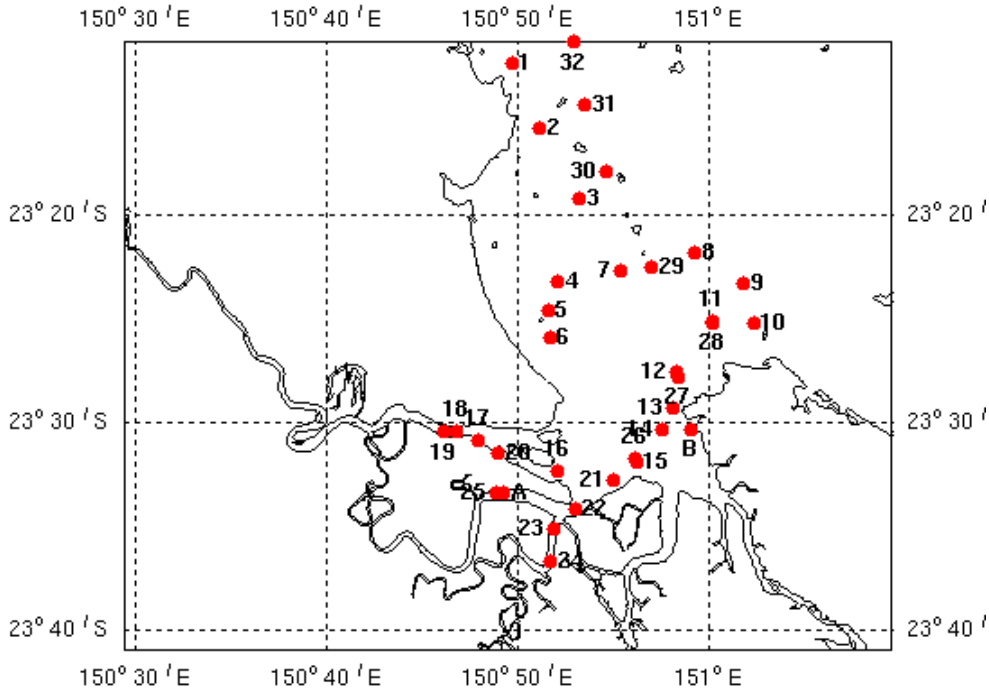


**Figure 6.2.11: Location of wet season CTD profiles**

A distinct oscillation in the temperature solution at the period of the neap-spring cycle (~14 days) is observed in both the modelled and measured temperature solution, perhaps a result of the passage of atmospheric systems. At Timandra Buoy during the first 10 days of the comparison the model is ~1$^{o}$C cooler than observed, otherwise the model compares to measurement remarkably well. Modelled salinity is consistently lower than observed, although the timing of neap–spring cycling, low salinity spikes during the first 40 days, the onset of the flood and the post-flood recovery are well captured by the model. The salinity magnitude during the flood and during flood recovery compares well to observation, although the magnitude of salinity oscillations at the period of the tide appears greater in the model, especially closer to the open boundary. The salinity offset is probably a result of the inaccuracy associated with the open boundary condition used in the model (see Section 5.3).

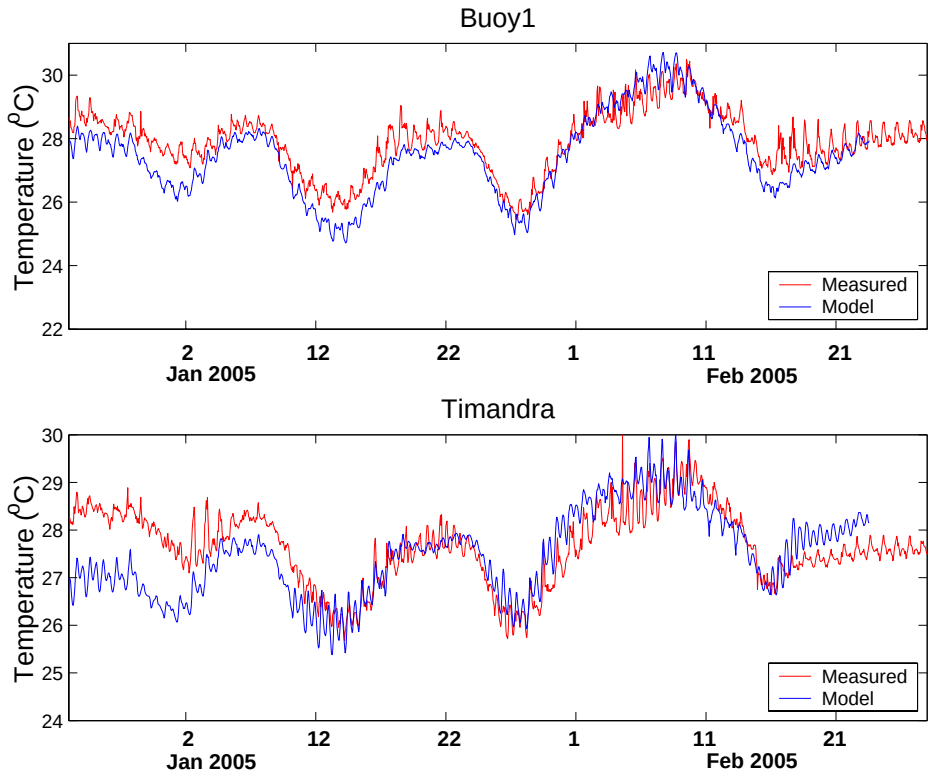


**Figure 6.2.12: Comparison of modelled and measured temperature at Buoy 1 and Timandra Buoy for the wet season (23 December 2004 to 28 February 2005)**

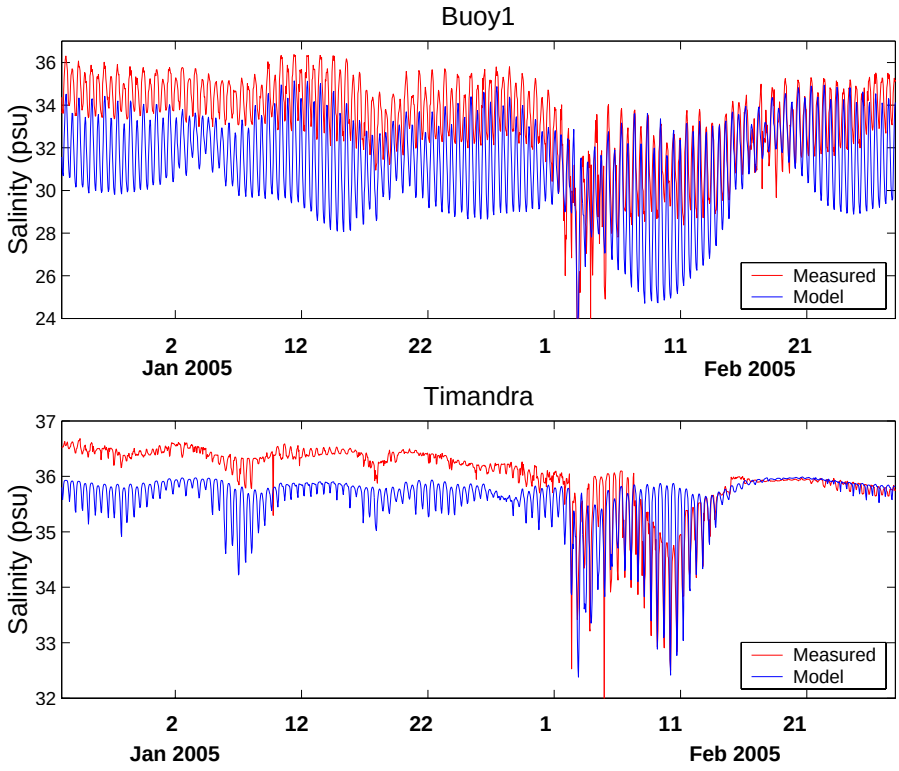

**Figure 6.2.13: Comparison of modelled and measured salinity at Buoy 1 and Timandra Buoy for the wet season (23 December 2004 to 28 February 2005)**

The modelled and measured surface temperature and salinity distributions are displayed in Figure 6.2.14. Salinity is fresher in the Fitzroy mouth and along the western side of Keppel Bay in both modelled and measured data, increasing offshore into Keppel Bay. Temperature is observed to increase in Connors Creek and midway along the western coast of Keppel Bay, with cooler water near the offshore boundary and adjacent to Curtis Island. Overall agreement between model and measurement is good.

Continuously profiled measurements are compared to model solutions for Station 26 only in Figure 6.2.15. The water column becomes fresher and warmer over the ebbing tide in both modelled and measured data. Changes in salinity, and to a lesser extent temperature, are much greater over the tidal cycle than during the dry season, due to the advection of the freshwater plume through the measurement site over the tidal cycle. Vertical stratification is also greater due to the presence of the freshwater plume. The model captures this well, exhibiting comparable changes in magnitude to the measured data. Overall the model can be considered to provide good agreement with measured data, in both the timing and magnitude of events.

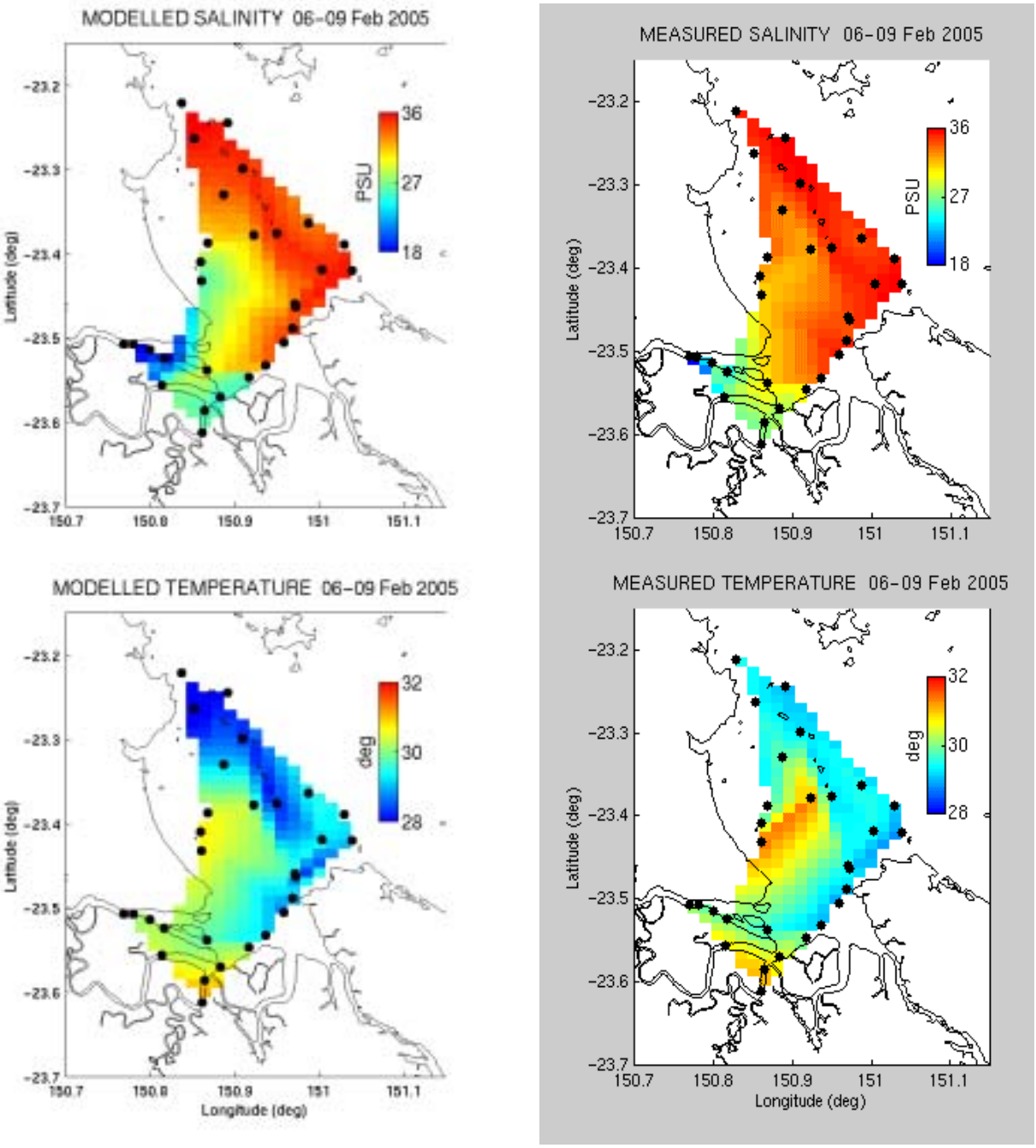


*Modelled* *Measured*

**Figure 6.2.14: Comparison of modelled and measured surface temperature and salinity for the wet season**

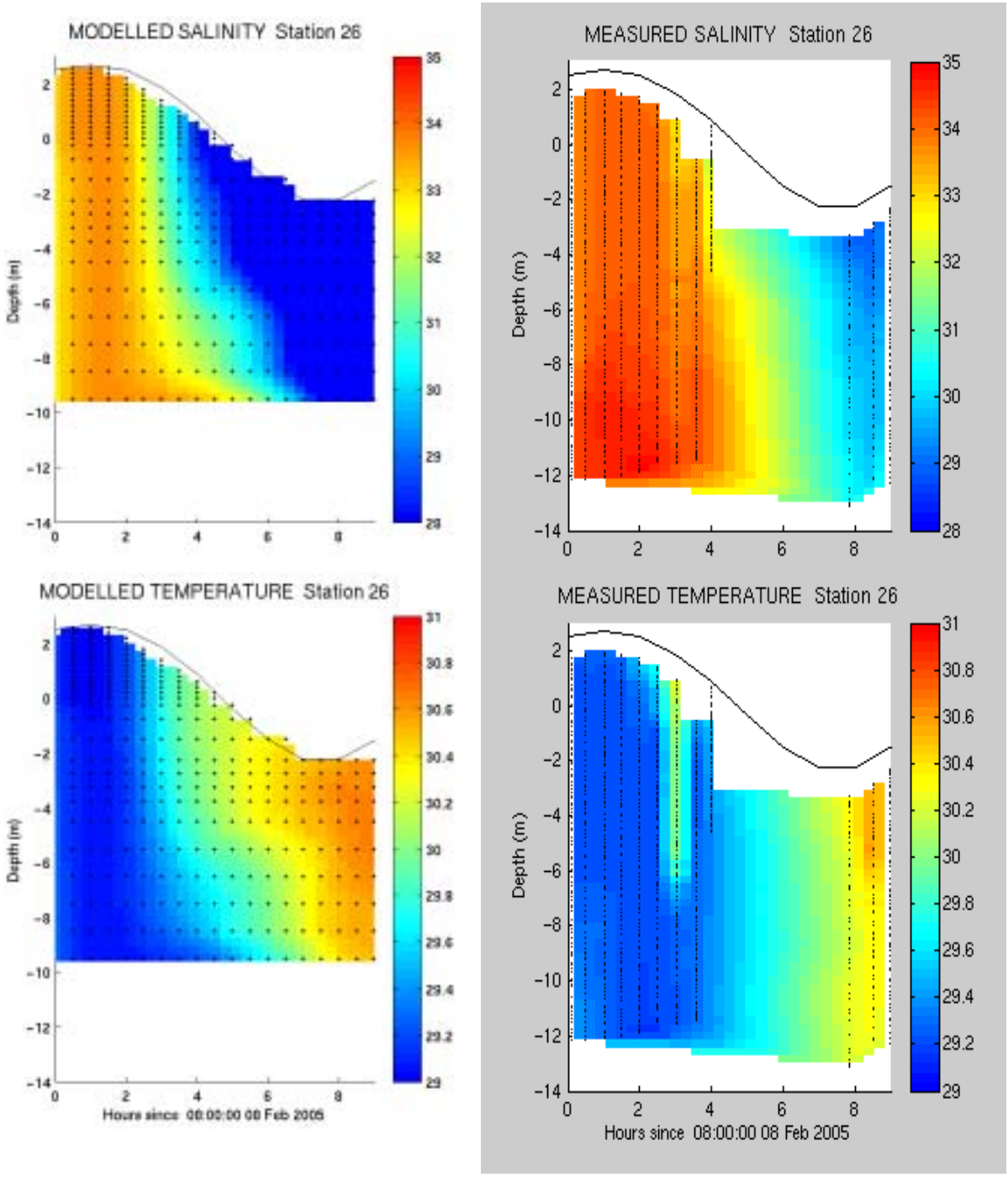


*Modelled* *Measured*

**Figure 6.2.15: Station 26 comparison of modelled and measured vertically profiled temperature and salinity for the dry season (25 August 2004)**

## 6.3 Sensitivity

During the calibration procedure an assessment of the sensitivity of model parameters and processes was made. This provides insight into the parameters and processes which may critically affect the model solutions. The calibration presented in Section 6.2 is the end result of the sensitivity analysis; the key parameters of the calibration procedure and model process requirements are detailed below.

The most critical process required to be included in the model was that of atmospheric heat and freshwater fluxes across the ocean surface. The fluxes were computed from standard meteorological measurements (Herzfeld, 2005, Chapter 9). These fluxes added heat to the system and allowed the temperature solution to realistically mirror the seasonal cycles. In shallow areas, particularly those subjected to wetting and drying over tidal cycles and further up the tidal creeks, localised temperature increases are observed in model output due to differential heating. Salinity was also observed to increase due to the same mechanism via evaporation.

The temperature solution compared to the moored measurement during the dry season without heat fluxes applied is displayed in Figure 6.3.1, from which it can be seen there exists no long-term trend. The choice of bulk scheme used to derive the sensible and latent heat fluxes across the sea surface proved to be critical also. There are numerous bulk schemes in existence; Blanc (1985) reviews ten schemes and concludes that each scheme provided different results when applied to the same data, highlighting the uncertainty inherent in the bulk method. The bulk scheme of Masagutov (1981) proved to provide the most favourable agreement between measured and model results. A comparison of modelled and measured temperature using the bulk scheme of Kitaigorodskii *et al.* (1973) demonstrates the variability possible due to the implementation of different bulk schemes (Figure 6.3.2).

The short-wave radiation component incident on the sea surface may be partitioned so that a fraction is input as the surface boundary condition (in addition to the sensible, latent and long-wave components) and the remaining fraction is allowed to penetrate the water column to a depth determined by an extinction coefficient. This partitioning represents the preferential absorption of longer wavelengths of short-wave radiation within the first few metres (Simpson & Dickey, 1981).

It was determined that the best temperature calibration occurred when all short-wave radiation was allowed to penetrate the water column with an extinction coefficient of 0.3 $m^{-1}$. Surface temperature solutions using a transmission coefficient of 0.5 and 1.0 are displayed in Figure 6.3.3, from which it is observed the full transmission results in a slightly cooler solution at the surface. The actual extinction coefficient in Keppel Bays exhibits large variability due to the presence of suspended solids. The use of a constant extinction in the model may account for some of the discrepancy between modelled and measured diurnal temperature in the mouth of the Fitzroy (Figure 6.2.9).

The bathymetry used in the model proved critical in accurately calibrating differential bathymetry effects on temperature and salinity due to surface fluxes. This required more accurate bathymetry in the mouth of the Fitzroy River, Casuarina Creek and the western side of Keppel Bay. Bathymetry was manually digitised in these regions to provide a more accurate bathymetric representation. Several of the major tidal flats were included and the code optimised to cope with wetting and drying over these regions. The bathymetry in the Fitzroy mouth before and after these enhancements is displayed in Figure 6.3.4. The latter (digitised) bathymetry was used for all model simulations.

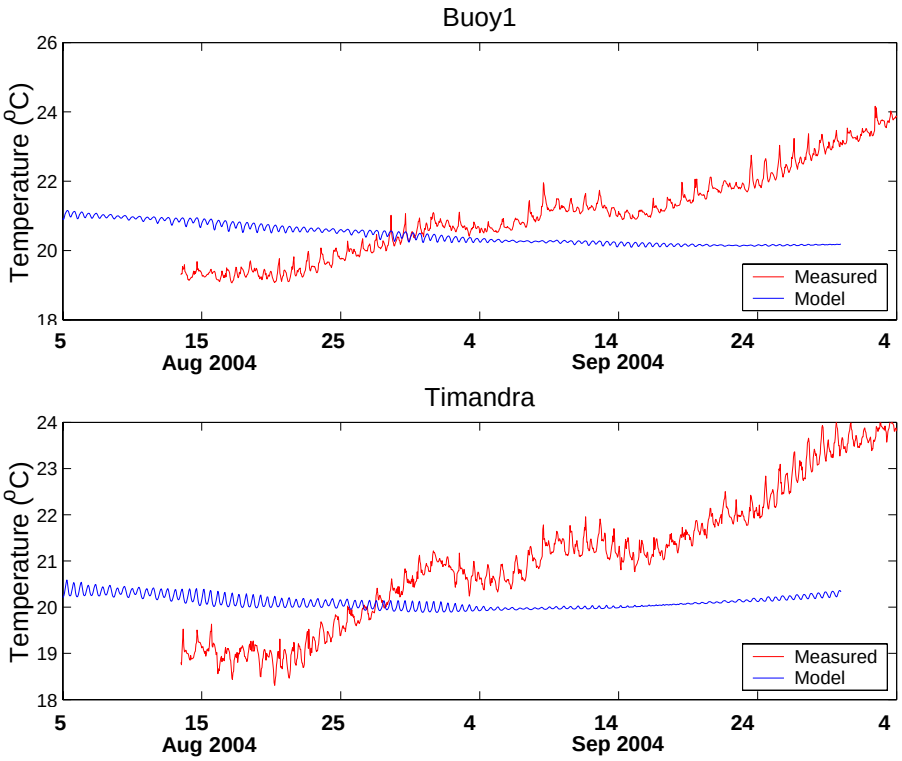


**Figure 6.3.1: Temperature solutions with no heat flux**

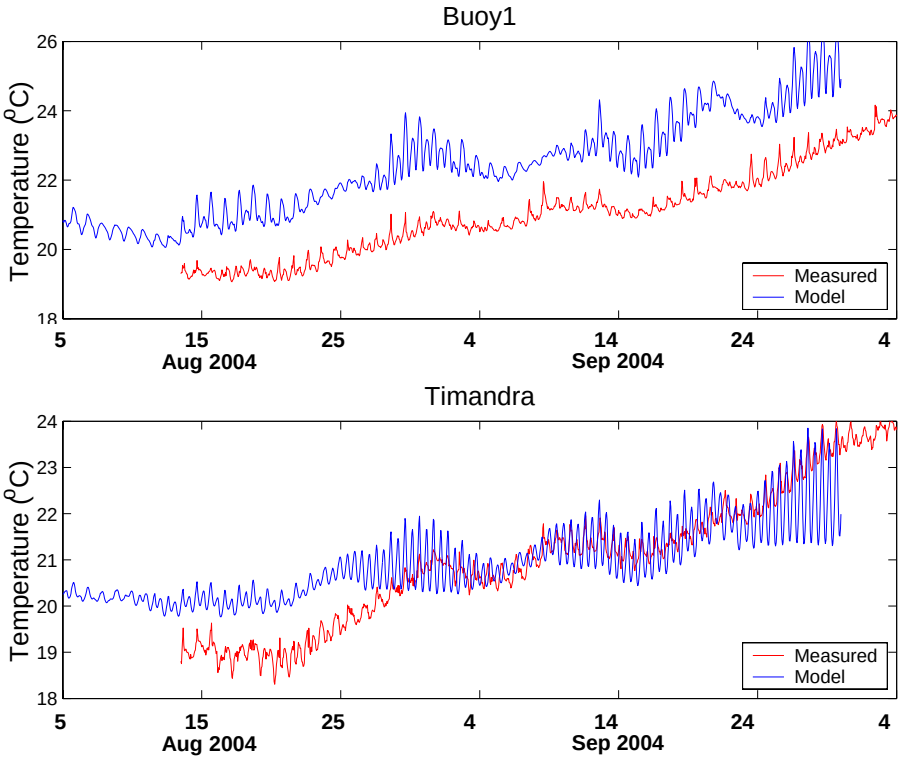


**Figure 6.3.2: Temperature solutions using the bulk scheme of Kitaigorodskii *et al.* (1973)**

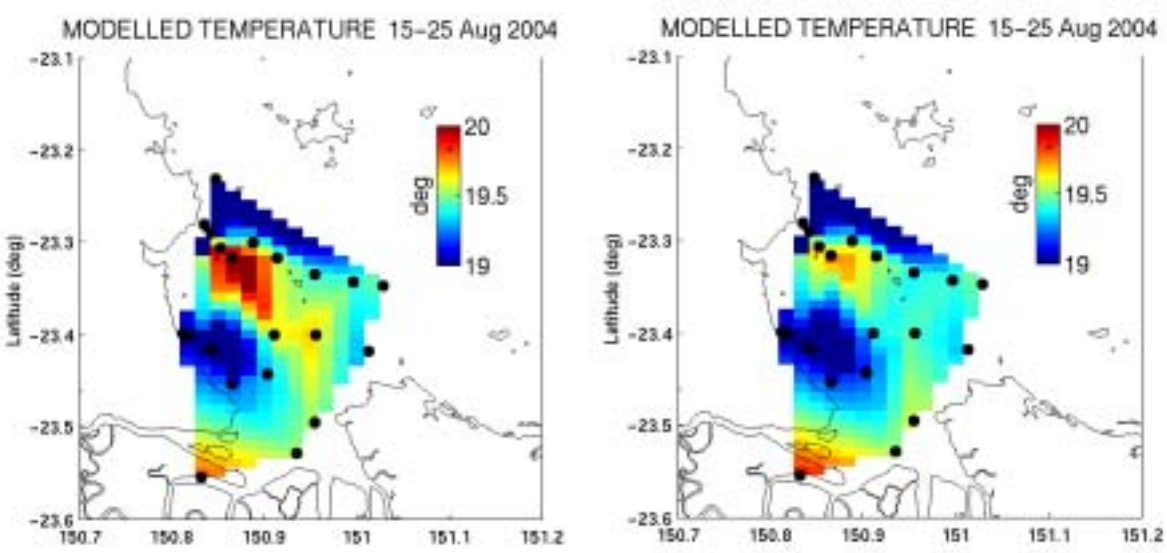


*(a) Transmission = 0.5* *(b) Transmission = 1*

**Figure 6.3.3: Temperature solutions variable short wave transmission (extinction = 0.3 $m^{-1}$)**

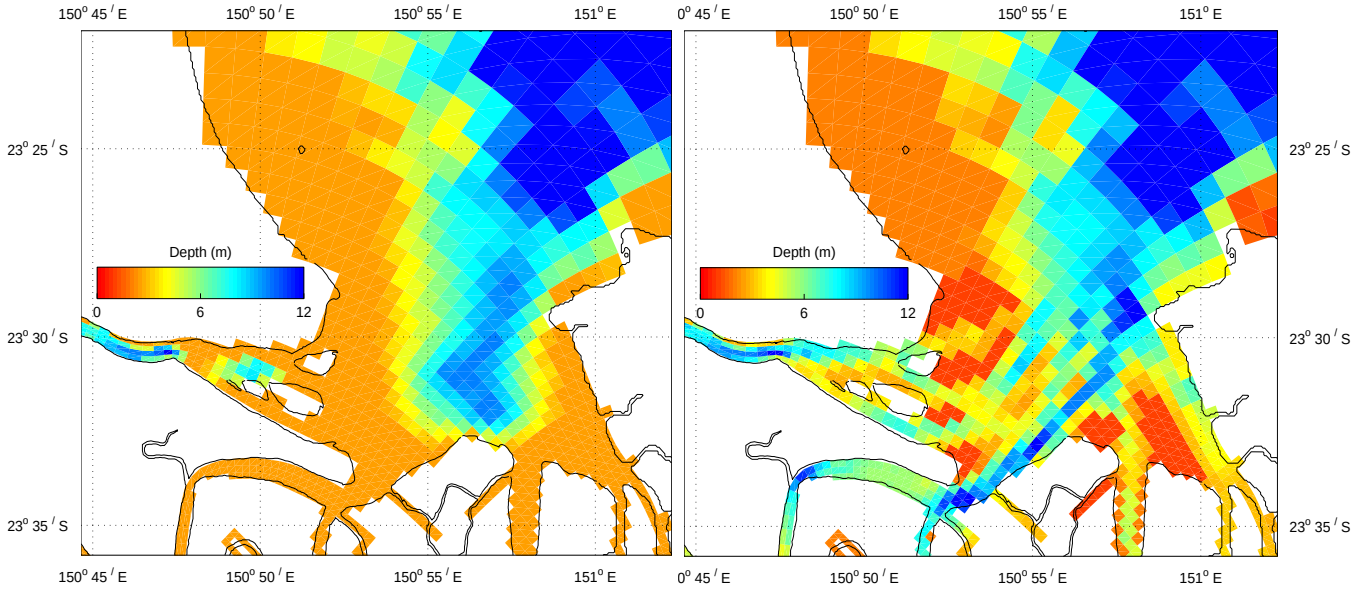


*(a) Before digitisation* *(b) After digitisation*

**Figure 6.3.4: Bathymetry in the vicinity of Fitzroy mouth**

The horizontal viscosity used was the shear dependent Smagorinsky formulation (Smagorinsky, 1963) where horizontal mixing coefficients are computed every time step based on the horizontal shear present. This proved to provide marginally better solutions than using constant coefficients (viscosity = 150 $m^2s^{-1}$, diffusion = 25 $m^2s^{-1}$), Figure 6.3.5.

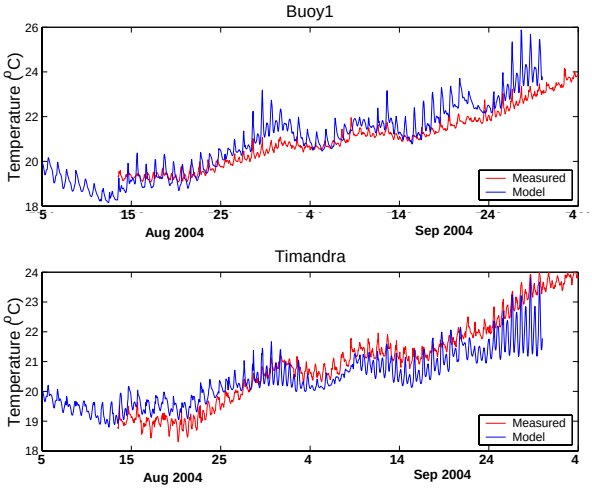


**Figure 6.3.5: Temperature solutions using constant mixing coefficients (viscosity = 150 $m^2s^{-1}$, diffusion = 25 $m^2s^{-1}$)**

The background vertical diffusion coefficients were set to $1x10^{-5}$ $m^2s^{-1}$, using the Mellor-Yamada 2.0 mixing scheme (Mellor & Yamada, 1982). Increasing or decreasing the background mixing by an order of magnitude had minimal effect on solutions (Figure 6.3.6). This insensitivity is probably due to vertical mixing

coefficients rarely prescribed to background values due to the vigorous tidal mixing in the region.

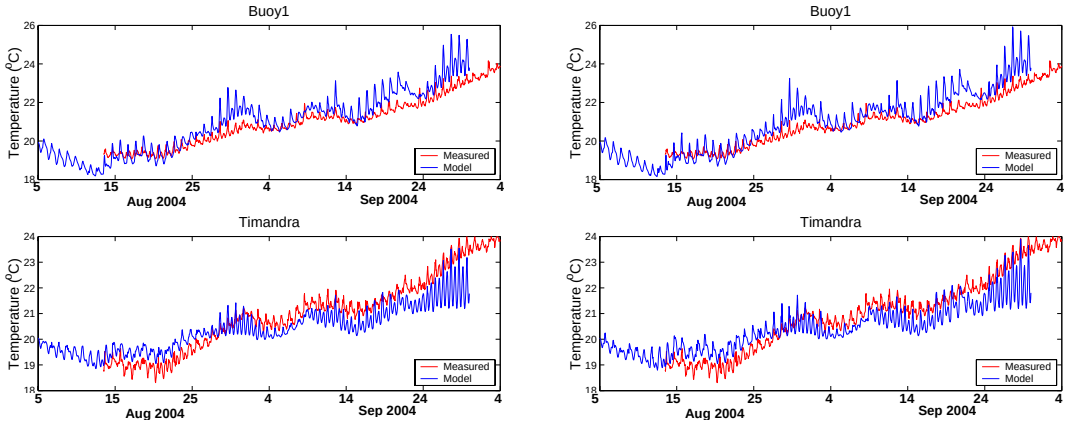


*(a) $V_z = K_z = 1x10^{-4}\ m^2s^{-1}$* *(b) $V_z = K_z = 1x10^{-6}\ m^2s^{-1}$*

**Figure 6.3.6: Temperature solutions using varied background vertical mixing coefficients**

As mentioned earlier, model solutions were not sensitive to the initial condition due to the rapid spin-up time. The large heat fluxes applied at the surface resulted in a faster spin-up of the temperature solution than the salinity solution, which was controlled more by boundary effects during the dry season. Salinity solutions using an initial condition of 36 and 38 psu are displayed in Figure 6.3.7, demonstrating this insensitivity.

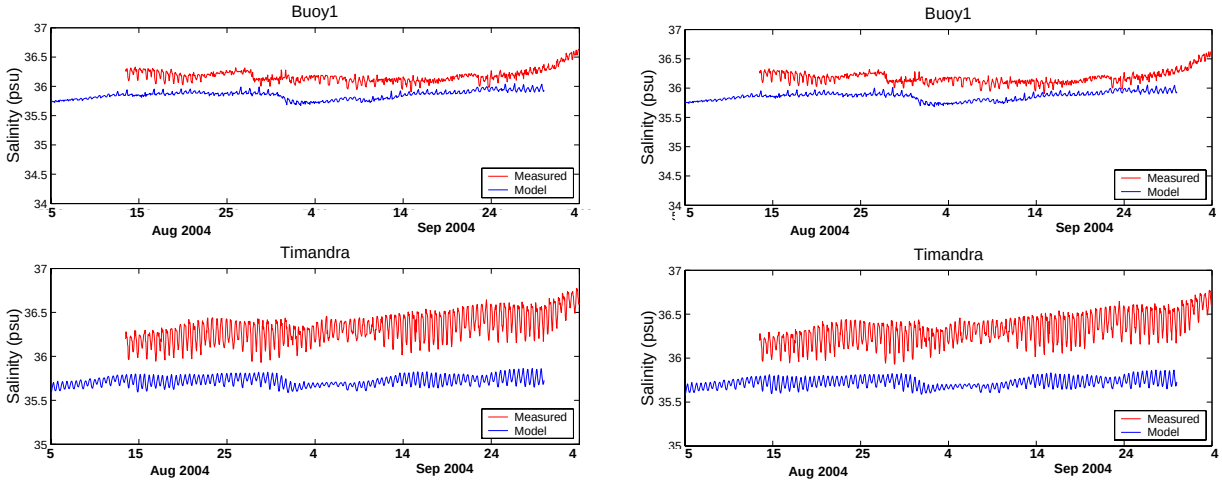


*(a) S = 36 psu* *(b) S = 38 psu*

**Figure 6.3.7: Salinity solutions using varied initial conditions**

There existed no suitable data to force the local Fitzroy model with temperature and salinity on the offshore open boundary (see Section 5.3). The Fitzroy model is always nested within the regional model, using output from this larger-scale model to drive its open boundaries. The choice of open boundary conditions for the regional model influences the T/S distributions throughout the regional domain, and hence impacts the open boundary forcing for the Fitzroy model. Available options for forcing the open boundaries of the regional model were to use the CARS climatological atlas or global model output from a previous year (since global model output was only available up to ~2002 at the time of these simulations). Either of these options was unsatisfactory, providing salinities in the Fitzroy region that were too fresh (Figure 6.3.8; compare with 6.2.9). The salinity solution in the Fitzroy model was strongly influenced by the offshore open boundary, and the temperature solution became more sensitive to the open boundary forcing in the wet season when solar irradiance was lower and increased humidity lead to lower latent heat losses, thus diminishing the influence of surface fluxes.

In order to generate acceptable solutions, the Fitzroy open boundaries derived from the CARS open boundary forced regional model were scaled so as to provide optimum model–measurement comparisons. Different values of the scaling were applied for the wet and dry seasons, and the scaling was applied uniformly along the boundary. The effect of boundary scaling on the salinity solution is illustrated in Figure 6.3.9, which may be compared to the un-scaled solution in Figure 6.3.7.

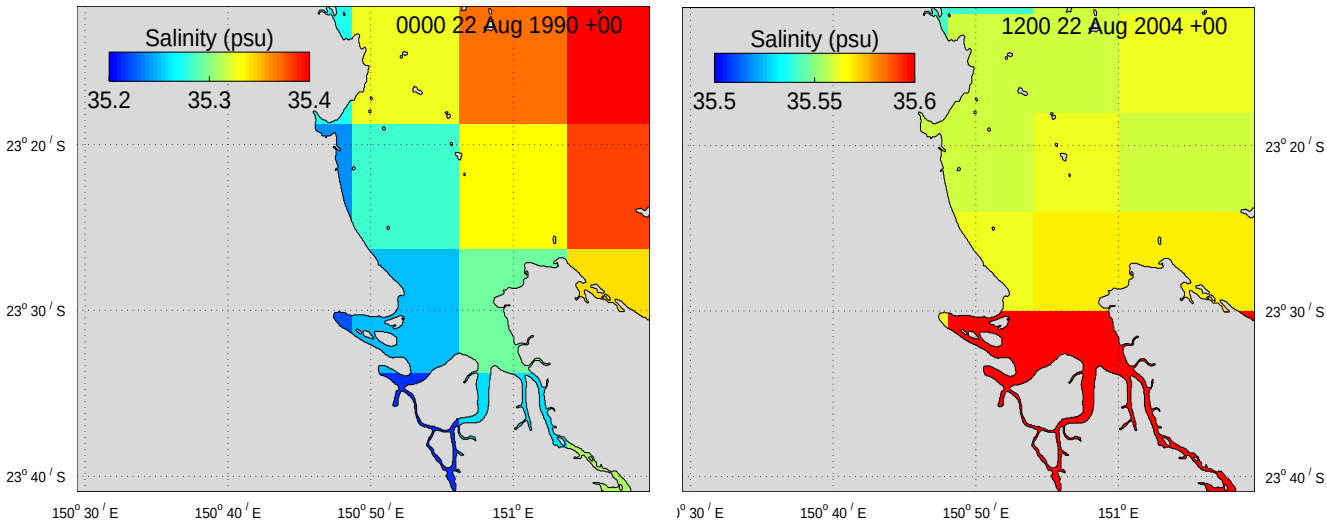


*(a) CARS* *(b) OFAM 2001*

**Figure 6.3.8: CARS and OFAM 2001 salinity distributions in the Fitzroy region**

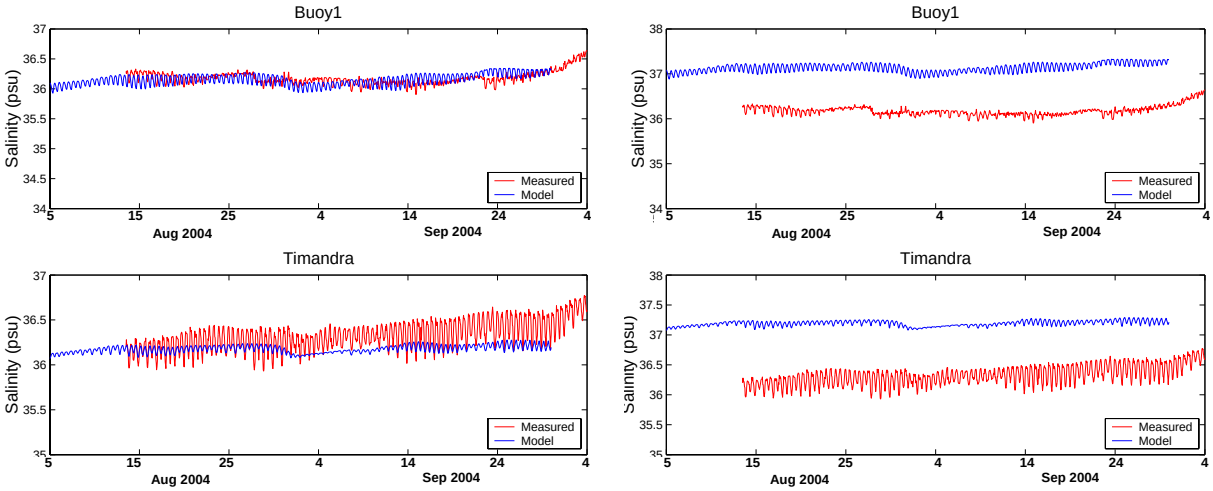


*(a) 0.5 psu added to CARS salinity* *(b) 1.5 psu added to CARS salinity*

**Figure 6.3.9: Salinity solutions using boundary scaling**

Final scaling was such that 0.5 psu was added to boundary salinities and no scaling was applied to temperature during the dry (March to December 2004), and 1.0 psu and 3$^{o}$C were added to salinity and temperature respectively during the wet (January to March 2005). The most crucial requirement for improving model solutions is the prescription of accurate temporally and spatially varying forcing for temperature and salinity on the offshore open boundary. The future use of high resolution global model output in this capacity may be adequate.

Finally, the treatment of freshwater inflow at the barrage impacted on the salinity in the domain. The boundary condition used at this location was a one-dimensional version of the advection equation (upstream method, Herzfeld 2005, Section 4.8). This method cannot distinguish between downstream flow due to an ebbing tide and that due to a large river discharge, and using this boundary condition the estuary becomes too fresh due to the tide bringing fresh water through the barrage boundary on every ebb. The upstream method was modified to ensure fresh water was only input into the system when the river flow dominates the tide. Salinity solutions using this adaptive upstream method are displayed in Figure 6.3.10 [note the moored data for Buoy 1 (red line) is deemed inaccurate due to fouling, see Section 6.2]. Buoy 1 was most clearly influenced due to its closer location to the Fitzroy mouth, hence any freshwater influence.

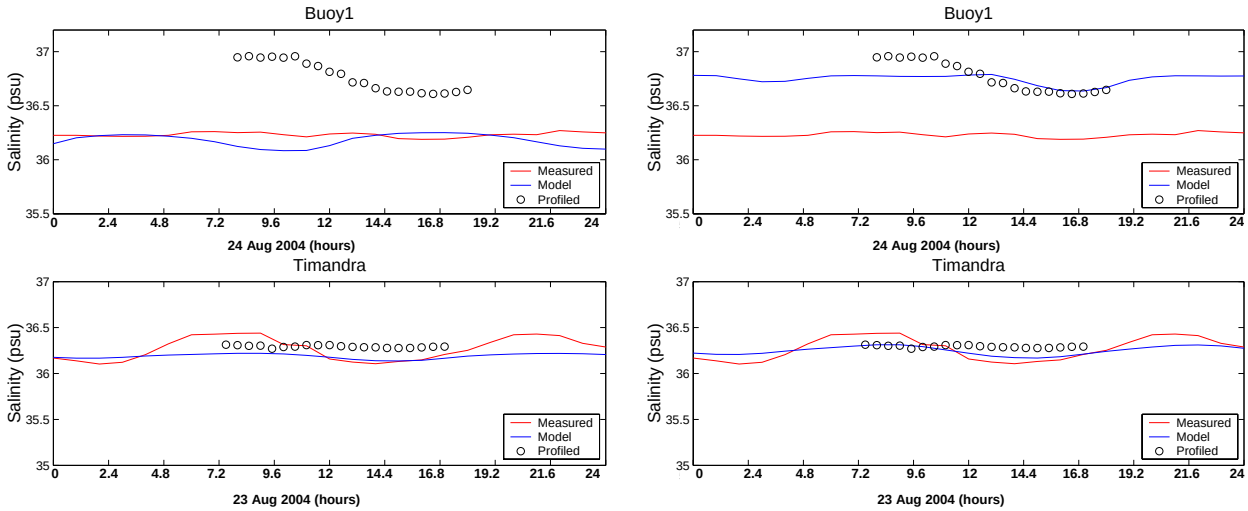


*(a) Standard upstream method* *(b) Adaptive upstream method*

**Figure 6.3.10: Salinity solutions using upstream boundary conditions at the barrage**

## 6.4 Longer simulations

Simulations of longer duration are desirable when analysing sediment transport and nutrient dynamics, since these processes are associated with long timescales. The model was run from June 2003 to February 2005, providing 20 months of simulation. The calibration was not, however, as good as the March 2004 to February 2005 simulation. In particular, the water near the Fitzroy mouth is fresher than was observed during the 2004 dry season (Figure 6.4.1). Note that the only difference in the model between the longer simulation, Figure 6.4.1, and original calibration, Figure 6.2.9, is a significantly different initial condition due to residual fresh water present from the 2003–2004 wet season. This indicates that the domain did not recover sufficiently after the 2003–2004 wet season flooding.

The comparisons of model temperature with moored measurement (Figure 6.4.2) and with profiled data appear satisfactory. Sea level comparisons remain good. The salinity response to the 2004–2005 floods was comparable to the response when the model was started in March 2004 (Figure 6.4.3; compare with Figure 6.2.13). Since open boundary forcing is the primary mechanism for regionally increasing salinity within the domain, the fresh bias in the model salinity is undoubtedly the result of inaccurate (i.e. low) salinity boundary forcing during and after the 2003–2004 wet season.

It appears that the CARS climatology-forced regional model solutions underestimate salinity at the end of the wet season in the Fitzroy region, and optimised scaling needs to be applied to the boundary values of the Fitzroy domain at quite a high temporal frequency to compensate. This scaling was not attempted due to time constraints (both project timelines and model run-time). Ultimately, adequate boundary forcing should ideally be applied to the model so scaling is not necessary. While salinity is underestimated through some periods of the simulation, it is anticipated that the tidally driven flow is accurately captured.

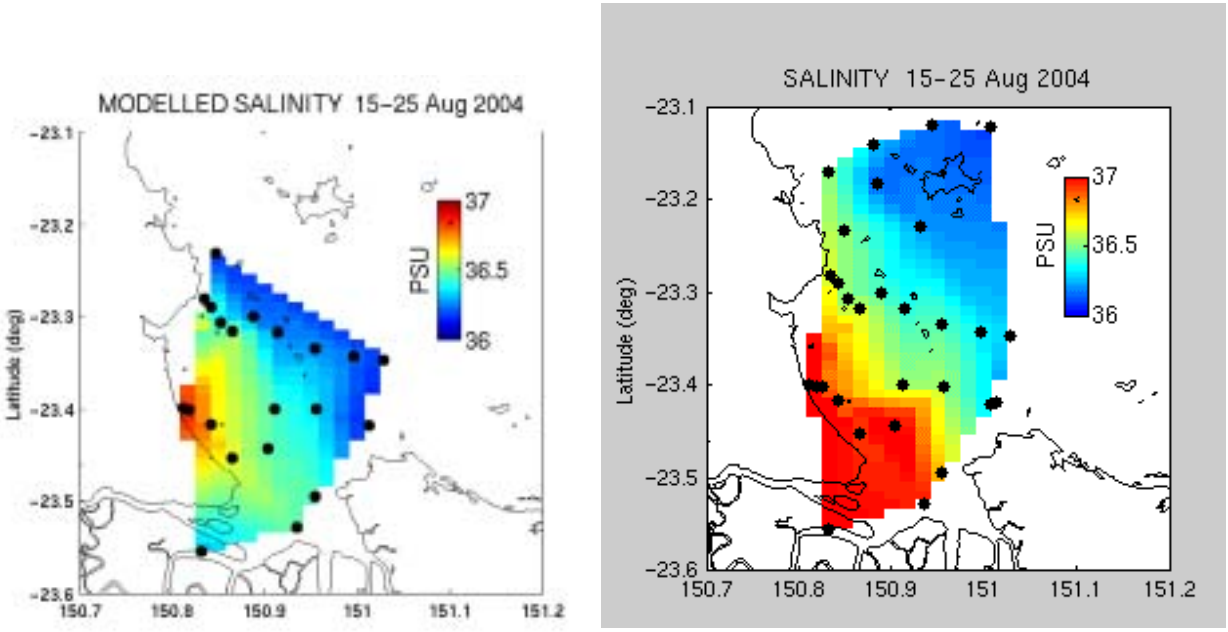


*Modelled* *Measured*

**Figure 6.4.1: Comparison of modelled and measured surface salinity for the dry season. Model start time is June 2003**

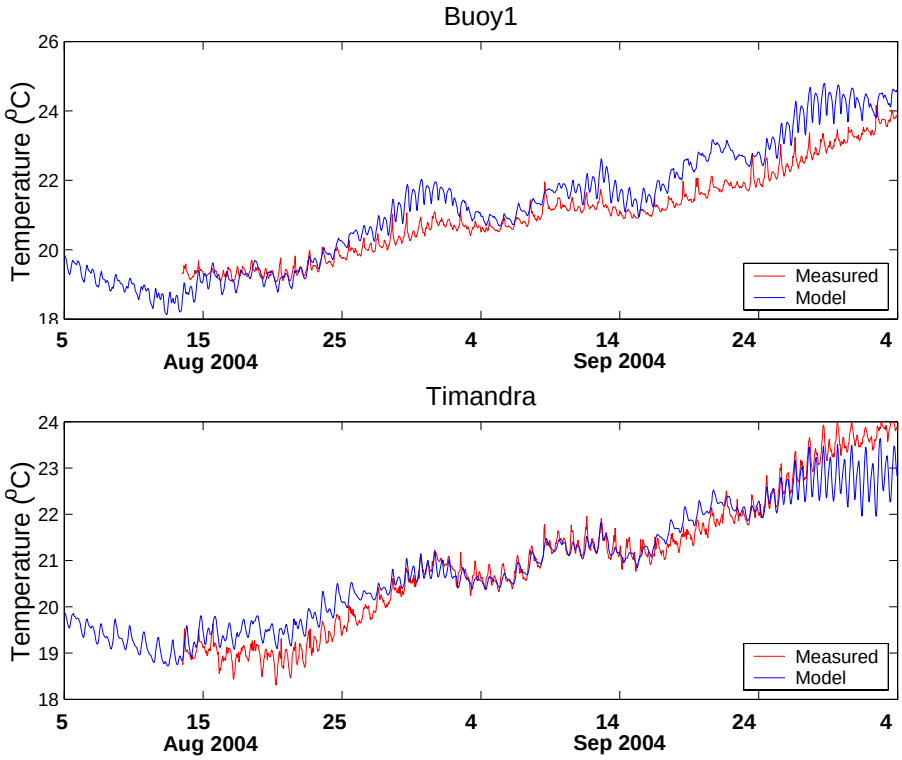


**Figure 6.4.2: Comparison of modelled and measured temperature at Buoy 1 and Timandra Buoy for the dry season (13 August 2004 to 15 October 2004). Model start time is June 2003**

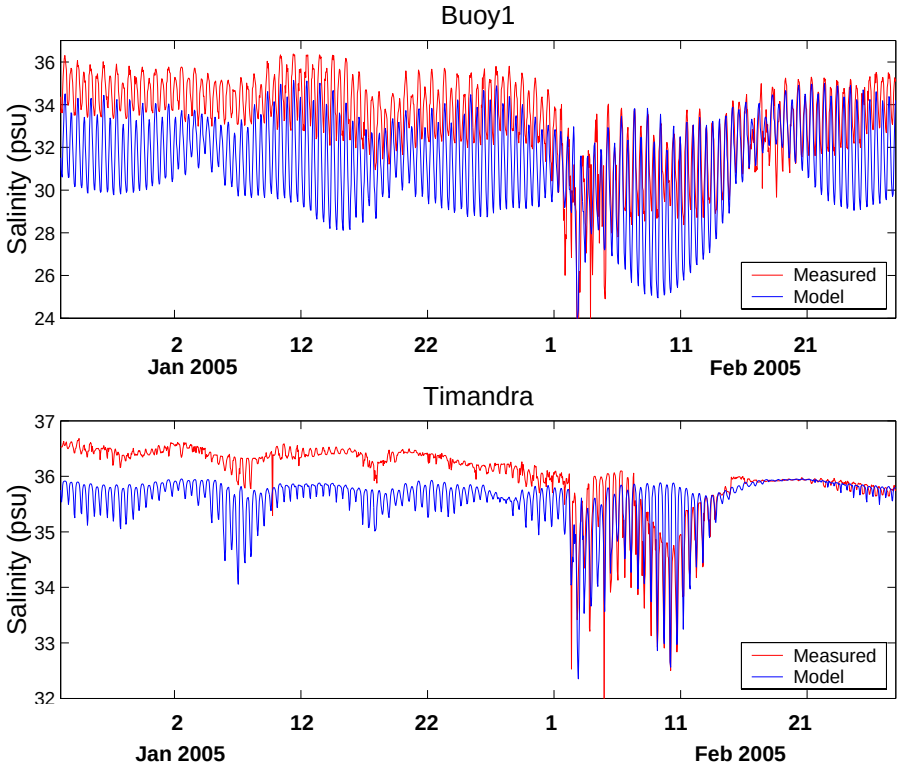


**Figure 6.4.3: Comparison of modelled and measured salinity at Buoy 1 and Timandra Buoy for the wet season (23 December 2004 to 28 February 2005). Model start time is June 2003**

# 7 Solutions

## 7.1 General solutions

The circulation in the Fitzroy Estuary/Keppel Bay region is dominated by the tide, with surface currents flowing into the estuary on the flood tide (Figure 7.1.1), and out of the estuary on the ebb (Figure 7.1.2). Currents are significantly weaker (up to a factor of 2) during the neap tide in comparison to the spring tide, where maximum current speeds approach 2 $ms^{-1}$. There exists a lag between the sea-level responses in the upper reaches of the Fitzroy and in Keppel Bay; that is, elevation is significantly lower in the upper Fitzroy than that in Keppel Bay at any point in time during the flood, and vice versa during the ebb.

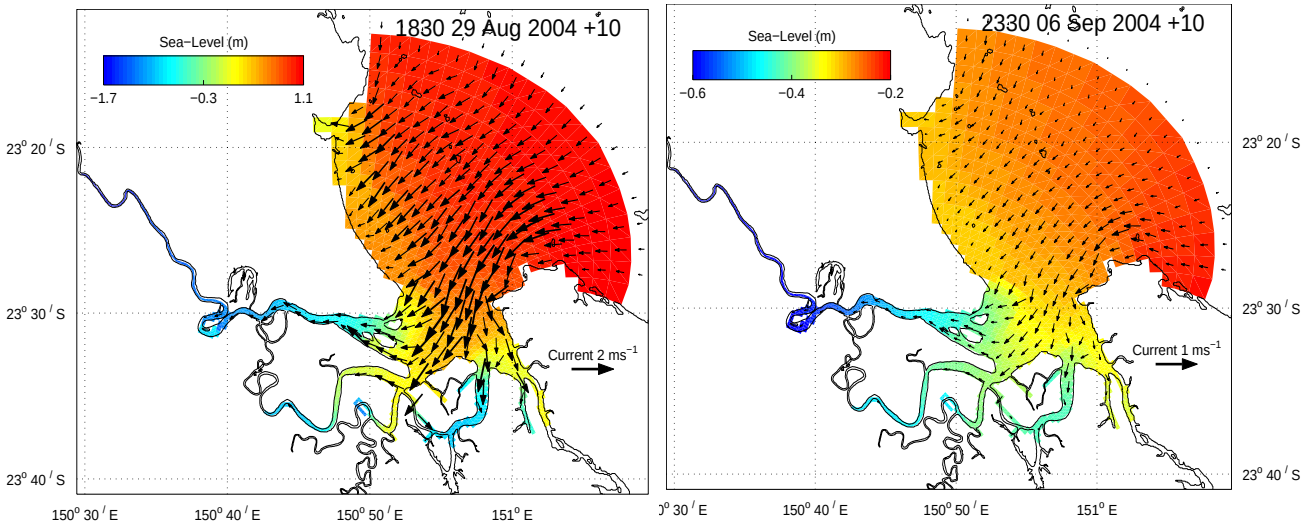


*(a) Spring tide* *(b) Neap tide*

**Figure 7.1.1: Surface currents at flood tide ($ms^{-1}$)**

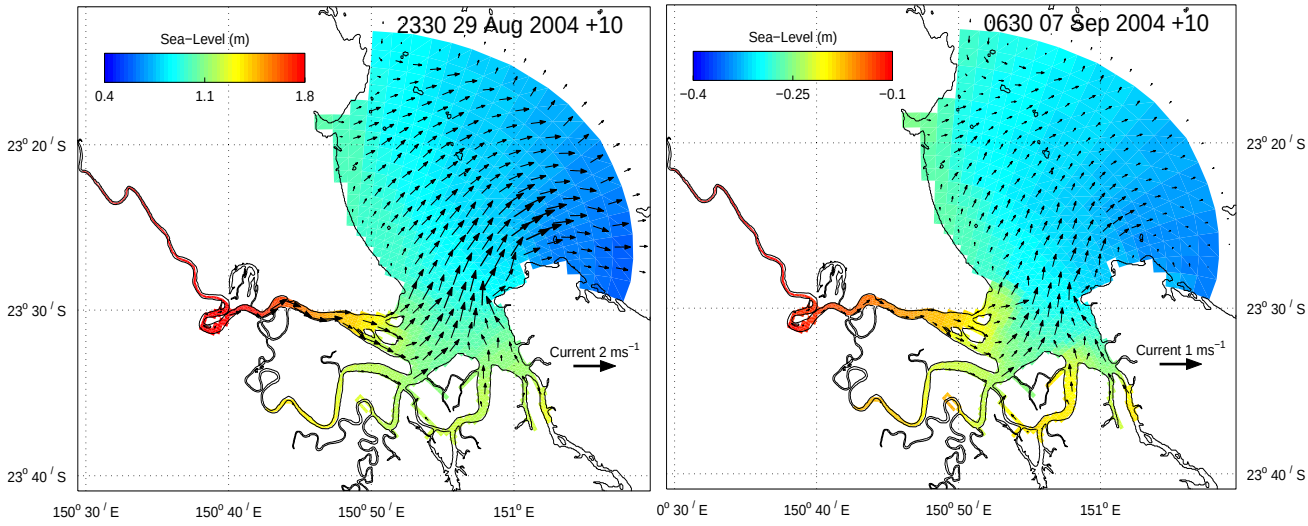


*(a) Spring tide* *(b) Neap tide*

**Figure 7.1.2: Surface currents at ebb tide ($ms^{-1}$)**

Depth-averaged and bottom currents distributions are very similar to the surface currents (Figure 7.1.3), indicating that momentum is quite well mixed vertically and there is little vertical structure to the three-dimensional flow. The large barotropic tide generates large currents, and combined with the shallow bathymetry, large bottom friction results, which generates a well mixed water column. This well mixed nature is also evident in the modelled and measured profiles of temperature and salinity displayed in Figure 6.2.10. However, as shown in Figure 6.2.15, the presence of the freshwater layer during the wet season can result in a stratified water column.

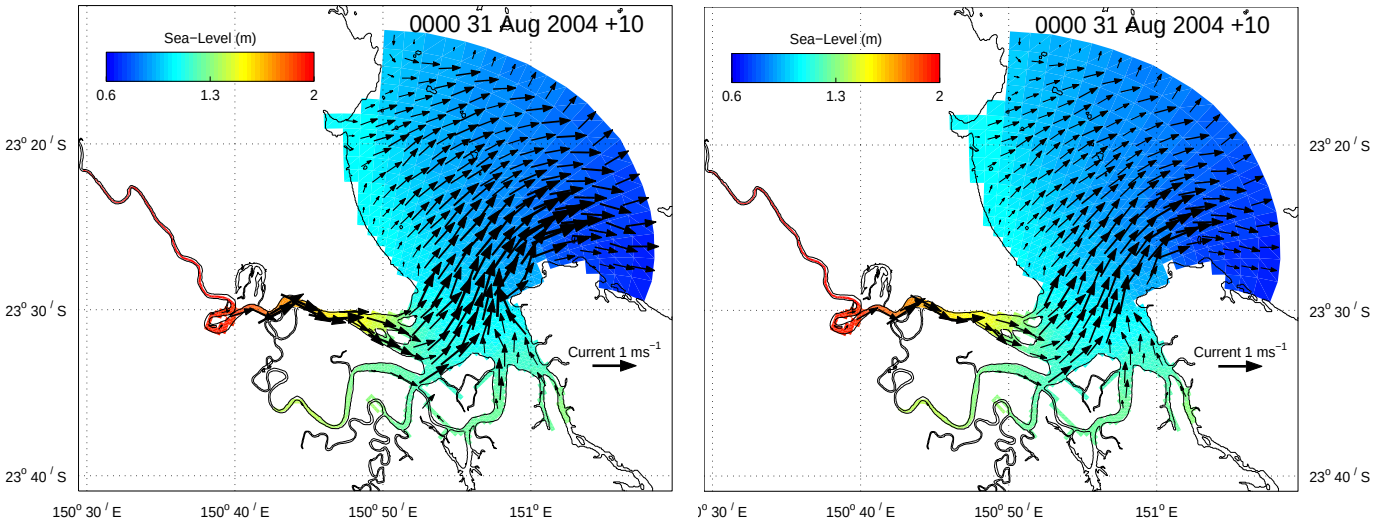


*(a) Surface currents*

*(b) Depth-averaged currents*

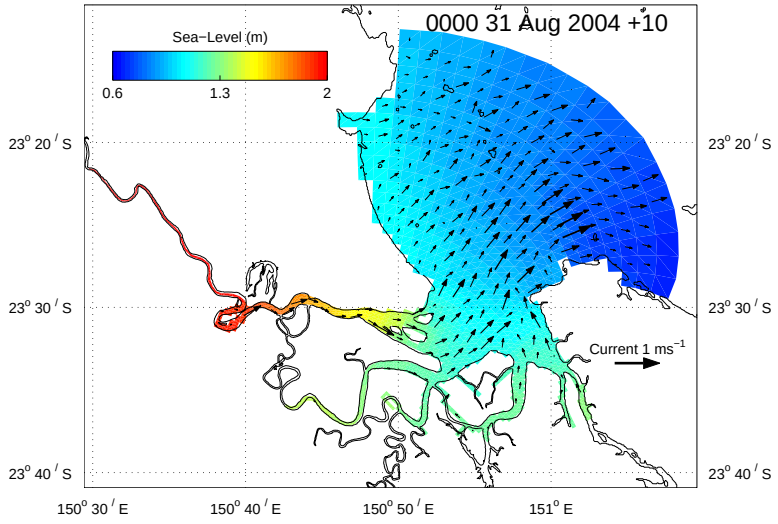


*(c) Bottom currents*

**Figure 7.1.3: Currents at ebb tide (ms$^{-1}$)**

The modelled surface elevation at Buoy 1 is displayed as a function of time in Figure 7.1.4. This shows that tidal ranges may reach ~5 m during spring tides and are generally confined to ~1 m during neaps. The neap–spring cycle has a period of ~14 days. The tide is mixed, mainly semi-diurnal in character, which may be quantified by the form factor F = ratio of diurnal to semi-diurnal amplitudes ($F = K_1+O_1 / M_2+ S_2$). In the case of the Fitzroy region, F ~0.28 verifies that the tide just falls into the semi-diurnal mixed category ($0.25 < F < 1.5$).

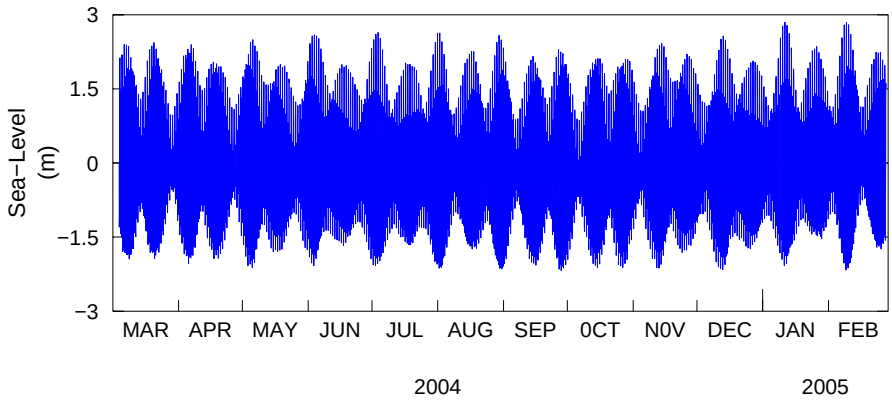


**Figure 7.1.4: Sea level at Buoy 1**

During the dry season local temperature increases are observed in shallow regions due to differential heating. This effect is most pronounced in the area around the cut-through, the upper reaches of the tidal creeks, the shallow expanse on the western side of Keppel Bay and at various tidal flats near the mouth of the Fitzroy (Figure 7.1.5). A similar trend is observed in the salinity solution (Figure 7.1.6), where evaporation increases salinity over the shallower regions. This is particularly evident in the upper reaches of Casuarina Creek, where salinity approaches 40 psu. This is consistent with anecdotal evidence, indicating the model is realistically representing the physics in this region. The western side of Keppel Bay also undergoes a noticeable salinity increase. Salinity is lowest in the upper Fitzroy due to base flow freshwater input at the barrage boundary.

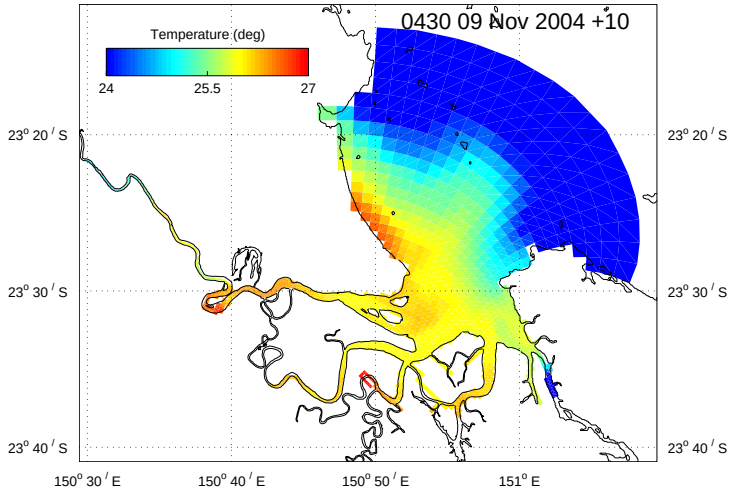


**Figure 7.1.5: Surface temperature during the dry season**

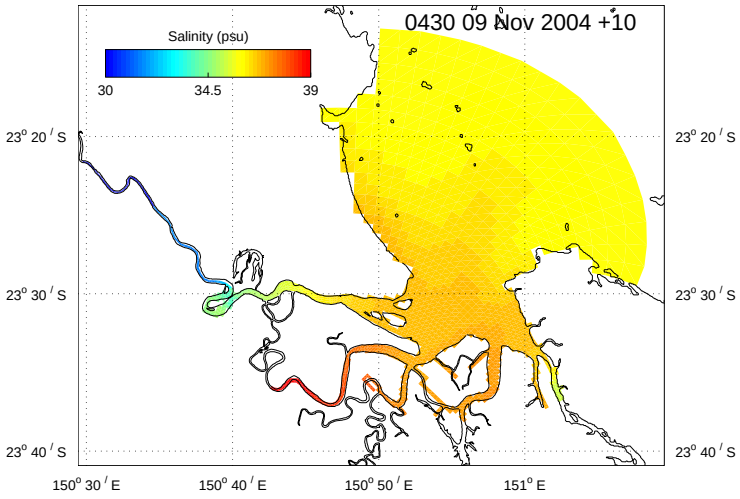


**Figure 7.1.6: Surface salinity during the dry season**

The large floods entering the Fitzroy Estuary during the wet season significantly alter the thermohaline distribution. The flood of February 2005 delivered a maximum flow of approximately 800 $m^3s^{-1}$ down the Fitzroy Estuary, which may be considered small by historical standards. Even so, this flood greatly retarded the tidal flow into the estuary on the flood tide (Figure 7.1.7). Under large floods of >10 000 $m^3s^{-1}$ it is possible that the tide would not reverse during the flood tide on the neap phase.

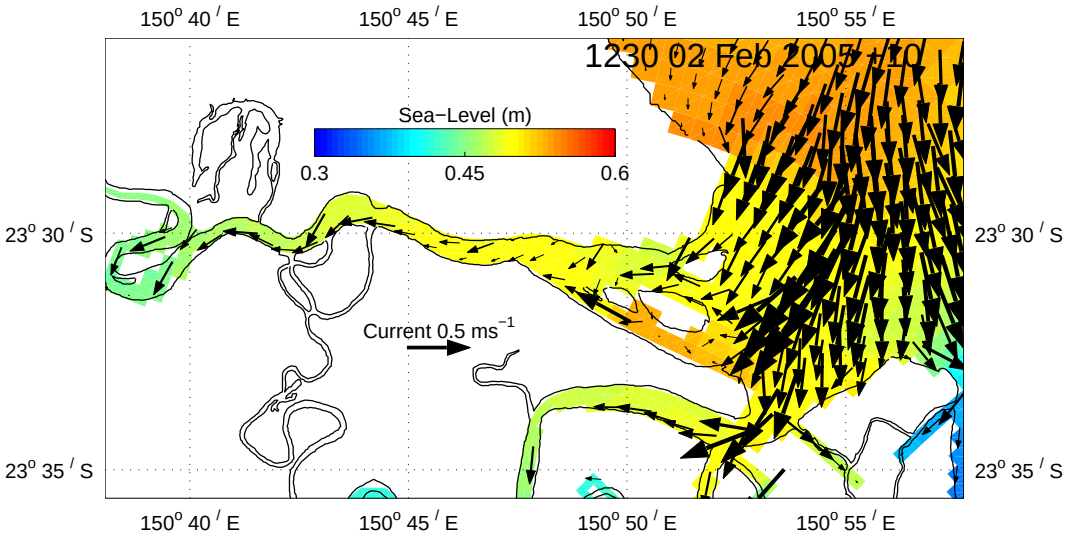


**Figure 7.1.7: Surface velocity during wet season flood: neap flood tide**

Three distinct flood events occurred during the 2004–2005 wet season (see Figure 5.4.1). These floods result in a plume of fresh water transported into Keppel Bay (Figure 7.1.8, after third flood peak). Salinity can be as low as 10 psu near the Fitzroy mouth, and significant salinity gradients occur throughout southern Keppel Bay. Salinity also decreases markedly in the tidal creeks. The Fitzroy Estuary has salinity of less than 1 psu along the majority of its length, and remains well mixed vertically above the cut-through. The presence of the freshwater plume in Keppel Bay increases stability of the water column, and consequently some stratification is observed (e.g. Figure 6.2.15). This stratification is quite spatially and temporally variable.

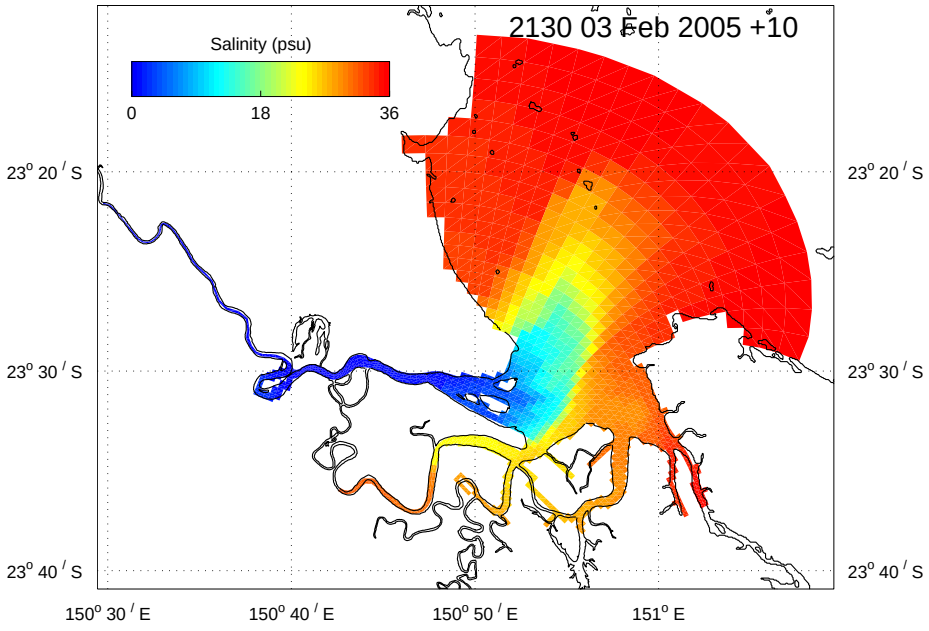


**Figure 7.1.8: Salinity distribution after ~800 $m^3s^{-1}$ flood**

The plume undergoes significant horizontal motion in response to the tidal pulsing (Figure 7.1.9). The plume position also responds to the effects of wind and the residual circulation; there appears to be no favoured direction of plume transport. Once the flood ceases the baroclinic pressure gradients drive saline water up the estuary. This process takes some time, and it may be many months before the upper reaches again experience marine (>30 psu) salinities. Figure 7.1.10 illustrates this recovery for the 2003–2004 wet season.

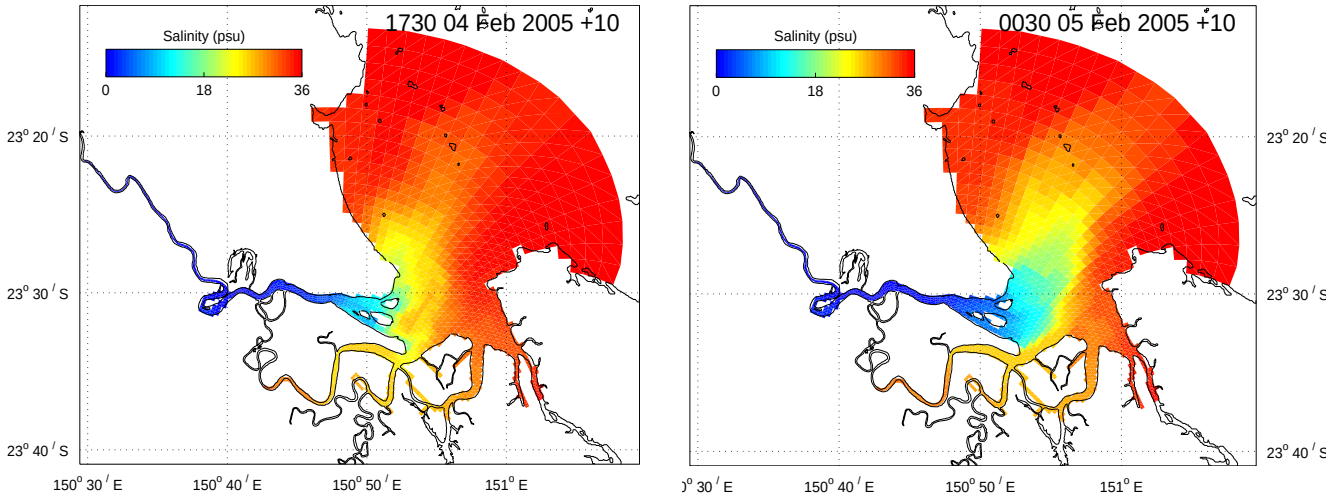


*(a) Flood tide* *(b) Ebb tide*

**Figure 7.1.9: Response of salinity plume to the tide**

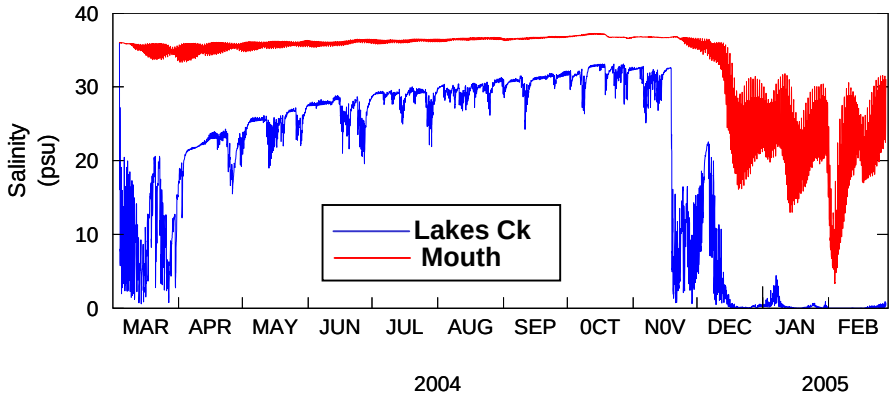


**Figure 7.1.10: Salinity time series**

Vertical diffusivity for the ebb tide is displayed in Figure 7.1.11. These mixing coefficients were generated using the Mellor-Yamada level 2.0 mixing scheme (Mellor & Yamada, 1982). Very large mixing is evident throughout Keppel Bay, with the largest mixing occurring near the Fitzroy mouth.

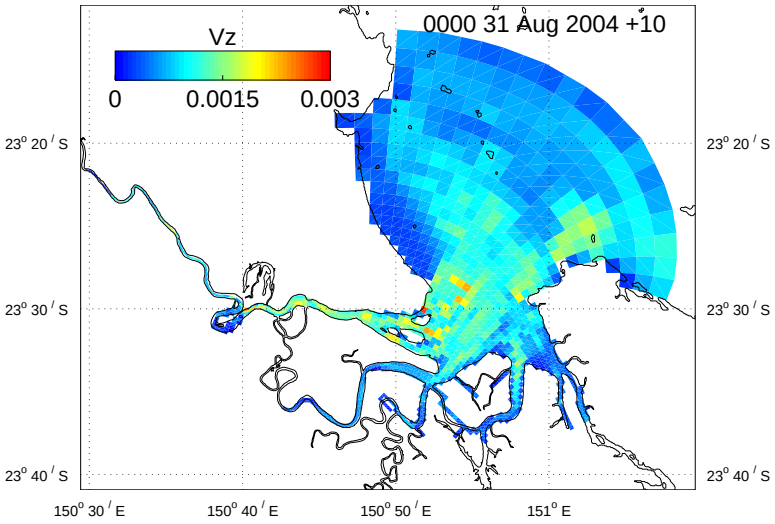


**Figure 7.1.11: Surface vertical viscosity ($m^2s^{-1}$), spring ebb tide**

## 7.2 Residual (net) currents

The long-term net flow in the domain was obtained by calculating a Eularian average of the model velocity components at every time step over 90- and 180-day periods. It is the net flow that is important from a flushing perspective, since transport by this flow provides a mechanism that may potentially remove material permanently from the estuary or Keppel Bay. The 90-day mean reveals no obvious coherent pattern in the residual flow (Figure 7.2.1). Flow is generally directed down-estuary, becoming stronger in the wet season [December to February, Figure 7.2.1(d)] due to flood waters propagating down the river. Flow is strongest near the mouth of the Fitzroy/Casuarina Creek, approaching 0.1 $ms^{-1}$. This down-estuary flow exits Keppel Bay generally along the western side of Curtis Island, becoming more evident in the wet.

A north-westward net flow can be seen at the north-western tip of Curtis Island, becoming stronger during and immediately after the wet season [Figure 7.2.1 (a,d)]. Apart from a vague north-eastward trend there exists no coherent flow in the remainder of Keppel Bay. An eastward boundary artifact is evident along the offshore open boundary. Apart from the strengthening of the down-estuary flow

in the wet season, there appears to be little seasonality in the residual circulation. The 180-day mean (March to August, Figure 7.2.2) exhibits the same trends as the 90-day means. These flow patterns reflect the distribution passive tracers are expected to follow in the long term.

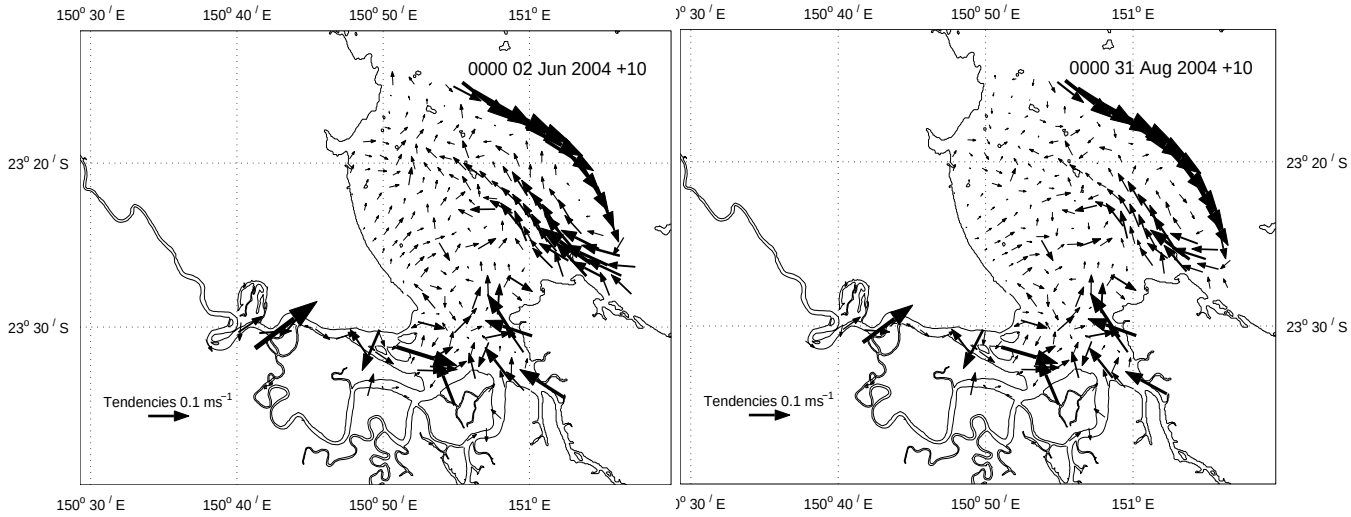


*(a) March–May* *(b) June–August*

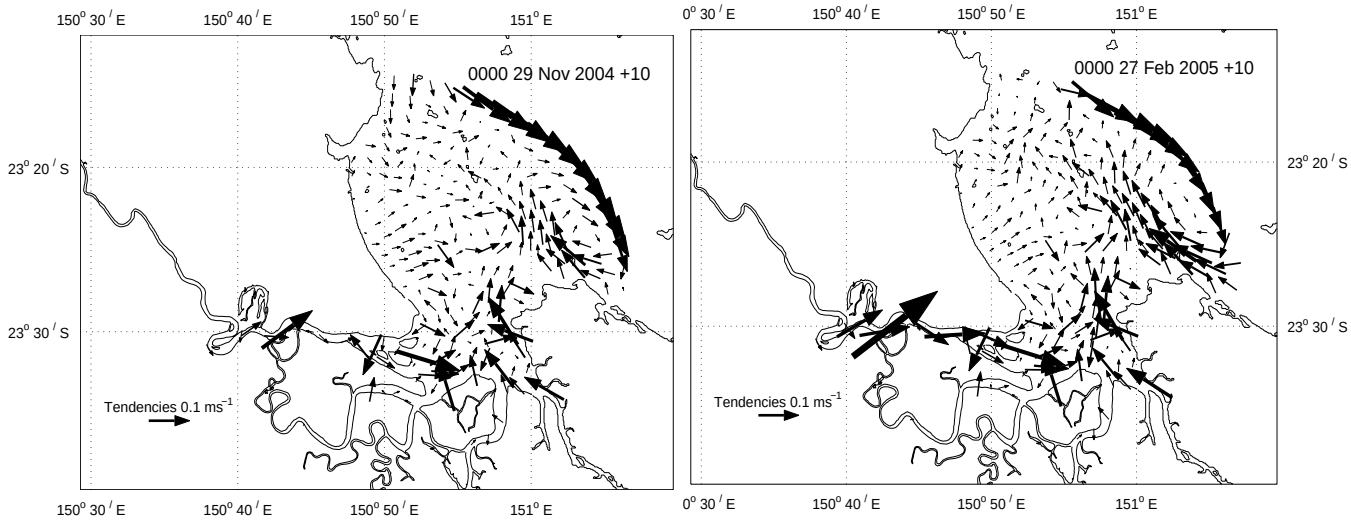


*(a) September–November* *(b) December–February*

**Figure 7.2.1: Mean surface currents, 90-day mean**

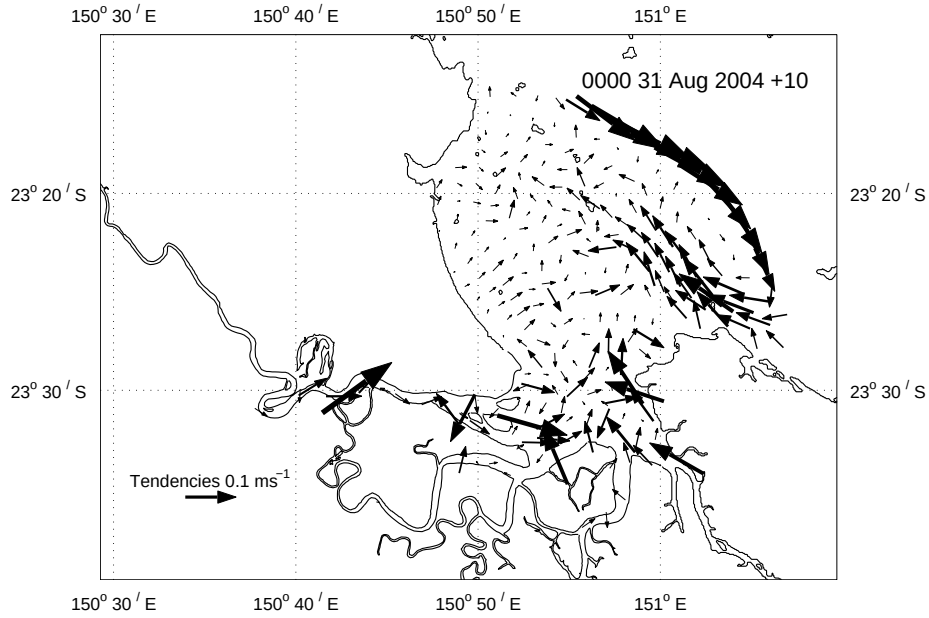


**Figure 7.2.2: Mean surface circulation, March–August, 180-day mean**

Although the currents generated by tidal forcing (sea-level driven or barotropic flow) are large, they are periodic by nature and only result in net flow through non-linear interactions with topography. These tidally rectified currents are small, ~$1x10^{-8}$ $ms^{-1}$ (Figure 7.2.3), and contribute almost nothing to the net flow. The baroclinic net circulation (density driven flow) also makes a negligible contribution to the mean flow throughout Keppel Bay (Figure 7.2.4); however, in the upper estuary this contribution is the largest (~$2x10^{-4}$ $ms^{-1}$ up-estuary) representing the propagation of saline water towards the barrage during the dry season.

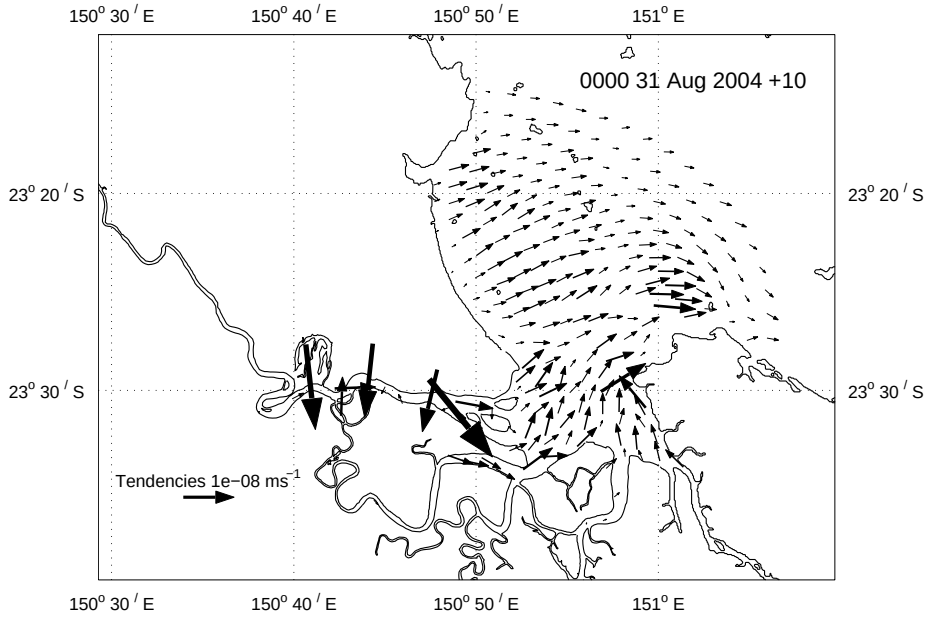


**Figure 7.2.3: Mean surface barotropic circulation (90 days, June–August)**

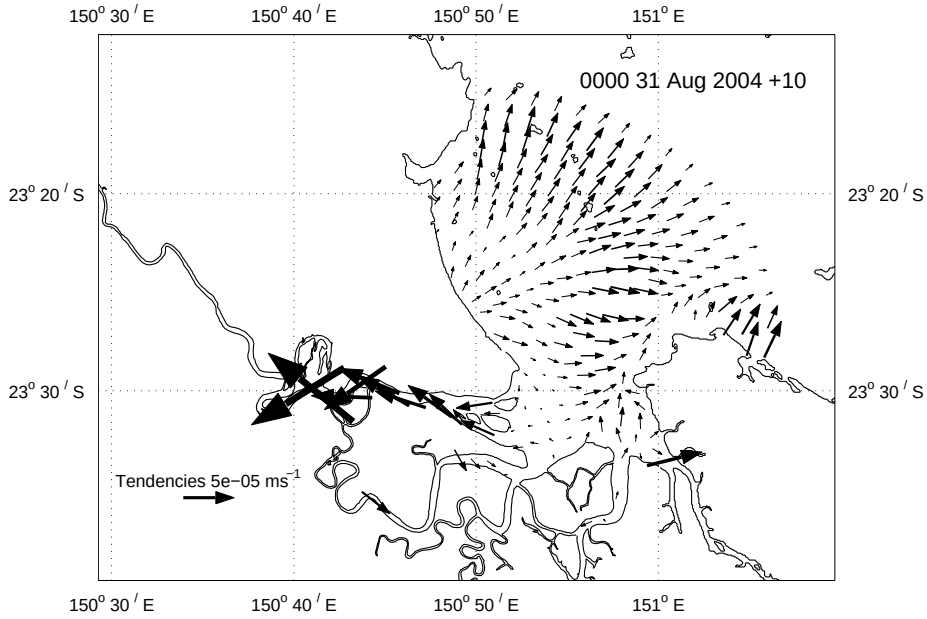


**Figure 7.2.4: Mean surface baroclinic circulation (90 days, June–August)**

The main contribution to the residual flow comes from the vertical diffusive component (Figure 7.2.5). Near the surface this may be loosely interpreted as the contribution due to the wind; however, this term actually represents $\frac{\partial}{\partial z}(V_Z \frac{\partial \bar{u}}{\partial z})$ in the momentum equation, where $V_z$ ($m^2s^{-1}$) is the vertical viscosity (i.e. coefficient of vertical mixing). The wind stress only acts as the surface boundary condition for this term, and there may be effects of vertical mixing of

momentum (i.e. bottom drag effects) present at the surface, especially if the water column is shallow and well mixed.

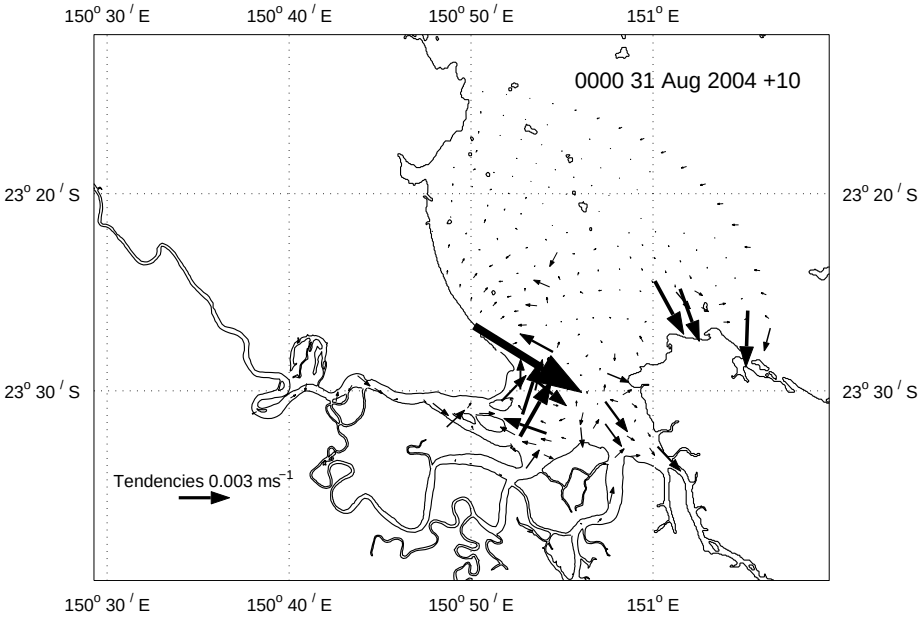


**Figure 7.2.5: Mean circulation due to vertical diffusion (90 days, surface)**

The mean wind (Figure 7.2.6) shows a south-easterly trend which, if the surface mixed layer were decoupled from the bottom boundary layer, would tend to drive surface flow in a roughly westward direction (surface currents are rotated approximately 45° to the left of the wind in the southern hemisphere). Clearly this is not evident in Figure 7.2.5, indicating boundary layer overlap and vertical mixing of sources (surface wind) and sinks (bottom drag) of momentum. Note that since bottom drag is non-linear (quadratic), the large tidal currents at the bottom may contribute to the mean vertical diffusive tendency through bottom drag even though they have little contribution via the barotropic tendency. The non-linear momentum advection terms provide the next-largest contribution to the mean flow (Figure 7.2.7), indicating that the net circulation is a non-linear balance between input of momentum at the surface via wind stress, loss of momentum due to bottom drag and redistribution of momentum via advection. The residual circulation in the domain is therefore complex and cannot be conceptualised through simple linear interactions.

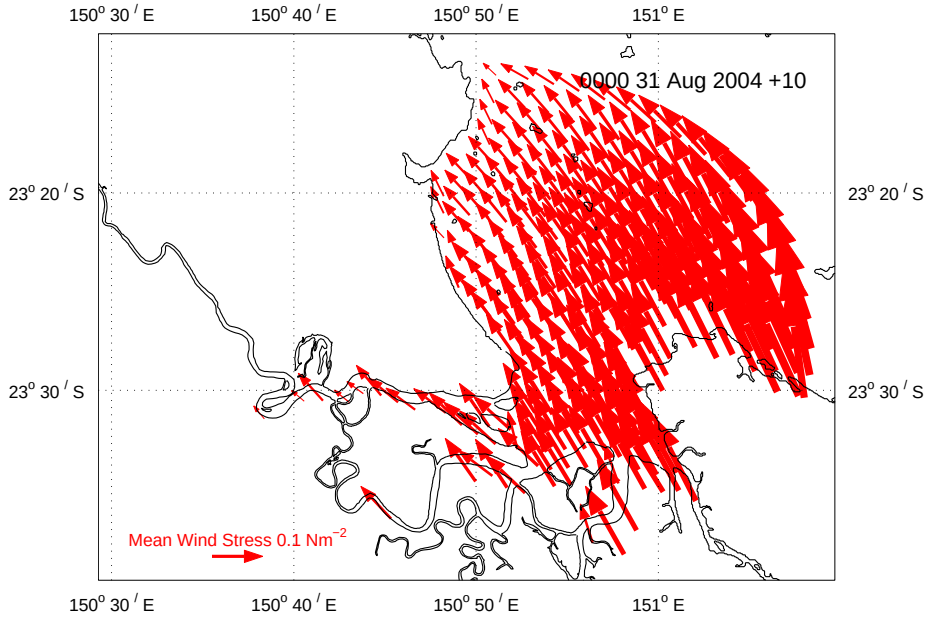


**Figure 7.2.6: Mean wind stress (90 days, surface)**

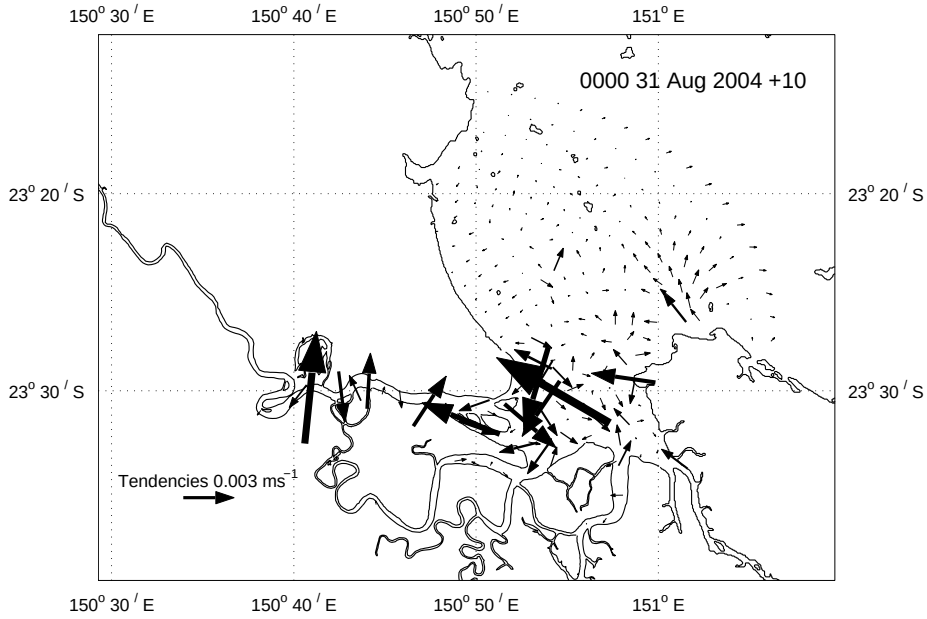


**Figure 7.2.7: Mean advective circulation (90 days, surface)**

## 7.3 Flushing characteristics

Passive tracers were used to obtain an estimate of the flushing characteristics of various regions within the Fitzroy Estuary and Keppel Bay. A passive tracer was initialised in a subregion of the estuary with a concentration of 1 and zero elsewhere, and the total mass in this subregion was calculated throughout the simulation. Full forcing was applied to the domain (i.e. wind, tide, low frequency sea level and temperature/salinity effects). The e-folding time for flushing this subregion is encountered when the total mass was reduced to 1/e (~38%) of the initial mass. This representation of the flushing time assumes that tracer is well mixed in the subregion and the total mass is assumed to decrease exponentially according to:

$$M(t) = M_0 e^{-t/\tau} \qquad \text{(Eqn 7.3.1)}$$

where $M_0$ is the initial mass and $\tau$ is the flushing time scale (Tartinville *et al.*, 1997). When $M = M_0/e$ then $t = \tau$, hence the flushing time can be recovered.

Dry season (August 2004) flushing times for various subregions of the domain are displayed in Figures 7.3.1 to 7.3.9. These figures include the initial tracer distribution which defines the subregion, the tracer distribution at the flushing time and the temporal evolution of normalised total mass in the subregion.

The flushing times are tabulated in Table 7.3.1; included in this table are the flushing times for the various subregions during the wet season (February 2005). The time series of the normalised total mass in the subregion indicates that total mass oscillates on the tidal frequency as tracer is brought into the domain on the flood and removed on the ebb. The general trend of tracer decrease is obtained by fitting a second- or third-order polynomial to the total mass, which aids in identifying the time $\tau$ when total mass is reduced to 1/e. The exponential curve of equation 7.3.1 is also fitted to the data, using the time scale $\tau$ identified from the polynomial fit.

**Table 7.3.1: Flushing times**

| Region | Start time | Flushing time (days) |
|---|---|---|
| **Fitzroy Estuary** | **1 Aug 2004** | **74** |
| **Fitzroy Estuary** | **2 Feb 2005** | **2.4** |
| **Casuarina creek** | **1 Aug 2004** | **34.5** |
| **Casuarina creek** | **2 Feb 2005** | **19** |
| **Connor/Deception creeks** | **1 Aug 2004** | **4.5** |
| **Connor/Deception creeks** | **2 Feb 2005** | **4.5** |
| **Cut-through** | **1 Aug 2004** | **5** |
| **Cut-through** | **2 Feb 2005** | **1.5** |
| **Keppel Bay** | **1 Aug 2004** | **6** |
| **Keppel Bay** | **2 Feb 2005** | **4.8** |
| **Whole region** | **1 Aug 2004** | **13.5** |
| **Whole region** | **2 Feb 2005** | **6.6** |

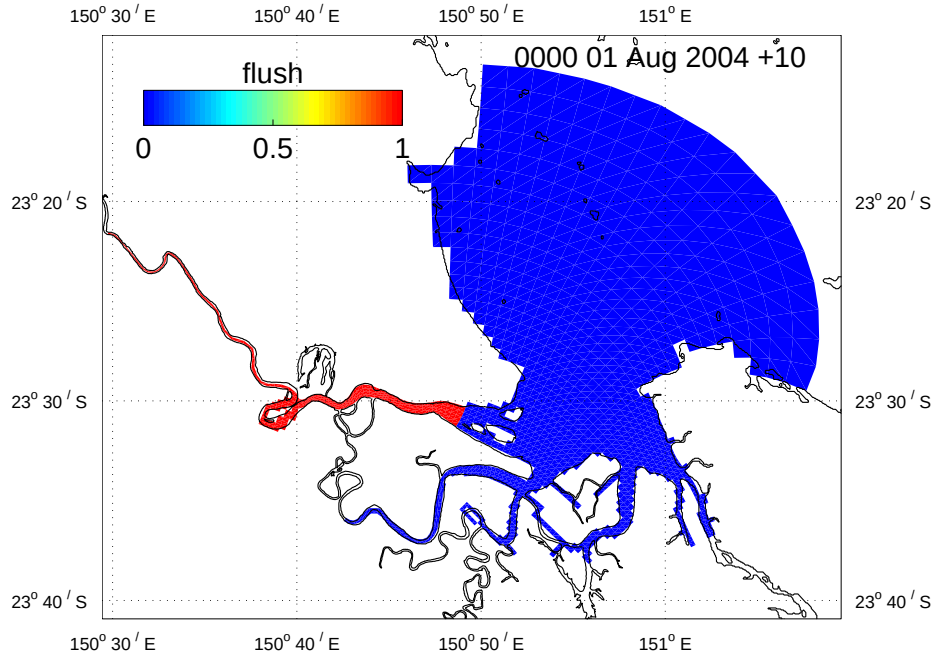


**Figure 7.3.1(a): Initial tracer distribution: Fitzroy Estuary**

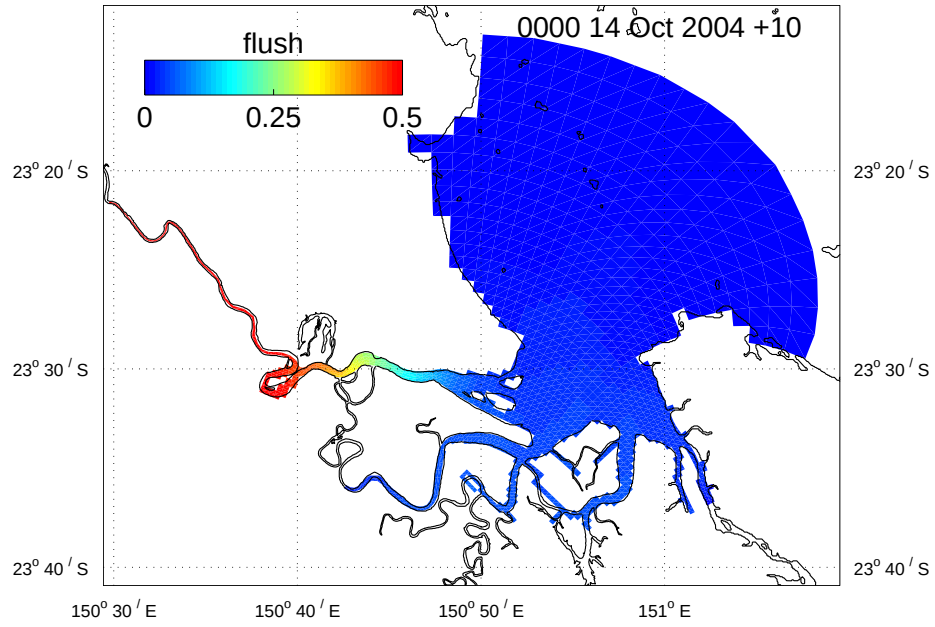


**Figure 7.3.1(b): Tracer distribution at 74 days**

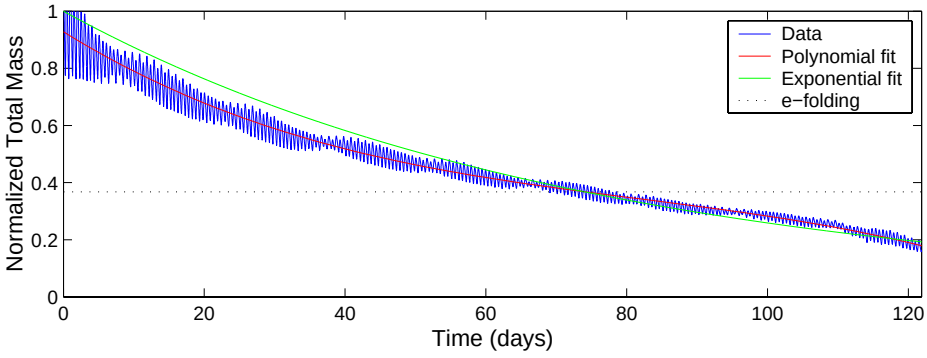


**Figure 7.3.1(c): Normalised total mass for the Fitzroy Estuary subregion**

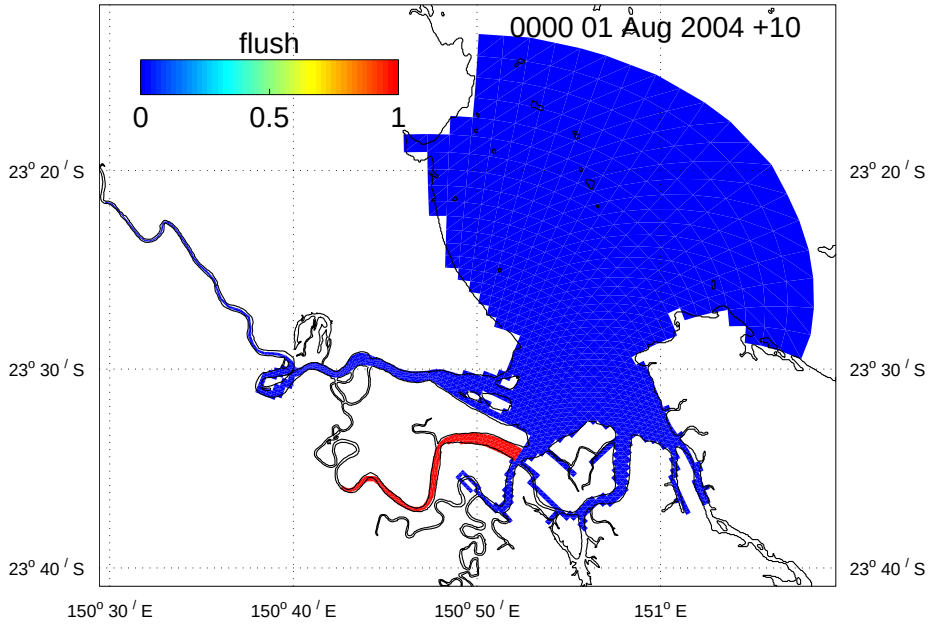


**Figure 7.3.2(a): Initial tracer distribution: Casuarina creek**

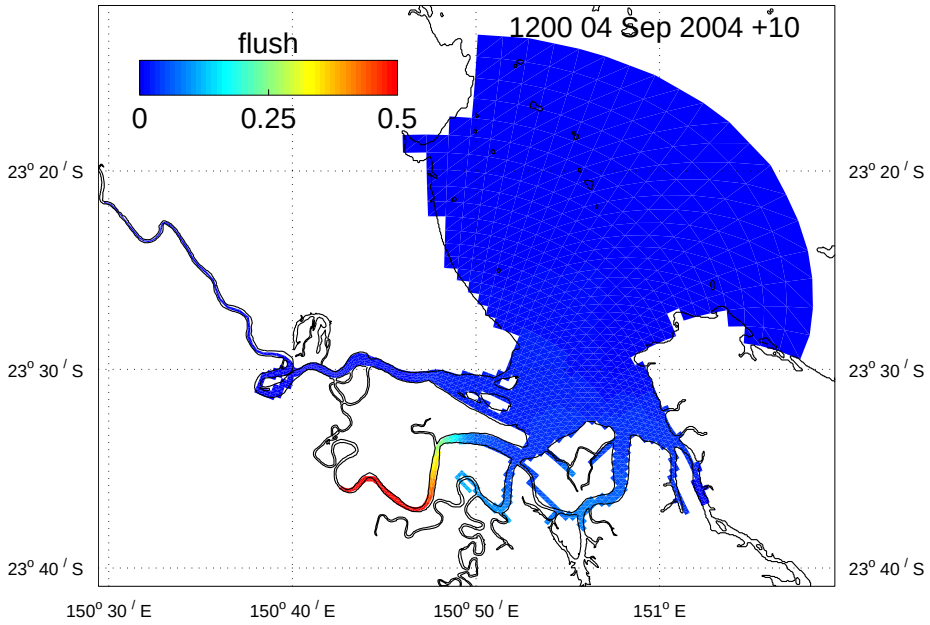


**Figure 7.3.2(b): Tracer distribution at 34.5 days**

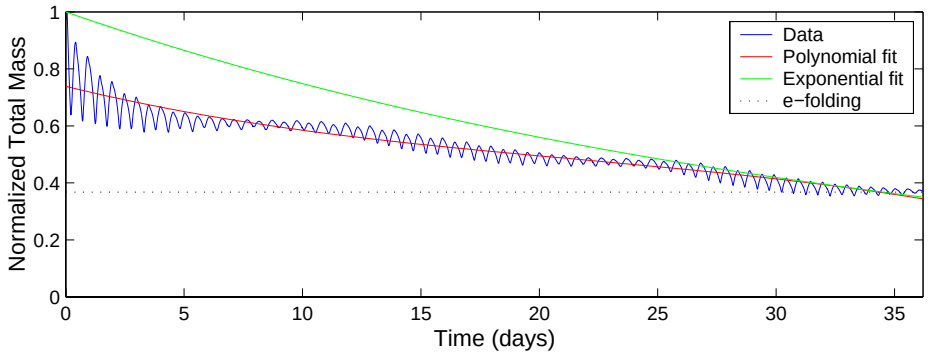


**Figure 7.3.2(c): Normalised total mass for the Casuarina creek subregion**

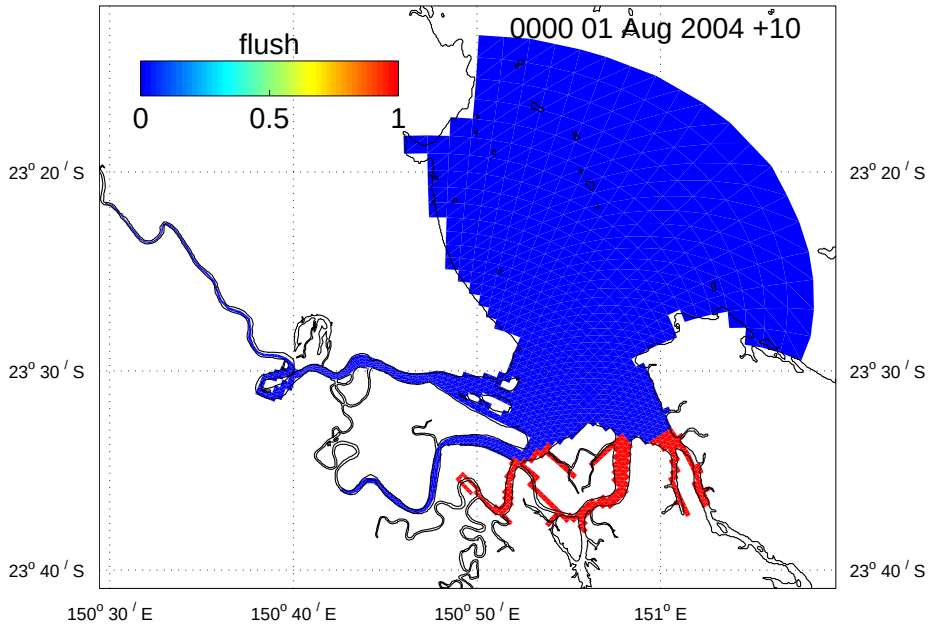


**Figure 7.3.3(a): Initial tracer distribution: Connor/Deception creeks**

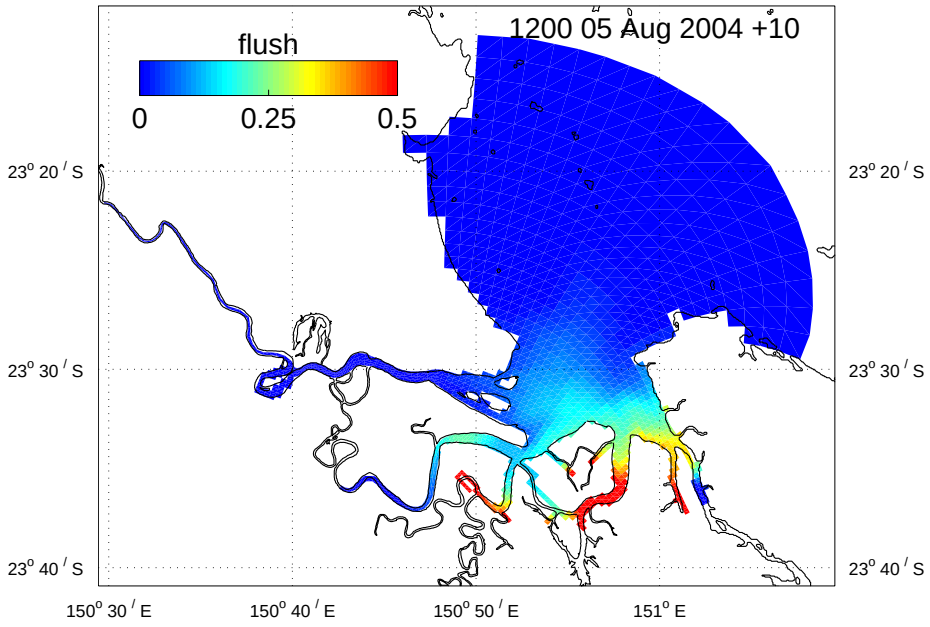


**Figure 7.3.3(b): Tracer distribution at 4.5 days**

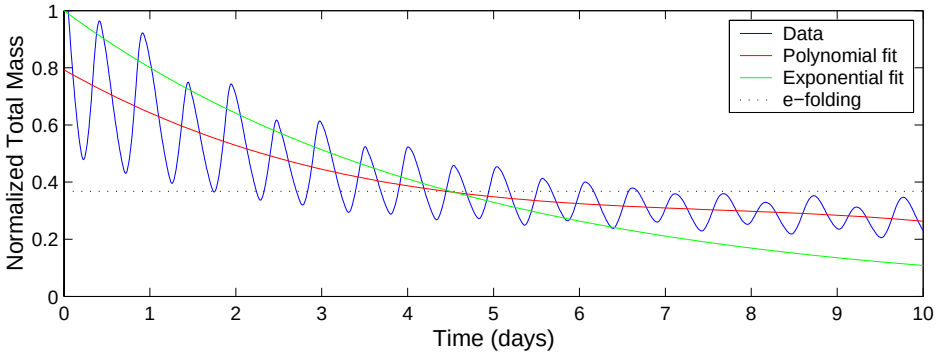


**Figure 7.3.3(c): Normalised total mass for the Connor/Deception creeks subregion**

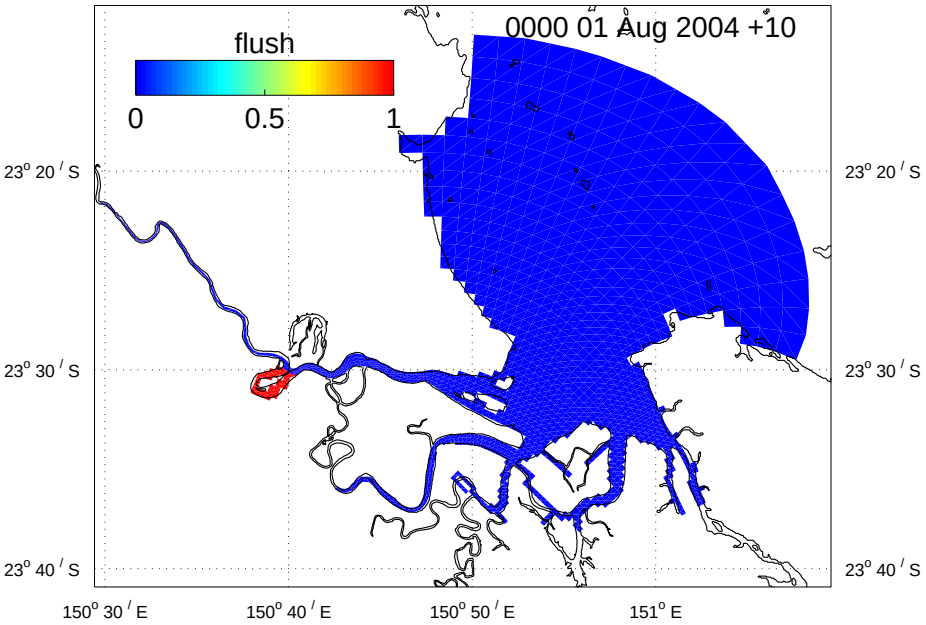


**Figure 7.3.4(a): Initial tracer distribution: cut-through**

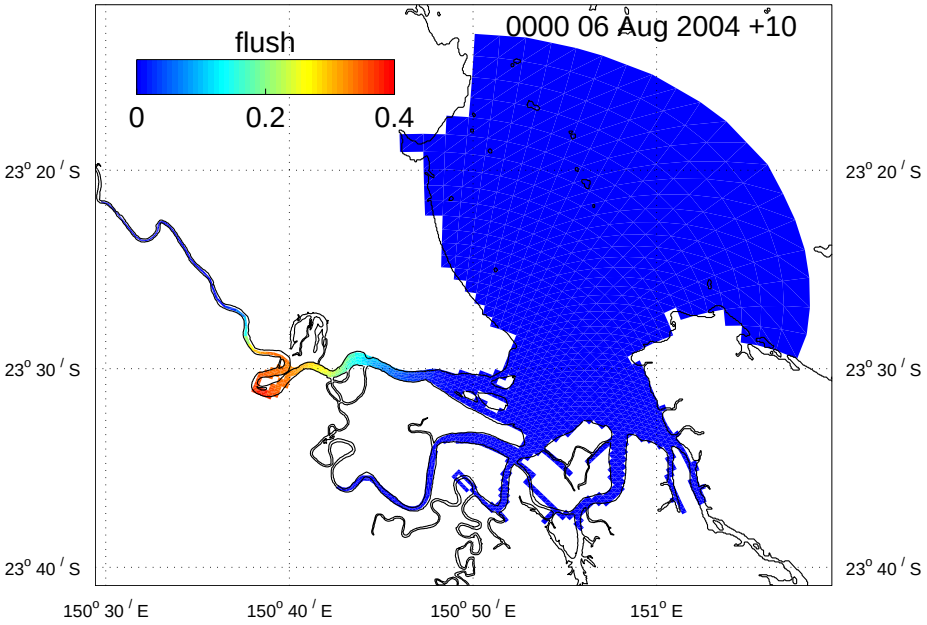


**Figure 7.3.4(b): Tracer distribution at 5 days**

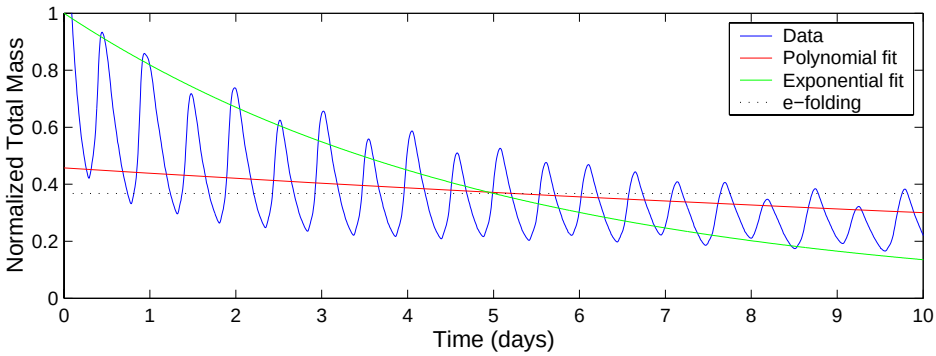


**Figure 7.3.4(c): Normalised total mass for the cut-through subregion**

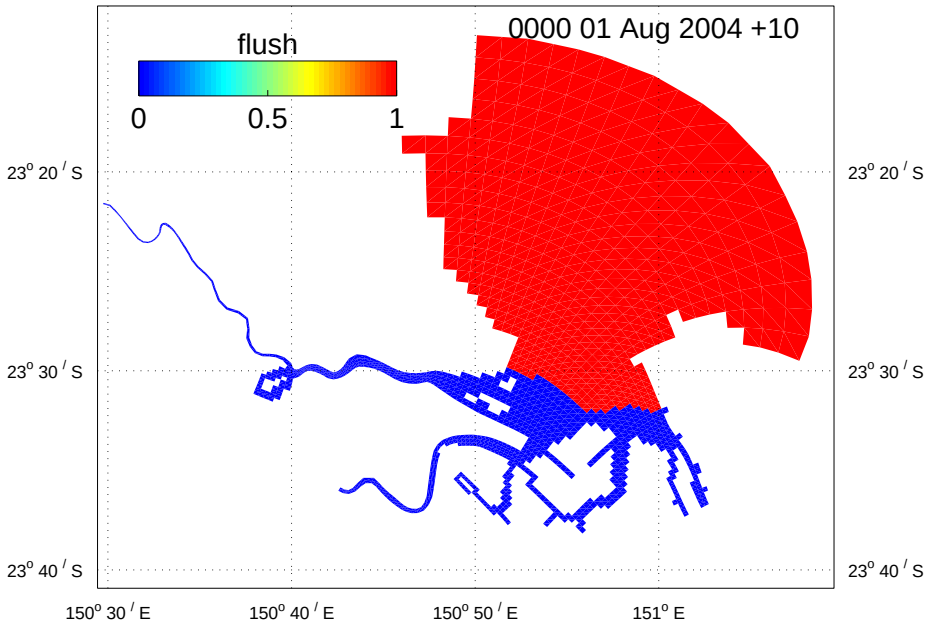


**Figure 7.3.5(a): Initial tracer distribution: Keppel Bay**

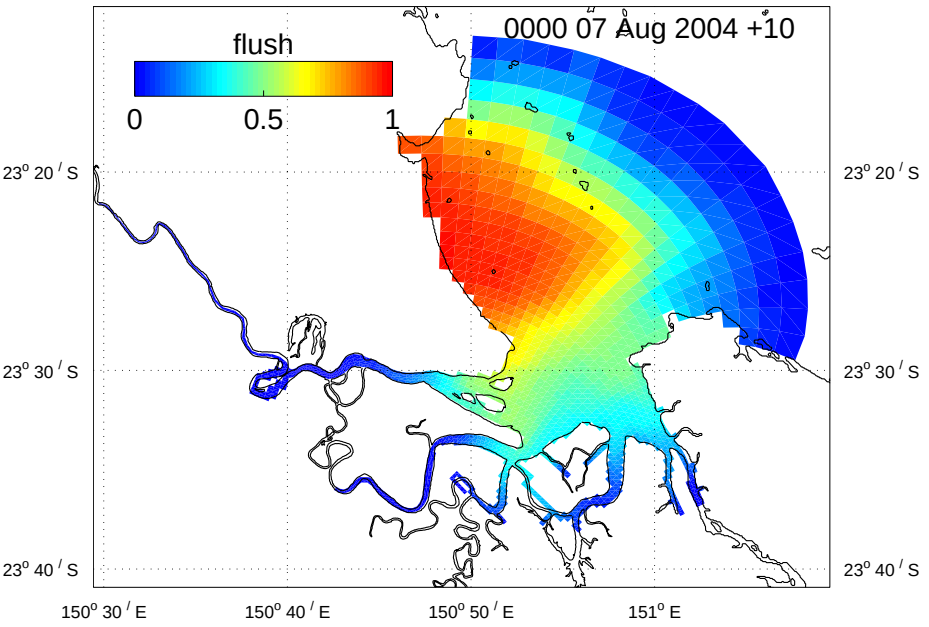


**Figure 7.3.5(b): Tracer distribution at 6 days**

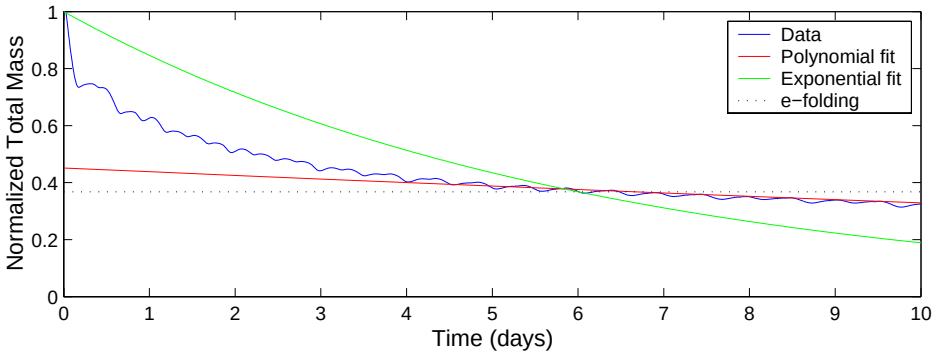


**Figure 7.3.5(c): Normalised total mass for the Keppel Bay subregion**

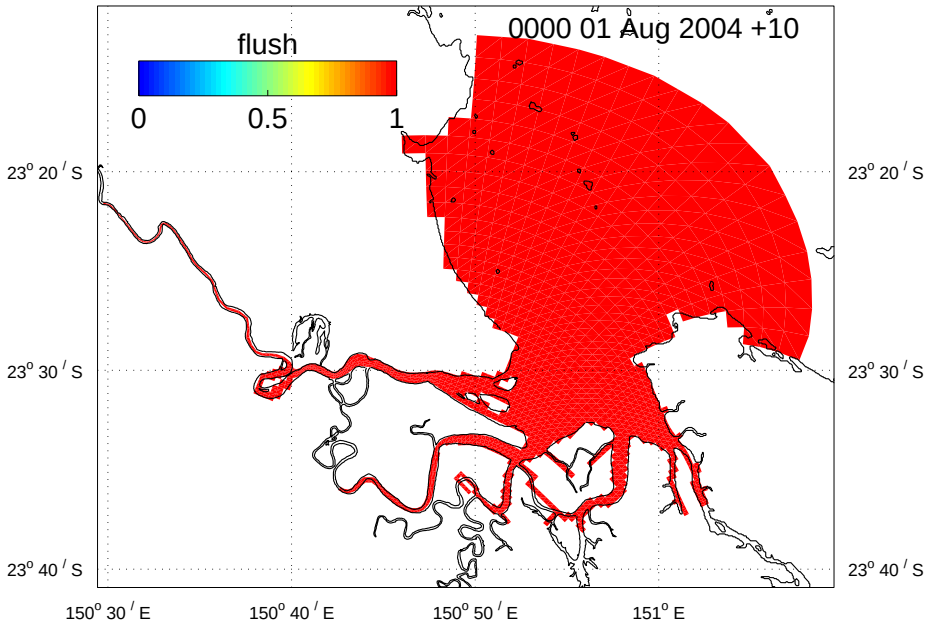


**Figure 7.3.6(a): Initial tracer distribution: whole region**

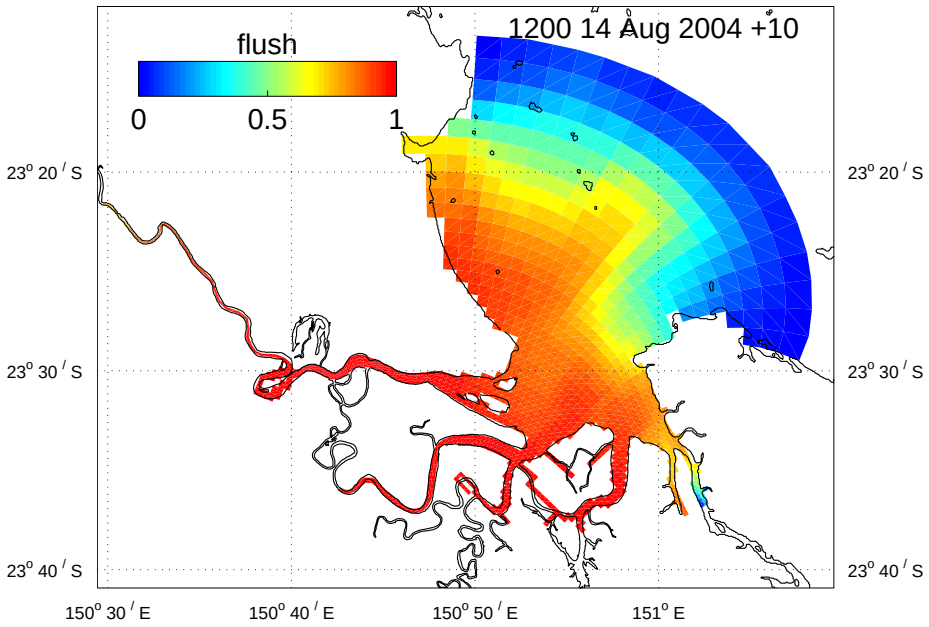


**Figure 7.3.6(b): Tracer distribution at 13.5 days**

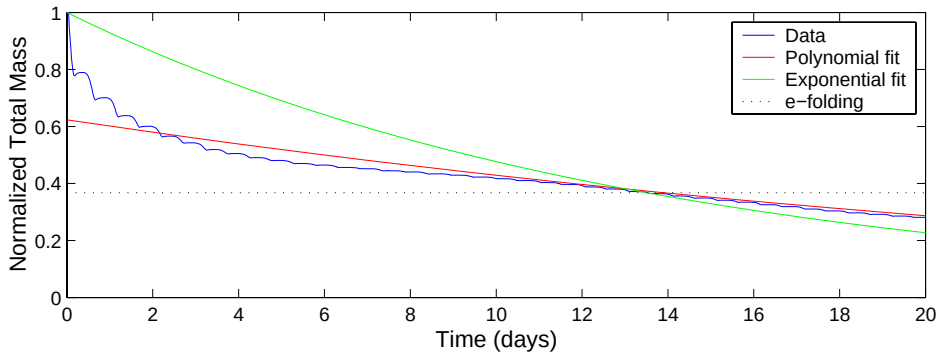


**Figure 7.3.6(c): Normalised total mass for the whole region subregion**

Table 7.3.1 indicates that there exists a wide range of flushing times depending on which region is flushed. The whole Fitzroy Estuary has the slowest flushing of ~2.5 months in the dry season, followed by Casuarina Creek with ~1 month. The disparity between the wet and dry season flushing times for these regions is large. The flushing for the Fitzroy is reduced from ~75 days in the dry to under 3 days in the wet when an ~800 $m^3s^{-1}$ flood is propagating down the Fitzroy. This wet season flushing is the second-fastest of any region during wet or dry seasons. Fastest flushing is the cut-through, which is a smaller subregion of the estuary and therefore expected to flush quickly in times of flood. For larger floods it is anticipated the Fitzroy flushing time would be even less.

During the dry season the estuary appears to be very poorly flushed, and relies on the wet season flooding for renewal of water. After 10 days following the February 2005 flood the estuary flushing results in significant amounts of tracer (up to 10% of initial concentration) in the adjacent tidal creeks (Figure 7.3.7). The tracer transport into these areas only occurs after ~day 5 of the flushing. During the dry season there is negligible tracer outside the estuary at the flushing time. Flushing time of Casuarina Creek is approximately halved during the wet season flooding.

Not much difference is observed in Keppel Bay flushing as a function of season, with the flushing during any season around 5 days. Exchange of water into Keppel Bay chiefly occurs via the open boundaries, thus flushing is reasonably independent of Fitzroy flooding. The initial rapid decrease in concentration in Figure 7.3.5(c) is a result of an inital loss of tracer through the offshore boundary. The flushing of the whole region is lengthened from the flushing of Keppel Bay due to the slow exchange within the estuary. Fast flushing of the estuary in the wet decreases this rate to approximately half. The Connor and Deception Creeks tidal flushing does not appear to be influenced by Fitzroy flooding. Exchange of water in these regions is primarily restricted to the lower reaches with Keppel Bay [Figure 7.3.3(b)].

The flushing estimates computed above are a somewhat subjective measure of exchange, since there are various methods of computing flushing (e.g. Tartinville *et al.*, 1997) which may potentially yield different results, and the assumptions made in deriving flushing times are often violated. The final tracer concentration distributions clearly show that tracer is not always well mixed throughout the flushing region, hence flushing estimates may be compromised. For example, tracer loss in Figure 7.5.3(b) is clearly overly influenced by the open boundary, hence the flushing time derived may not refect the flushing of the Keppel Bay region as a whole.

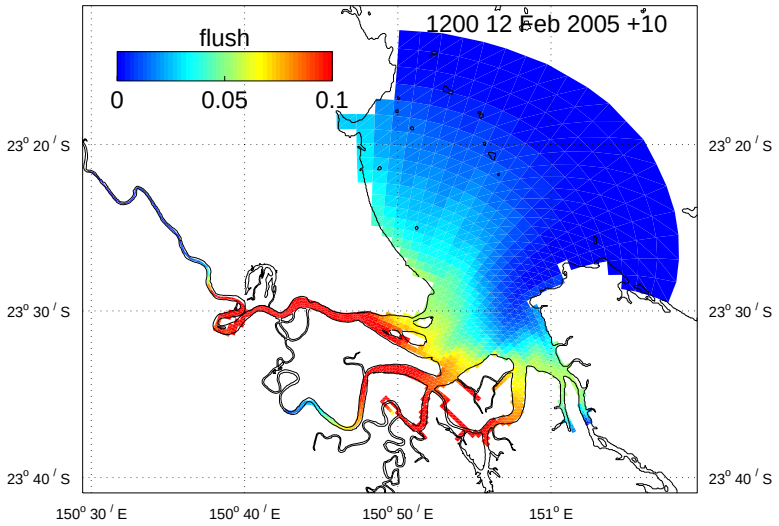


**Figure 7.3.7: Tracer distribution after 10 days, Fitzroy Estuary flushing, wet season**

## 7.4 Mixing zones

Point sources of tracers were continuously input to the water column at locations corresponding to a number of sites (Figure 7.5.1) with unit loads (assumed to be 1 $gs^{-1}$ ~ 31 500 kg/year, giving output concentrations in units of $gm^{-3}$, or $mgL^{-1}$) for the 12-month simulation period of March 2004 to February 2005. Tracers were released into surface waters. The continuous tracer input will be advected and mixed to result a quasi steady distribution, which will vary according to the forcing (wind, tide and river flow) in effect at any point in time. These distributions at any given time are not particularly useful to characterise the general tracer distribution, hence a statistical tracer distribution representing the whole simulation period was generated.

Surface tracer distributions were output at one-hour intervals and post-processed to compute the 5th, 50th (median) and 95th percentile concentration distributions for the whole simulation, providing a statistical description of the distributions resulting from tracer transport over this period. Owing to the volume of information that must be stored to compute the statistical distributions, only distributions for the surface layer where attempted and it was not feasible to create plots in bottom waters or along sections down the estuary. Note that the response of the tracers to the interaction of the point source input with the system dynamics is linear, so that if the load were scaled by some arbitrary factor then the corresponding concentrations can be scaled accordingly.

Results are displayed in Figures 7.4.2 to 7.4.9. Results are interpreted thus: given that a continuous unit load is input at the Port Alma site and its distribution throughout the domain allowed to reach quasi-steady state, at any given location in the domain one would expect to find the concentrations less than those shown in Figure 7.5.2(a) for 5% of the time; less than those in Figure 7.5.2(b) for 50% of the time; and less than those in Figure 7.5.2(c) for 95% of the time. These percentile plots provide a statistical description of the tracer concentration throughout the domain expected from various point source releases. Note that the concentration scales in the figures for the three percentiles generally differ from one another.

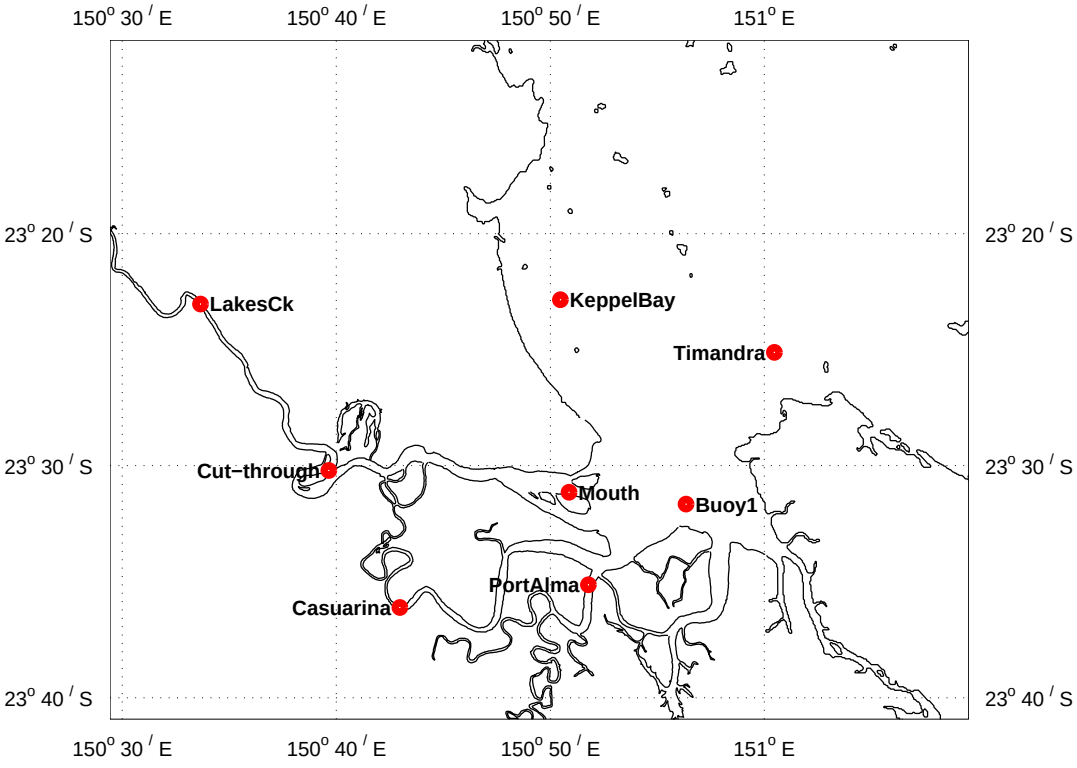


**Figure 7.4.1: Point source release locations**

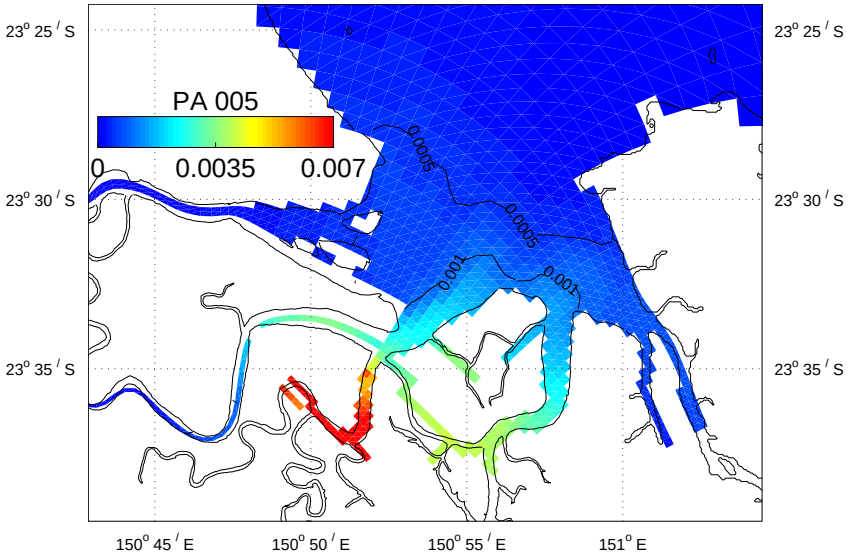


**Figure 7.4.2(a): Port Alma release 5 percentile distribution**

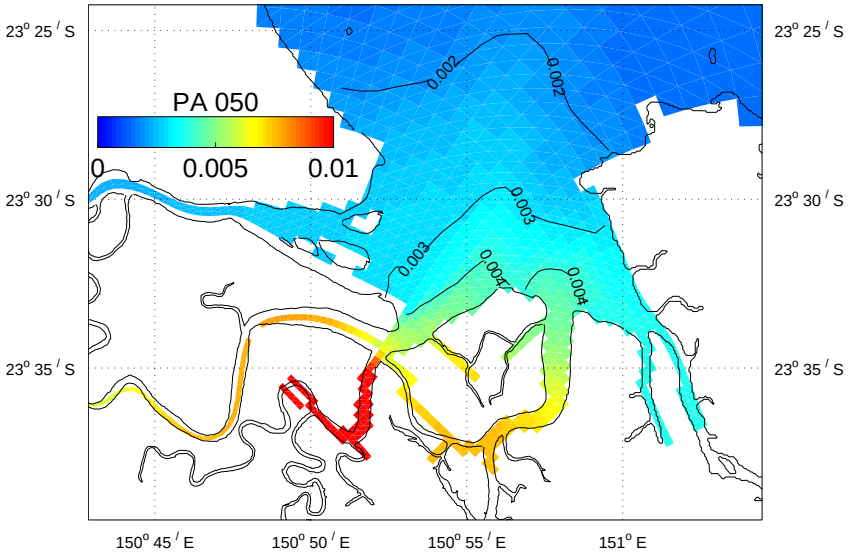


**Figure 7.4.2(b): Port Alma release median distribution**

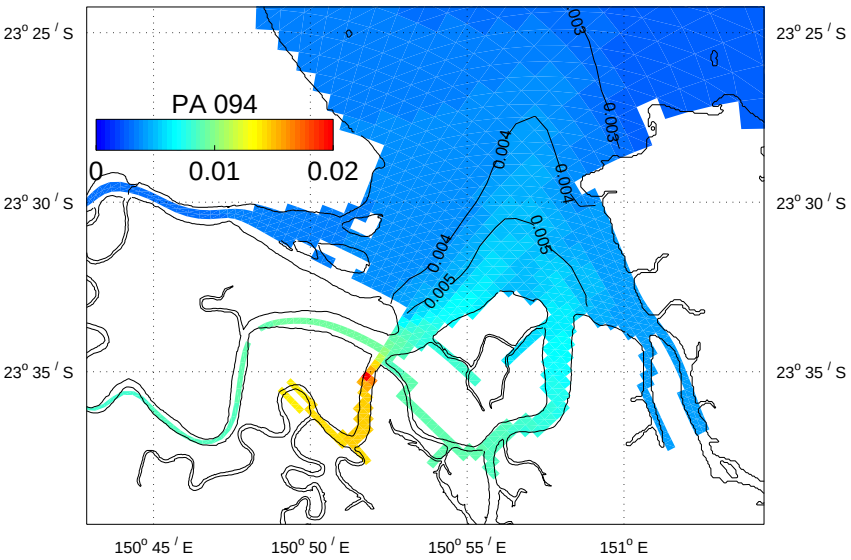


**Figure 7.4.(c): Port Alma release 95 percentile distribution**

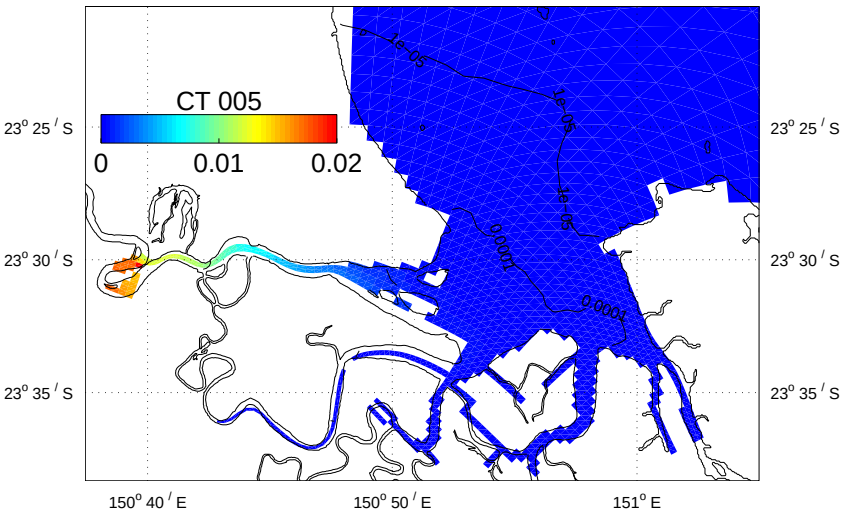


**Figure 7.4.3(a): Cut-through release 5 percentile distribution**

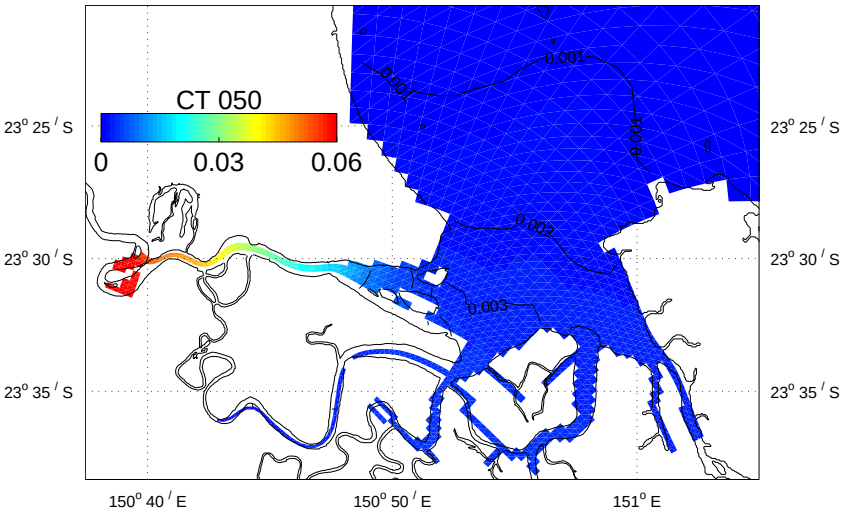


**Figure 7.4.3(b): Cut-through release median distribution**

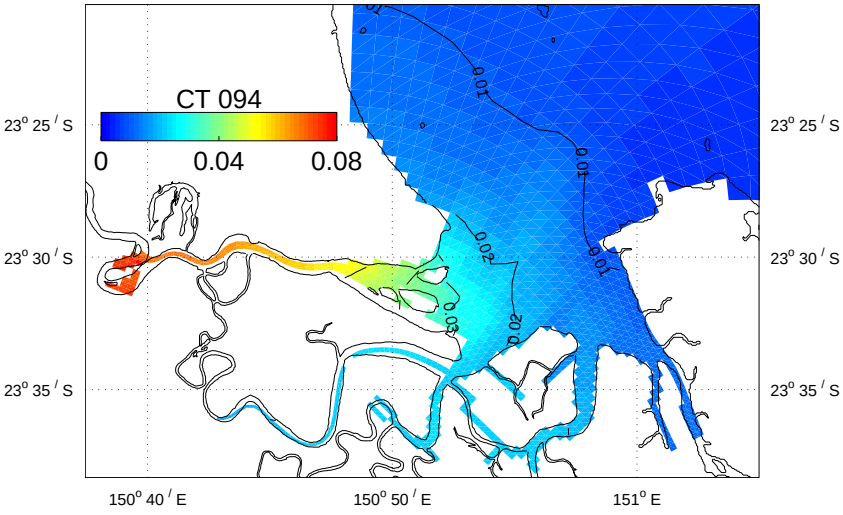


**Figure 7.4.3(c): Cut-through release 95 percentile distribution**

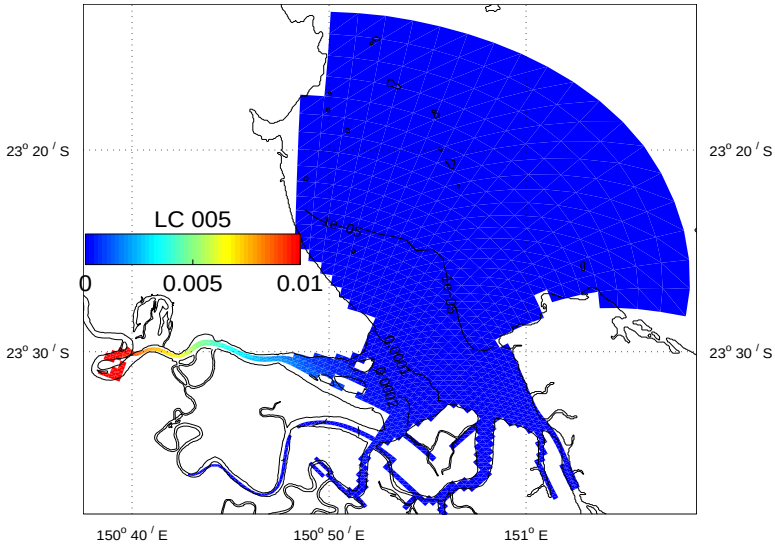


**Figure 7.4.4(a): Lakes Creek release 5 percentile distribution**

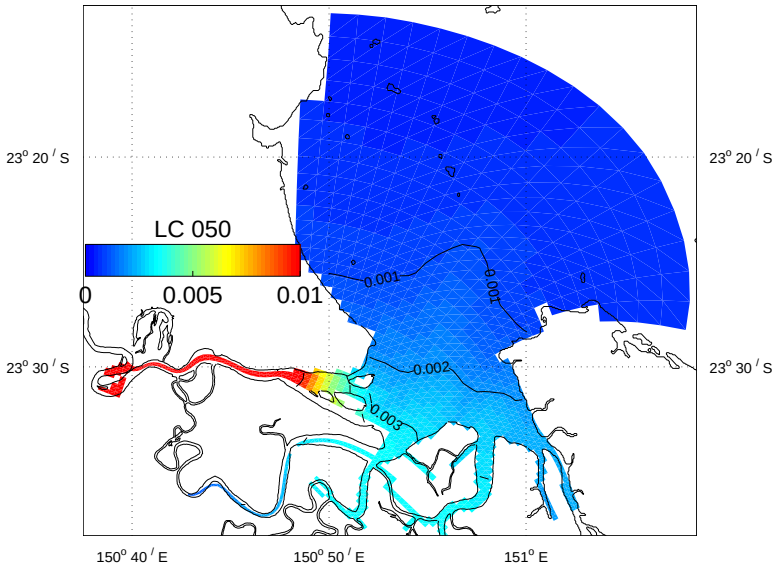


**Figure 7.4.4(b): Lakes Creek release median distribution**

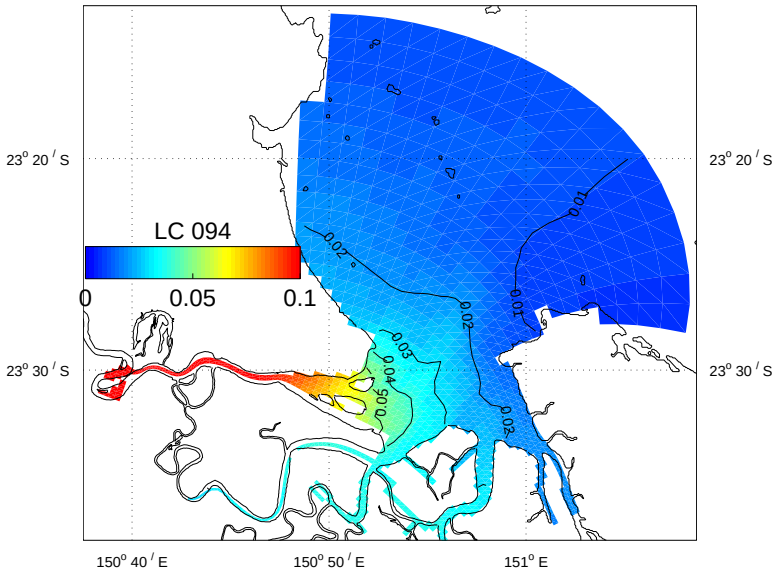


**Figure 7.4.4(c): Lakes Creek release 95 percentile distribution**

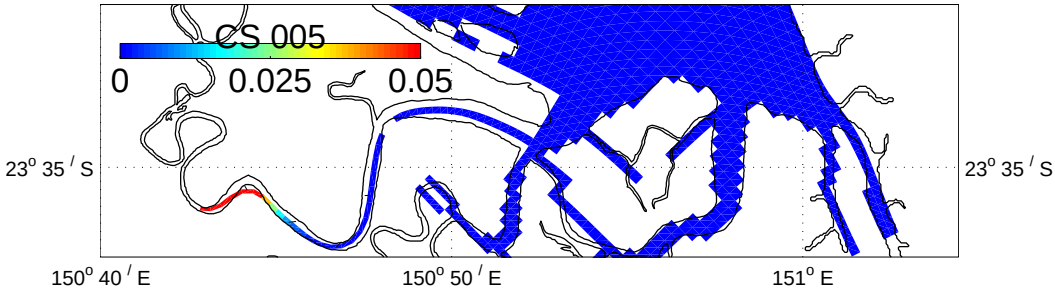


**Figure 7.4.5(a): Casuarina Creek release 5 percentile distribution**

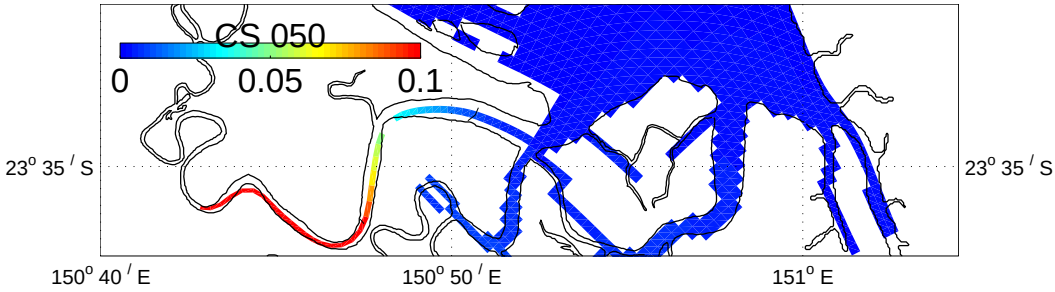


**Figure 7.4.5(b): Casuarina Creek release median distribution**

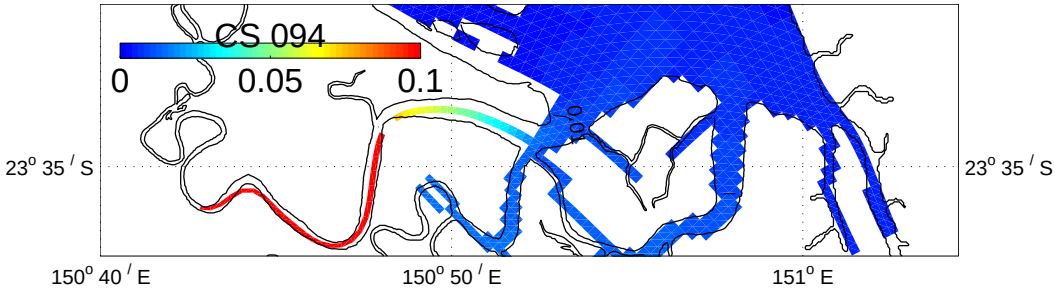


**Figure 7.4.5(c): Casuarina Creek release 95 percentile distribution**

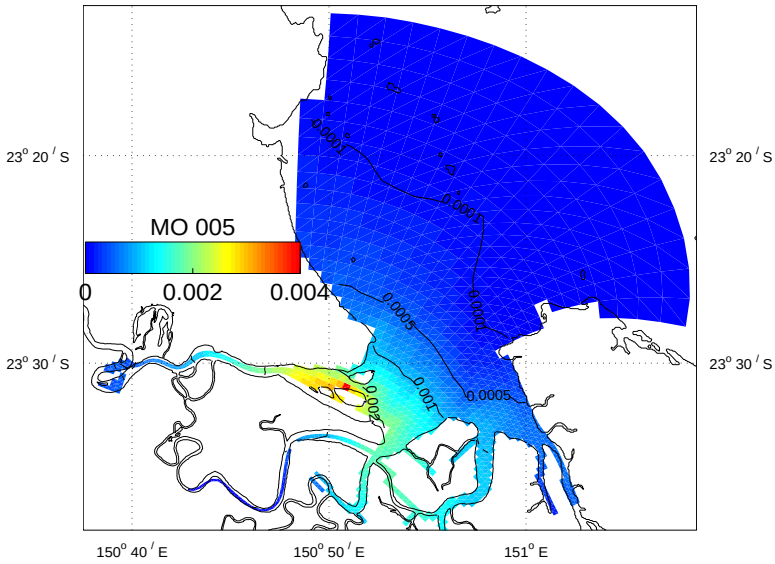


**Figure 7.4.6(a): Fitzroy mouth release 5 percentile distribution**

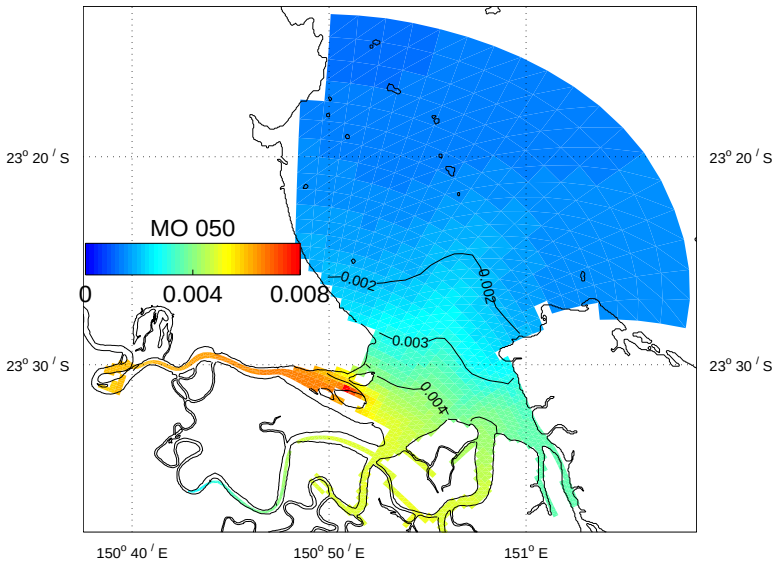


**Figure 7.4.6(b): Fitzroy mouth release median distribution**

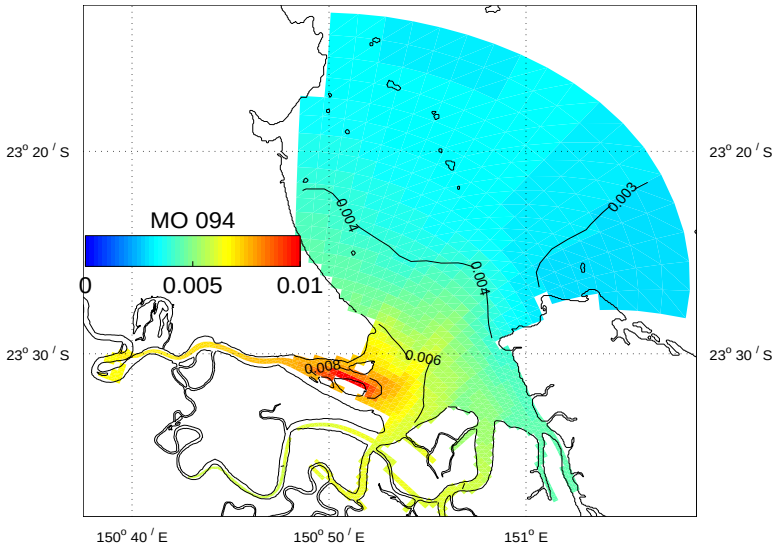


**Figure 7.4.6(c): Fitzroy mouth release 95 percentile distribution**

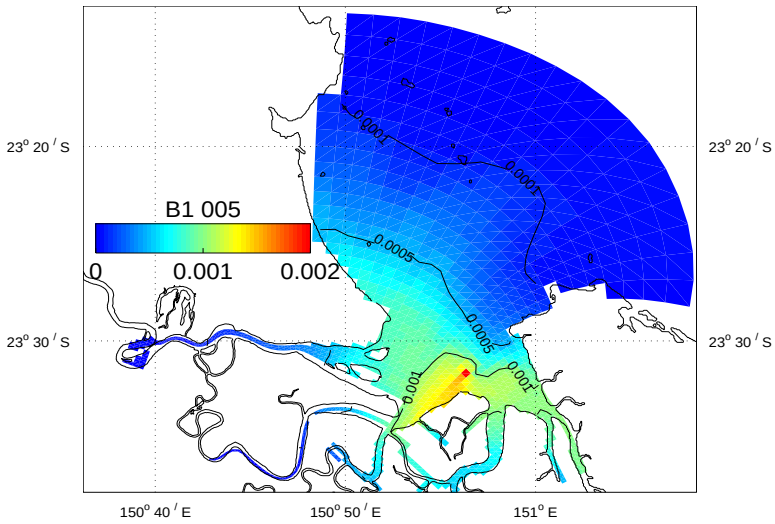


**Figure 7.4.7(a): Buoy 1 release 5 percentile distribution**

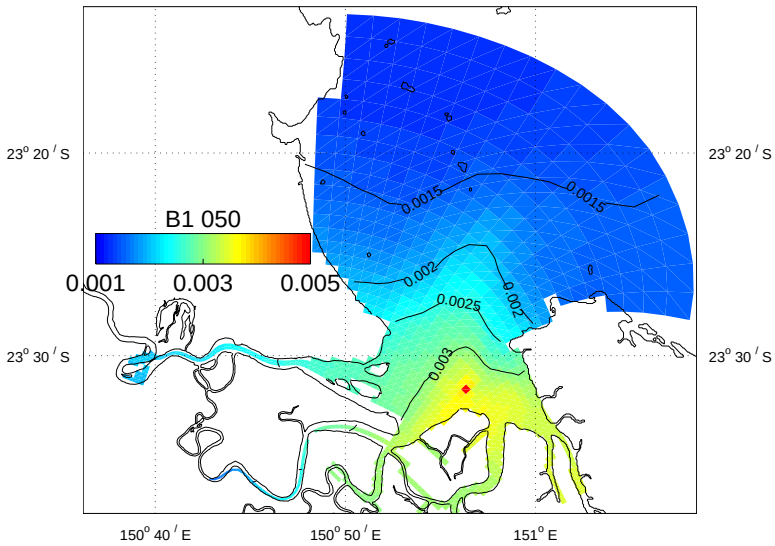


**Figure 7.4. (b): Buoy 1 release median distribution**

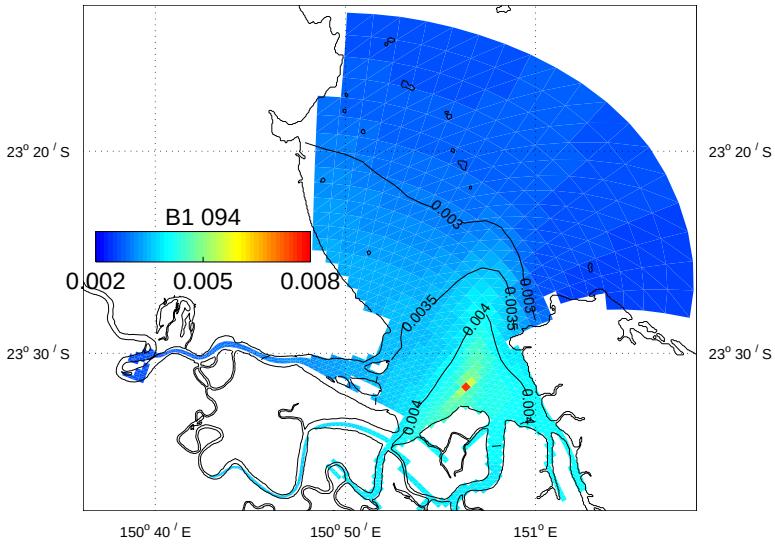


**Figure 7.4.7(c): Buoy 1 release 95 percentile distribution**

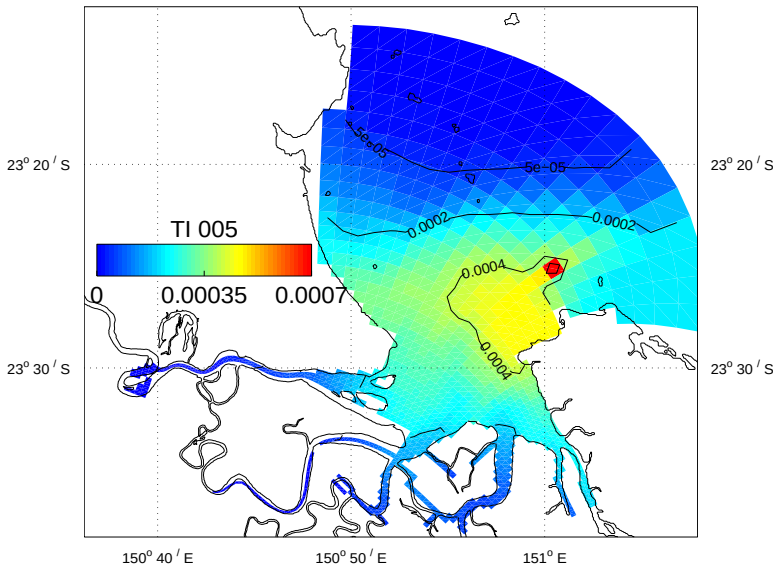


**Figure 7.4.8(a): Timandra buoy release 5 percentile distribution**

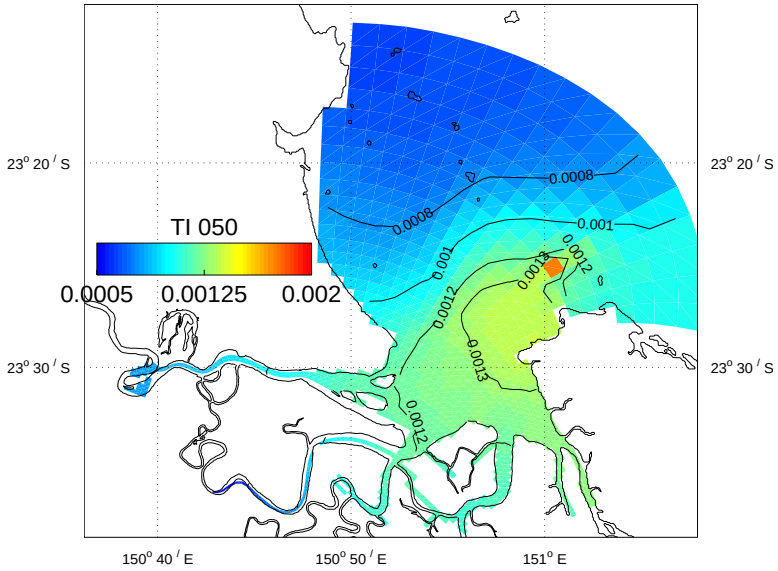


**Figure 7.4.8(b): Timandra buoy release median distribution**

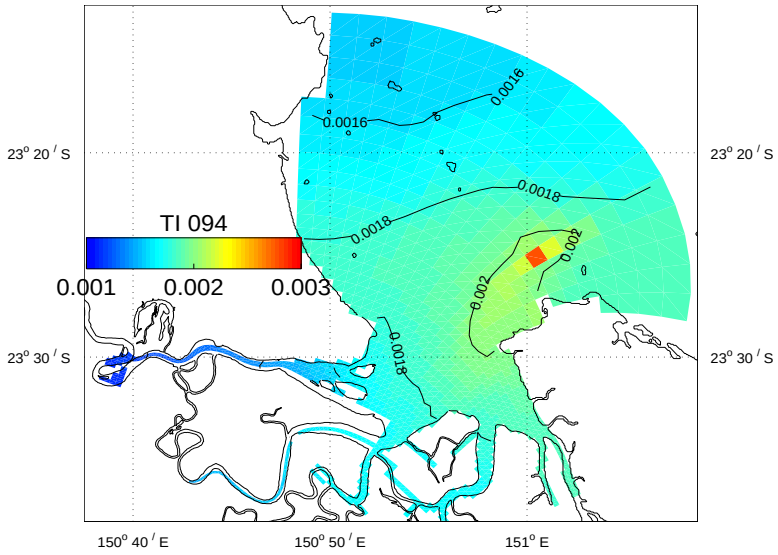


**Figure 7.4.8(c): Timandra buoy release 95 percentile distribution**

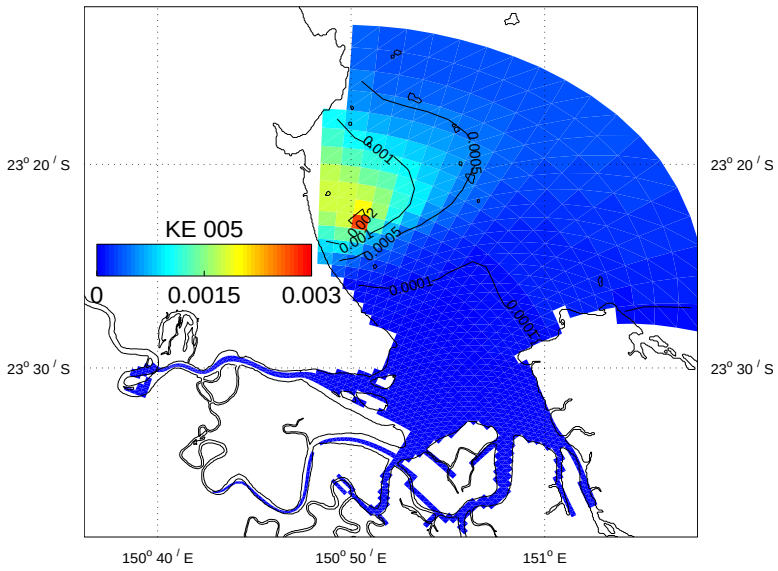


**Figure 7.4.9(a): Western Keppel Bay release 5 percentile distribution**

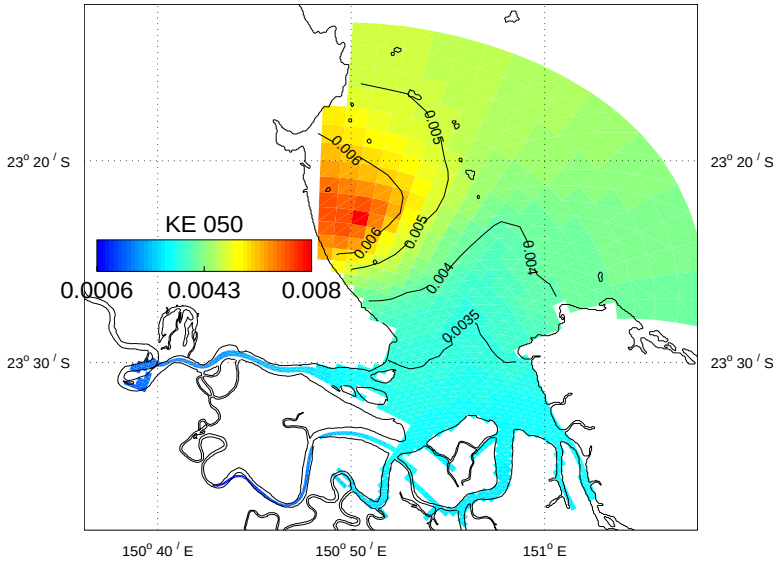


**Figure 7.4.9(b): Western Keppel Bay release median distribution**

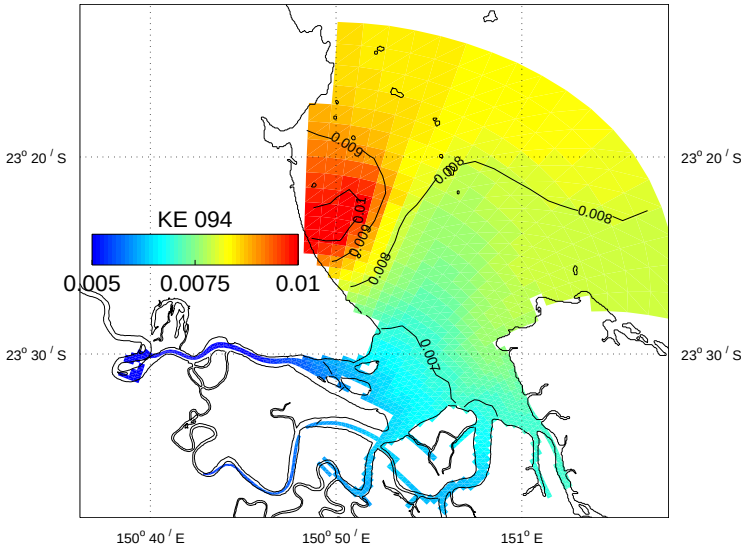


**Figure 7.4.9(c): Western Keppel Bay release 95 percentile distribution**

The distributions in these figures indicate that the Fitzroy Estuary/Keppel Bay region is relatively poorly connected. The release sites within the estuary or tidal creeks result in tracer distribution confined to the estuary or creek, with low concentrations encountered in Keppel Bay. Conversely, those sites located in Keppel Bay resulted in reasonable concentrations throughout the bay, with little tracer being transported into the estuary or creeks.

The site with the best connectivity was located on the western side of Keppel Bay. This release resulted in appreciable concentrations throughout Keppel Bay (>0.003 median), and noticeable concentrations in the lower reaches of the Fitzroy and tidal creeks (>0.002 median). The worst was the Casuarina Creek site, where very high concentrations of tracer (relative to tracer distributions from other release locations) were found within the creek (median 0.1), and negligible concentrations elsewhere. The Lakes Creek and cut-through releases resulted in similar distributions, having mid-estuary median concentrations of ~0.06.

Maximum surface concentrations are confined to the immediate vicinity of the release for all releases. These were generally lowest for the sites in Keppel Bay (95 percentile ~0.005), increased in the mouth of the estuary and tidal creeks (95 percentile ~0.01) and were greatest in the upstream reaches of the estuary and tidal creeks (95 percentile close to 1 for the Casuarina release, 0.07 for the cut-through). Note that these statistics are relevant to the dry and wet seasons of March 2004 to February 2005. A longer wet season with larger flows may bias the distributions in the estuary towards lower concentrations. Conversely, a persistently dry year may result in higher concentrations in the estuary.

## 7.5 Connectivity

The connectivity of the domain can be examined by observing the behaviour of neutrally buoyant particles released from the same locations and depths as the point source releases in Section 7.4. The particles were released at a rate of two particles per hour from an initial pool of 10 000 particles. These particles were subsequently advected with the circulation to provide insight into how various regions of the domain are connected. The particles are also subjected to random motion representing the effect of diffusion (i.e. sub-grid scale effects). Therefore, any two particles released from the same place at the same time are expected to undergo different trajectories due to this random motion. When a particle crosses the offshore open boundary it is replaced in the initial pool for subsequent re-release. The particle distributions after 12 months of simulation are displayed in Figures 7.5.1 to 7.5.8. This distribution is the projection of particles at all depths onto the surface. Particles are colour-coded according to their age since being released over the range 0–40 days (i.e. blue particles are 0 days old, red particles are >40 days old).

The connectivity of the domain inferred from the particle distributions is in agreement with the point source distributions (Section 7.4), that is, the Fitzroy Estuary and tidal creeks are not particularly well connected with Keppel Bay. Particle releases in Casuarina Creek or the Fitzroy Estuary generally remain confined to the creek or estuary respectively. Those particles that are advected into Keppel Bay are associated with old ages, that is, it takes a long time for particles to exit the estuary or tidal creek and make their way into the bay. The Casuarina Creek release, Figure 7.5.2, shows this particularly well. Distributions resulting from releases at the cut-through and Lakes Creek are very similar, indicating that trajectories of particles are not critically dependent on the release locations in the mid to upper estuary. The Fitzroy mouth and Buoy 1 releases result in relatively uniform particle distributions throughout Keppel Bay and the lower reaches of the estuary and tidal creeks. Again only older particles are found in the upper reaches of the estuary or creeks.

Releases further into Keppel Bay (Timandra Buoy and western Keppel) are confined to the bay with few particles advected into the estuary or creeks; the western Keppel distribution particularly so, where particles are confined to the northern bay. These releases also have quite young particles throughout, indicating particles are able to exit the domain relatively quickly. Over the wet season (October to February) the average age of 23 163 particles that exited the domain from all release sites was 45 days. This is probably a more realistic measure of the turnover time of the whole region, since the flushing estimates of

Section 7.3 did not maintain uniform tracer concentrations throughout the domain (i.e. violated the well mixed assumption) due to the influence of the offshore open boundary.

Note that these images are a snapshot of the particle distribution at the end of the wet season, and will vary in accordance with the forcing in effect. An animation of the particle motion over time best conveys the connectivity of the region, although observation of isolated particle trajectories does supply insight into the dynamics of the system. Trajectories were plotted during the wet season flood (3 February 2005) for one tidal cycle (low water to low water; neap tides were in effect at this time) in Figure 7.5.9, and during dry season spring and neap flood and ebb tides in Figures 7.5.10 to 7.5.13. Note that circles correspond to the start of the trajectory and squares to the end in these figures.

Particles trajectories are superimposed on the surface from all depth levels. The trajectories during the wet season flood clearly shows the impact of the fresh water propagating down the Fitzroy Estuary, where particles near the head of the estuary undergo displacement of over 15 km in 15 hours. Since the tide is of mixed mainly semi-diurnal character, particle trajectories are expected to undergo two excursions per day (i.e. one approximately every 6 hours), with the net displacement of start and end locations being indicative of the residual flow.

The trajectories in Keppel Bay reflect this oscillatory motion, where trajectories are directed toward the estuary during the flood tide and away during the ebb. Although the excursion may be large, net movement is usually small, with the particle returning to a location near its original position. Only those particles influenced by the flood waters undergo significant net down-estuary motion. There also appears to be some net motion up Casuarina Creek. The ebb tide during the dry season results in motion out of the estuary, tidal creeks and Keppel Bay towards the open boundary (Figures 7.5.10, 7.5.12). These motions are reversed on the flood tide (Figures 7.5.11, 7.5.13). Large tidal excursions associated with the strong tidal currents are clearly observed during the spring phase, where tidal excursions reach up to 15 km. The neap tide is associated with smaller tidal excursions, approaching 10 km.

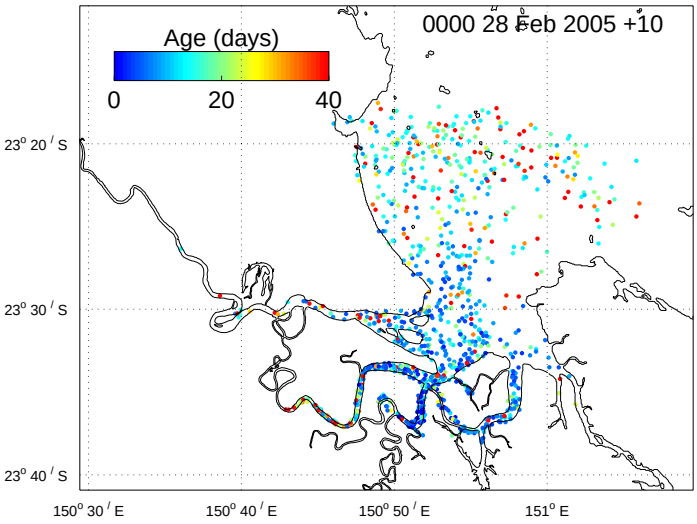


**Figure 7.5.1: Port Alma**

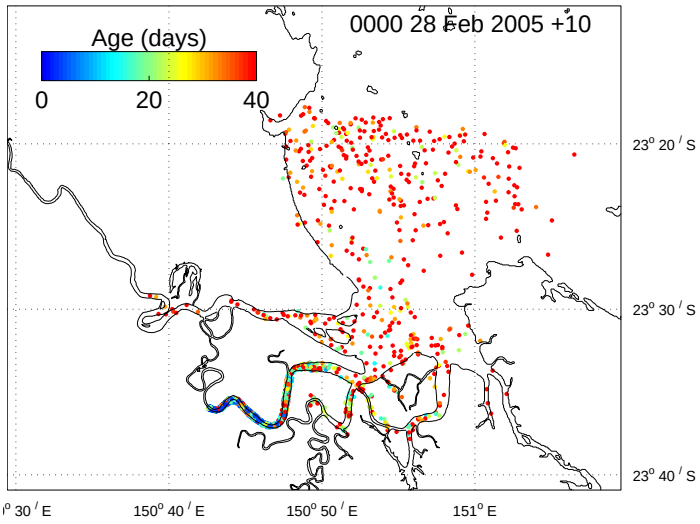


**Figure 7.5.2: Casuarina Creek**

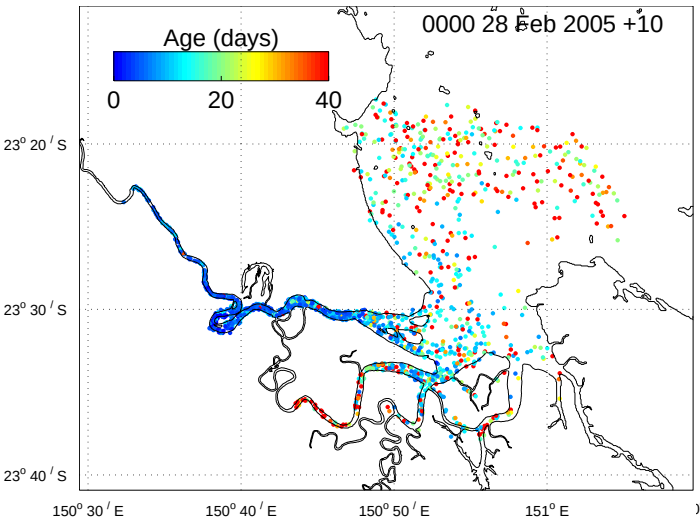


**Figure 7.5.3: Cut-through**

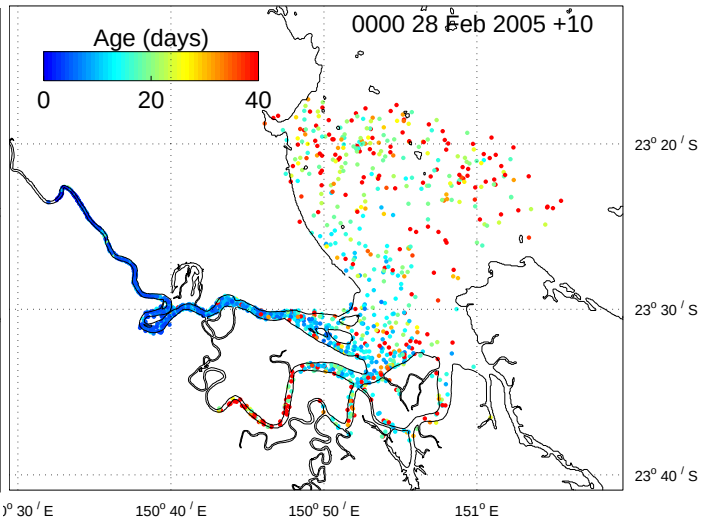


**Figure 7.5.4: Lakes Creek**

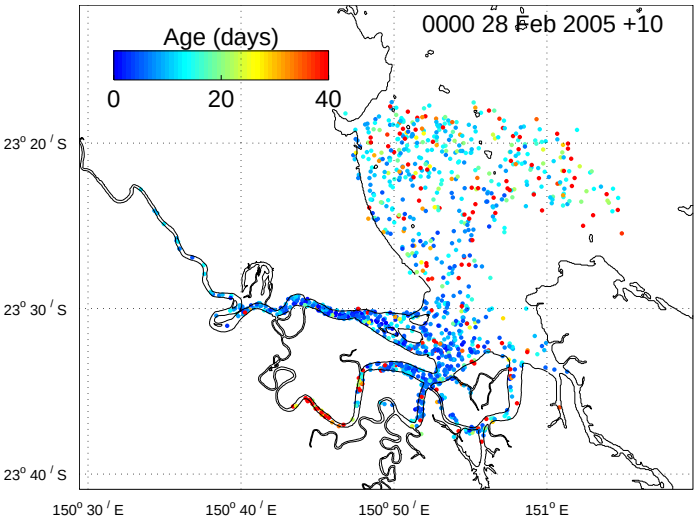


**Figure 7.5.5: Fitzroy mouth**

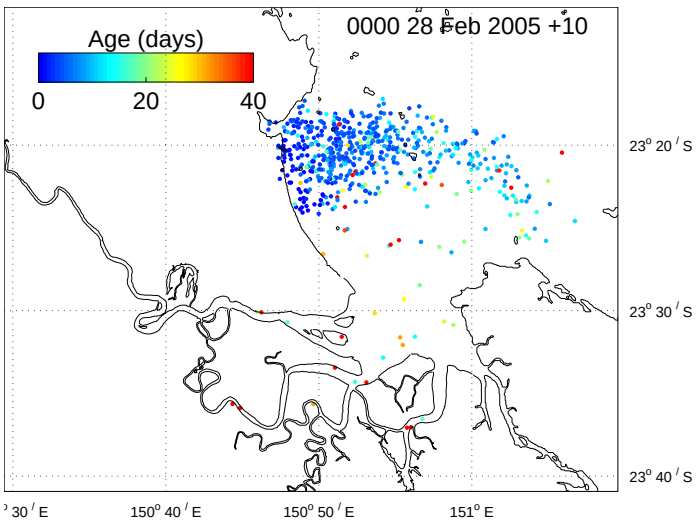


**Figure 7.5.6: Western Keppel Bay**

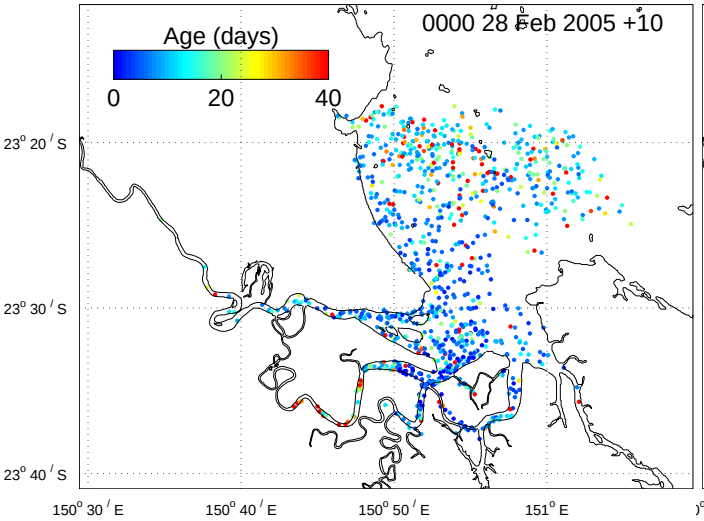


**Figure 7.5.7: Buoy 1**

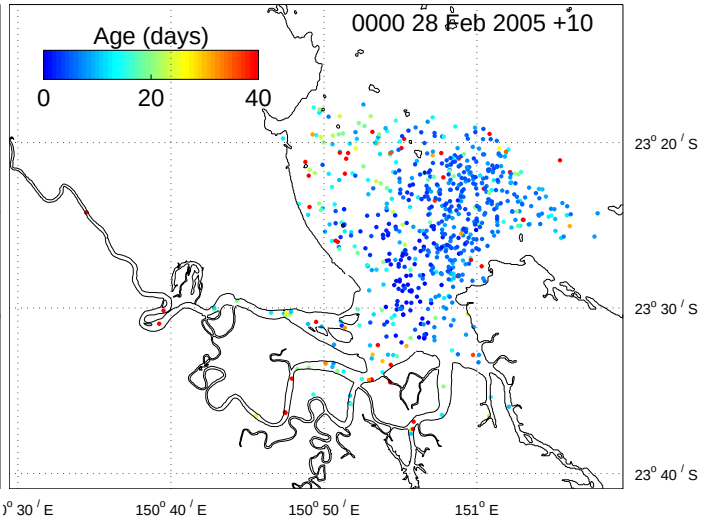


**Figure 7.5.8: Timandra Buoy**

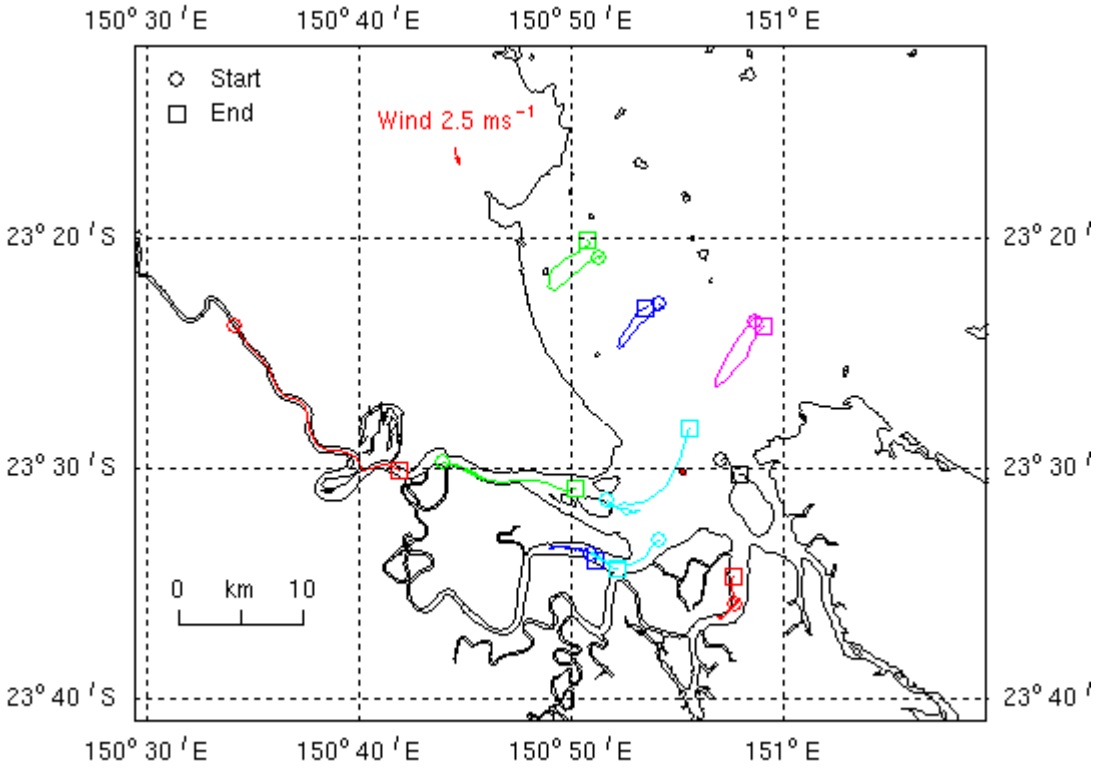


**Figure 7.5.9: Particle trajectories, neap tide (2.06 m range), wet season (21:00, 2 February 2005 – 11:00, 3 February 2005)**

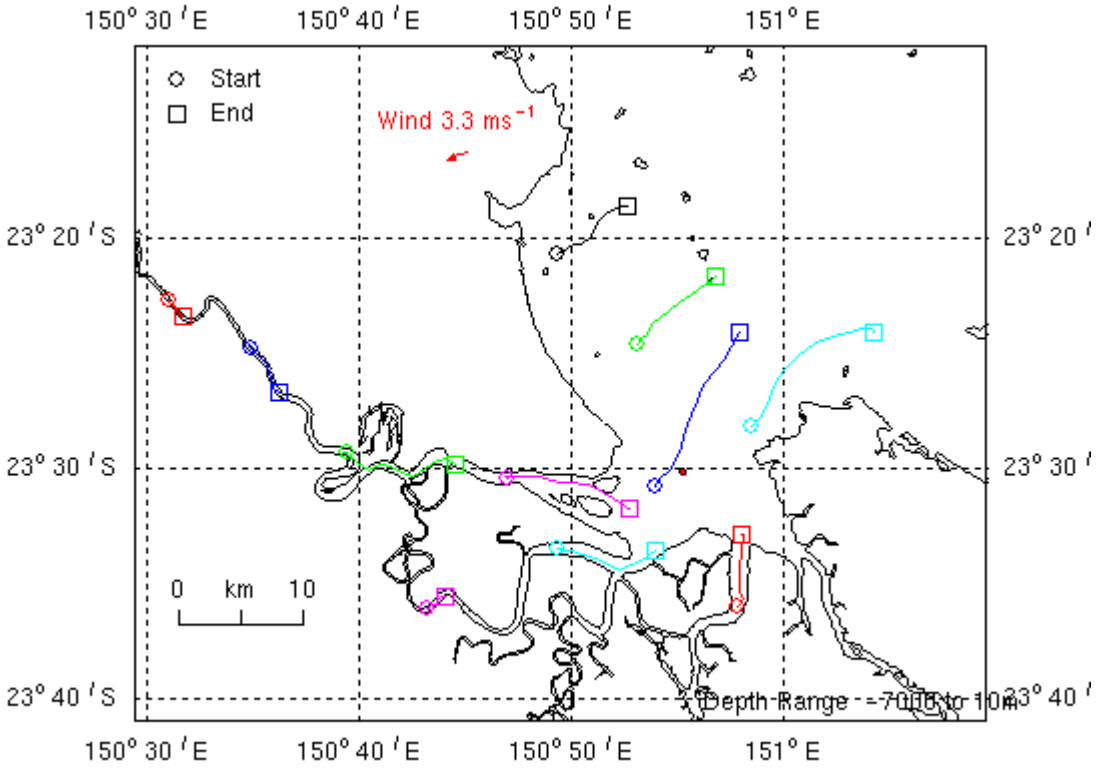


**Figure 7.5.10: Particle trajectories, spring ebb tide (3.86 m), dry season (14 October 2004, 10:00–16:00)**

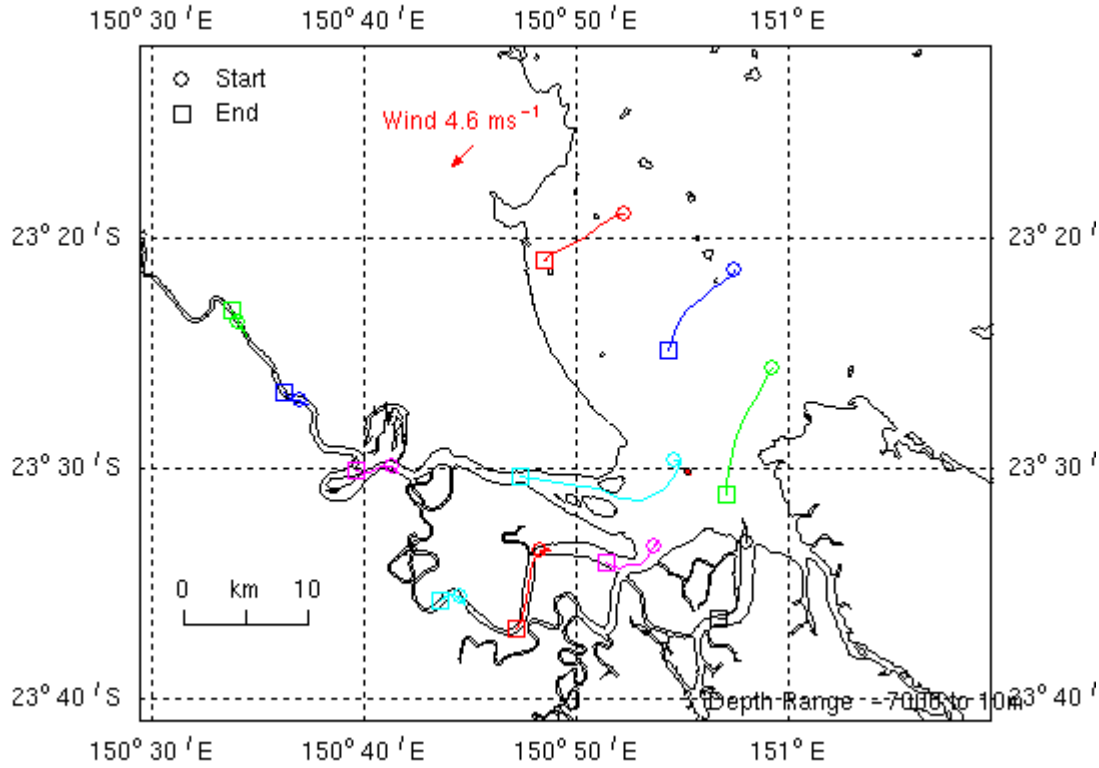


**Figure 7.5.11: Particle trajectories, spring flood tide (3.78 m), dry season (14 October 2004, 10:00–21:00)**

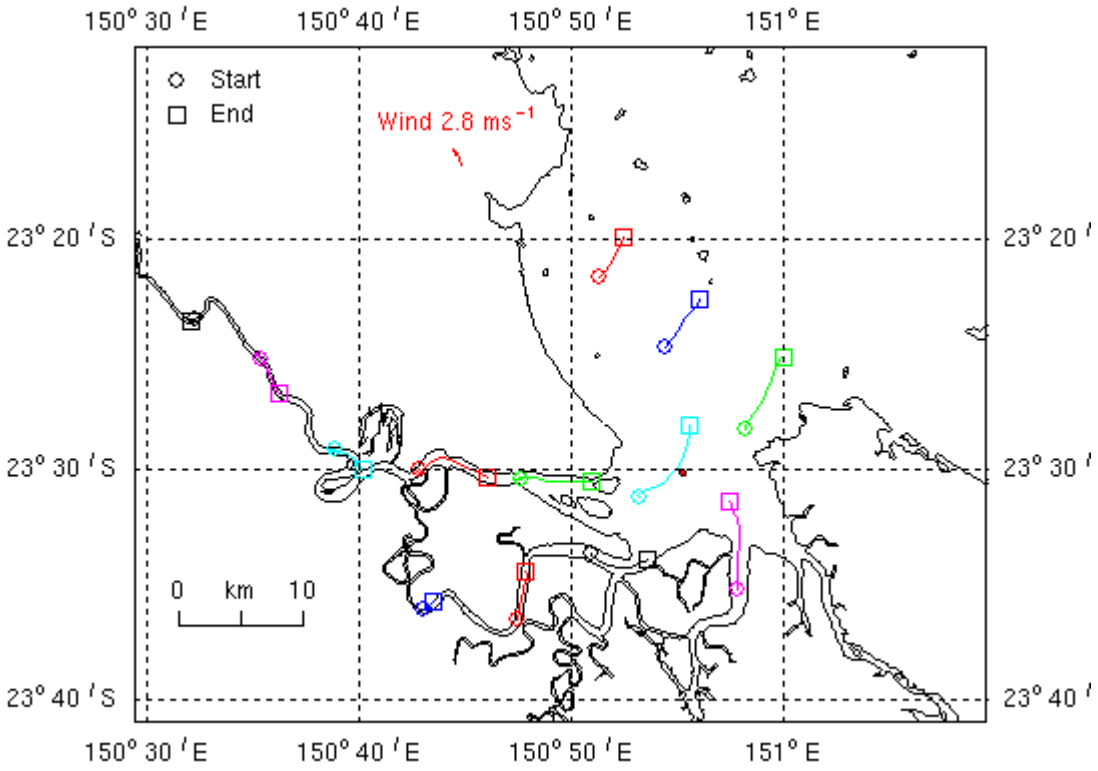


**Figure 7.5.12: Particle trajectories, neap ebb (1.47 m), dry season (20 October 2004, 02:00–08:00)**

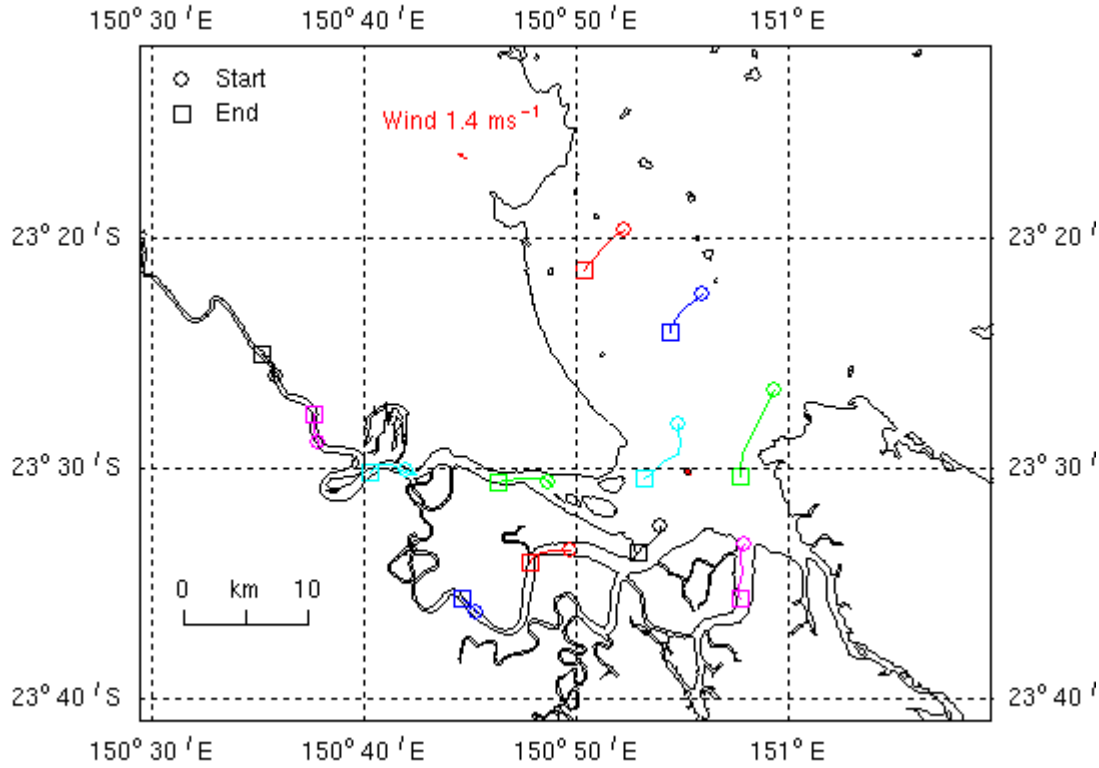


**Figure 7.5.13: Particle trajectories, neap flood (1.53 m), dry season (19 October 2004, 21:00–01:00)**

# 8 Conclusions

A 3D primitive equation model was applied to the Fitzroy Estuary and Keppel Bay to examine the hydrodynamics of the region. Using a nesting process the region was represented with high resolution while incorporating forcing due to wind stress, tides, low frequency sea-level oscillations and pressure gradients due to temperature and salinity distributions. The model was simulated for 12 months and calibrated to data collected in the field.

The model solutions proved to be sensitive to the prescription of heat and salt fluxes input through the ocean surface. The method of specifying latent and sensible bulk fluxes proved critical. Temperature solutions were predominantly controlled by atmospheric exchange during the dry season, with more influence from the offshore open boundary during the wet when surface fluxes begin to decrease. Salinity solutions were primarily controlled by the offshore open boundary.

There existed no adequate data to force the offshore boundaries, which were inversely scaled to attain a satisfactory calibration. Prescription of accurate open boundary conditions for temperature and salinity is an important requirement if the model is to generate adequate solutions. The effect of temperature and salinity on circulation (density driven flows) in Keppel Bay is small in comparison to tidal and wind-driven effects; however, these T/S may be important in controlling primary productivity and sediment flocculation, hence accurate representation is advantageous. Density driven flow is also the primary mechanism for propagating saline water up the estuary after the wet season.

The model results confirm that the Fitzroy Estuary/Keppel Bay region is tidally dominated. Large, predominantly semi-diurnal, tidal amplitudes of up to 2 m result in large currents that may attain speeds approaching 2 $ms^{-1}$ in the lower Fitzroy Estuary. Flow is directed up the estuary and tidal creeks on the flood tide, and down the estuary on the ebb. Flow in Keppel Bay is directed towards the estuary mouth on the flood, and away on the ebb. Surface elevation undergoes a neap-spring tidal cycle with a period of approximately 14 days.

The water column is well mixed in the estuary and Keppel Bay during the dry season, with negligible vertical gradients of momentum or density. This is attributed to large bottom stress generated by the strong tidal flow. The wet season floods effectively flush the estuary, lowering salinity in Keppel Bay and the tidal creeks and creating a degree of vertical stratification in Keppel Bay in the process. Subsequent to the floods the density-driven flow forces the salt

wedge up the estuary towards the barrage, rendering the estuary marine again. It may take 6–8 months for salinities at the head of the estuary to attain marine character after the wet season.

Although the currents are large in the estuary, the residual (net) flow appears small. The tidally and density-driven currents contribute very little to the net flow. Flow resulting from vertical diffusive effects and momentum advection appear to be the largest contributors, indicating that the long-term flow is a balance between sources of momentum at the surface (wind), sinks at the sea bed (bottom drag) and redistribution via momentum advection. The residual circulation in the domain is therefore complex and cannot be readily conceptualised through simple linear interactions.

The three-monthly mean circulation solutions exhibit no obvious coherent pattern to the flow structure. Mean flow is generally directed down-estuary, becoming stronger in the wet season due to flood waters propagating down the river. Net currents are strongest near the mouth of the Fitzroy/Casuarina Creek, approaching 0.1 $ms^{-1}$ during the 2004–2005 wet season. Generally these currents would be proportional to the magnitude of the Fitzroy discharge. The model shows the flow out of the Fitzroy appears to transverse Keppel Bay generally along the western side of Curtis Island; this phenomena needs to be verified with targeted measurements. A westward net flow can be seen at the north-western tip of Curtis Island. There appears to be little seasonal variation in the residual circulation.

The flushing estimates for various subregions of the domain revealed dramatic differences between flushing rates in different areas, and between rates in the same area during the wet and dry season. The Fitzroy Estuary is basically poorly flushed during the dry season, with flushing times generally of several months. This is despite the large tidal excursions, since these are associated with little net exchange. The impact of flood waters during the wet is to flush the system very effectively. The mean flow due to the flood pushes residual water out of the estuary reducing flushing times to the order of several days.

The flood events in the wet season appear to be predominantly responsible for annually renewing water in the estuary. The flushing of Keppel Bay appears to be primarily controlled by exchange across the open boundary, and is relatively insensitive to wet season floods, as is the whole region (estuary plus Keppel Bay plus tidal creeks). Connor and Deception Creeks have relatively short flushing timescales, and also appear to be unaffected by wet season floods. Casuarina Creek has a relatively long flushing time of ~1 month, which is approximately halved during times of Fitzroy flood. These flushing estimates are applicable to

a ~800 $m^3s^{-1}$ flood event, and flushing times are expected to decrease as wet season flows increase.

The analysis of statistical representations of mixing zones due to continuous point source release of unit loads at various locations throughout the estuary, combined with particle tracking analysis, indicate the system is relatively poorly connected as a whole. The upper estuary and tidal creeks exchange little water with Keppel Bay on an annual basis. The head of Casuarina Creek displays the worst connectivity with the rest of the system; this is reflected in the high salinities of ~40 psu that this area attains in the dry season. Keppel Bay appears somewhat better connected to the mouths of the estuary and tidal creeks, but again connectivity with the upper reaches is poor. The western side of Keppel Bay exhibits the best connection to the remainder of the system.

Particle trajectories display the expected up-estuary displacement on flood tides, and down-estuary on the ebb. Spring tidal excursions of ~15 km in Keppel Bay are greater than those during the neap phase, which approach 10 km. Tidal excursions are considerably less in the Fitzroy Estuary and tidal creeks. During the wet season floods particle displacement down the Fitzroy Estuary is large, up to 15 km over a tidal cycle. There also appears to be some net motion up Casuarina Creek during the wet season floods. Although the excursion may be large over a complete tidal cycle in Keppel Bay, net movement is usually small, with the particle returning to a location near its original position.

A simple conceptual overview of the system is one where there are essentially three independent systems in existence in the region. Firstly, Keppel Bay appears well connected to regions further offshore, which exchange water readily with the bay. The bay does not readily exchange water with the estuary or tidal creeks, with transport only influencing the lower reaches of these systems. Secondly, the Fitzroy Estuary is almost de-coupled from Keppel Bay during the dry season, with very little exchange being driven by the slow propagation of the saline water up-estuary. During the wet season the floods effectively flush the estuary, emptying water into Keppel Bay where subsequent exchanges with offshore water masses eventually renew the water in the system. Thirdly, the tidal creeks are also poorly coupled to Keppel Bay during the dry (exchange being restricted to the lower reaches of the creeks), and have only limited benefit from large freshwater flows during the wet to assist in flushing. The further east from the Fitzroy these creeks reside, the less impact the wet season floods appear to have. Note that no freshwater inputs were included in these tidal creeks, which if included would be expected to improve connectivity with Keppel Bay.

# References

Atkinson, I., Ford, P., Noble, R., Oubelkheir, K., Radke, L., Robson, B., Tindall, C., Verwey, P. & Webster, I. (2004) *Field report on the second survey of dry season water column and sediment properties in the Fitzroy Estuary and Keppel Bay, Rockhampton Queensland, August 15 – September 1, 2004*. Coastal CRC, Contaminants dynamics subproject. Milestones AC09, AC11, AC43 and AC44.

Blanc, T.V. (1985) Variation of bulk-derived surface flux, stability, and roughness results due to the use of different transfer coefficient schemes. *Journal of Physical Oceanography*, 15, 650–669.

Blumberg, A.F. & Herring, J. (1987) Circulation modelling using orthogonal curvilinear coordinates. In: *Three-dimensional models of marine and estuarine dynamics*, eds. J.C.J. Nihoul & and B.M. Jamart, Elsevier.

Eanes, R. & S. Bettadpur (1995) *The CSR 3.0 global ocean tide model*. Center for Space Research, Technical Memorandum, CST-TM-95-06.

Herzfeld, M. (2005) SHOC, sparse hydrodynamic ocean code, scientific manual. CSIRO Marine and Atmospheric Research.

Kitaigorodskii, S.A., Kuznetsov O.A. & Panin G.N. (1973) *Coefficients of drag, sensible heat and evaporation in the atmosphere over the surface of the sea.* Izvestiya Academy of Sciences, USSR.

Leonard, B.P. (1979) A stable and accurate convective modelling procedure based on quadratic upstream interpolation. *Computer Methods in Applied Mechanics and Engineering*, 19, 59–98.

Leonard, B.P. (1991) The ULTIMATE conservative difference scheme applied to unsteady one-dimensional advection. *Computer Methods in Applied Mechanics and Engineering*, 19, 17–74.

Margvelashvili, N., Herzfeld, M. & Webster, I. (2006) *Modelling of fine sediment transport in Fitzroy Estuary and Keppel Bay.* Technical Report No. 39, CRC for Coastal Zone, Estuary and Waterway Management, Brisbane.

Masagutov, T.F. (1981) Calculation of the vertical turbulent fluxes in the near-water atmospheric layer over the ocean in tropical latitudes. *Meteorologiya i Gidrologiya* 12, 61–68.

Mellor, G.L. & Yamada, T. (1982) Development of a turbulence closure model for geophysical fluid problems. *Reviews of Geophysics and Space Physics*, 20(4), 851–875.

Ridgway K.R., Dunn, J.R. & Wilkin, J.L. (2002) Ocean interpolation by four-dimensional least squares – Application to the waters around Australia, *Journal of Atmospheric and Oceanic Technology*, 19, 1357–1375.

Simpson, J.J. & Dickey T.D. (1981) The relationship between downward irradiance and upper ocean structure. *Journal of Physical Oceanography*, 11, 309–323.

Smagorinsky, J. (1963) General circulation experiments with the primitive equations, I. The basic experiment. *Monthly Weather Review*, 91, 99–164.

Tartinville, B., Deleersnijder, E. & Rancher, J. (1997) The water residence time in the Mururoa atoll lagoon: Sensitivity analysis of a three-dimensional model. *Coral Reefs*, 16, 193–203.

Walker, S.J. & Waring J.R. (1998) *A multiple grid, 3-dimensional, non-linear, variable-density hydrodynamic model with curvilinear horizontal coordinates and level (z) vertical coordinates.* CSIRO Marine Research, Report OMR-118/120.

Webster, I.T., Ford, P.W., Robson, B., Margvelashvili, N. & Parslow, J. (2004) Conceptual models of the hydrodynamics, fine sediment dynamics, biogeochemistry and primary production in the Fitzroy Estuary. Technical Report No. 8, CRC for Coastal Zone Estuary and Waterway Management, Brisbane.